

RADC-TR-81-166

In-House Report

June 1981

12

FILED



AD A107039

# PROPAGATION STUDY FOR A TROPOSPHERIC TRANSHORIZON RADAR

Kurt Toman

APPROVED FOR PUBLIC RELEASE; DISTRIBUTION UNLIMITED

DTIC  
ELECTE  
NOV 9 1981  
S D  
B

**ROME AIR DEVELOPMENT CENTER**  
**Air Force Systems Command**  
**Griffiss Air Force Base, New York 13441**

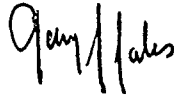
FILED  
THE FILE COPY

81 11 09137

This report has been reviewed by the RADC Public Affairs Office (PA) and is releasable to the National Technical Information Service (NTIS). At NTIS it will be releasable to the general public, including foreign nations.

RADC-TR-81-166 has been reviewed and is approved for publication.

APPROVED.



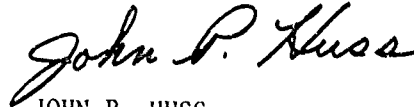
GARY S. SALES  
Acting Chief, Propagation Branch  
Electromagnetic Sciences Division

APPROVED:



ALLAN C. SCHELL  
Chief, Electromagnetic Sciences Division

FOR THE COMMANDER:



JOHN P. HUSS  
Acting Chief, Plans Office

If your address has changed or if you wish to be removed from the RADC mailing list, or if the addressee is no longer employed by your organization, please notify RADC (EEP ) Hanscom AFB MA 01731. This will assist us in maintaining a current mailing list.

Do not return this copy. Retain or destroy.

Unclassified

SECURITY CLASSIFICATION OF THIS PAGE (When Data Entered)

REPORT DOCUMENTATION PAGE		READ INSTRUCTIONS BEFORE COMPLETING FORM	
1. REPORT NUMBER <b>(14)</b> RADC-TR-81-166	2. GOVT ACCESSION NO. AD-A207039	3. RECIPIENT'S CATALOG NUMBER	
4. TITLE (and Subtitle) <b>(6)</b> PROPAGATION STUDY FOR A TROPOSPHERIC TRANSHORIZON RADAR		5. TYPE OF REPORT & PERIOD COVERED In-House	
7. AUTHOR(s) <b>(10)</b> Kurt/Toman		6. PERFORMING ORG. REPORT NUMBER	
9. PERFORMING ORGANIZATION NAME AND ADDRESS Deputy for Electronic Technology (RADC/EEP) Hanscom AFB Massachusetts 01731		10. PROGRAM ELEMENT, PROJECT, TASK AREA & WORK UNIT NUMBERS 62702F 45061730	<b>(16)</b> <b>(17)</b> 27
11. CONTROLLING OFFICE NAME AND ADDRESS Deputy for Electronic Technology (RADC/EEP) Hanscom AFB Massachusetts 01731		12. REPORT DATE June 1981	<b>(11)</b>
14. MONITORING AGENCY NAME & ADDRESS (if different from Controlling Office) <b>(9)</b> Technical Repts		13. NUMBER OF PAGES 82	<b>(12)</b> 83
		15. SECURITY CLASS. (of this report) Unclassified	
16. DISTRIBUTION STATEMENT (of this Report)  Approved for public release; distribution unlimited.		15a. DECLASSIFICATION/DOWNGRADING SCHEDULE	
17. DISTRIBUTION STATEMENT (of abstract entered in Block 20, if different from Report)			
18. SUPPLEMENTARY NOTES			
19. KEY WORDS (Continue on reverse side if necessary and identify by block number) Tropospheric propagation      Scatter cross section Transhorizon propagation      Noise temperature Path attenuation                  Signal-to-noise ratio Propagation loss			
20. ABSTRACT (Continue on reverse side if necessary and identify by block number) Computation methods for tropospheric propagation losses in transhorizon propagation are used to provide estimates for the detectability of over-the-horizon targets. Losses depend on frequency, distance, climate, refractivity, and on an empirically derived attenuation function which also takes into account the effects of antenna heights. Equivalent antenna temperatures are assumed to be due to galactic noise. Receiver noise is characterized by noise figure F. Signal-to-noise ratios are illustrated for several target cross-sections as a function of frequency and distance, parametric in antenna heights, distance or			

DD FORM 1 JAN 73 1473

Unclassified

SECURITY CLASSIFICATION OF THIS PAGE (When Data Entered)

1 309050 xlt

Unclassified

SECURITY CLASSIFICATION OF THIS PAGE(When Data Entered)

20. (Cont)

frequency, for the median loss 50%, as well as 1, 10, 90, and 99% levels of variability.

Unclassified

SECURITY CLASSIFICATION OF THIS PAGE(When Data Entered)

## Preface

This propagation study was initiated by EEP in response to the RADC Technology Tasking Order "Low VHF Radar Propagation Study" dated 8 September 1980.

Programming for computing and plotting was done by Mr. Joseph S. Bamford, Arcon Corporation contract F19628-78-C-0202. The document search/retrieval effort was aided by the outstanding staff of the AFGL Research Library. The MIT Lincoln Lab library also provided some support.

Accession For	
NTIS GRA&I	<input checked="" type="checkbox"/>
DTIC TAB	<input type="checkbox"/>
Unannounced	<input type="checkbox"/>
Justification	
By	
Distribution/	
Availability Codes	
Avail and/or	
Dist	Special
<b>A</b>	

## Contents

1. INTRODUCTION	7
2. DEFINITIONS	8
3. ESTIMATING PATH ATTENUATION	9
3.1 Attenuation Function $F(\theta d)$	10
4. SIGNAL-TO-NOISE RATIO	17
5. AVAILABLE BANDWIDTH AND COHERENCE TIME	33
6. CLUTTER FACTOR	25
7. CONCLUSION	25
8. RECOMMENDATIONS	27
REFERENCES	29
APPENDIX A: Five Plots of Two-way Loss (dB) vs Frequency (MHz)	31
APPENDIX B: Three Plots of Two-way Loss (dB) vs Distance (km)	37
APPENDIX C: Fourteen Plots of Signal-to-Noise Ratio (dB) vs Frequency (MHz) for Median Loss	41
APPENDIX D: Nine Plots of Signal-to-Noise Ratio (dB) vs Frequency (MHz) for 1 to 99% Loss Variability	49
APPENDIX E: Thirty-three Plots of Signal-to-Noise Ratio (dB) vs Distance (km) for Median Loss	55
APPENDIX F: Eighteen Plots of Signal-to-Noise Ratio (dB) vs Distance (km) for 1 to 99% Loss Variability	73

## Illustrations

1.	Curved-earth Geometry for Transhorizon Propagation Between Elevated Antennas	11
2.	Attenuation Function $F(\theta d)$ , in dB, Parametric in Surface Refractivity, as a Function of the Product $\theta d$	11
3.	Geometry for the Asymmetry Parameter $s = \alpha_0 / \beta_0$	13
4.	For Tropospheric Transhorizon Propagation, the Two-way Median Path Attenuation, in dB, Relative to Free Space as a Function of Frequency, Parametric With Distance for Pairs of Equal Antenna Heights, Standard Refraction, and Continental Temperate Climate	14
5.	For Tropospheric Transhorizon Propagation, the Signal-to-Noise Ratio, in dB, Available at a Mono-static Radar From a Target, as a Function of Frequency, With Frequency Independent Scattering Cross Section	17
6.	For Tropospheric Transhorizon Propagation, the Signal-to-Noise Ratio, in dB, Available at a Mono-static Radar From Three Different Types of Targets, as a Function of Frequency	20
7.	For Tropospheric Transhorizon Propagation, the Signal-to-Noise Ratio, in dB, Available at a Mono-static Radar From a Composite Target	21
8.	Tentative Estimate of the Usable Frequency Band of a Tropospheric Transhorizon Propagation Link as a Function of Range for Several Values of Free-space Antenna Gains	24
9.	Variation of Clutter Factor $\beta$ With Frequency Derived From Experimental Studies and From C. C. I. R. (Comité Consultatif International des Radiocommunications) Predictions	26

## Tables

1.	Look-up Table for $V(d_e)$	12
2.	Look-up Table for Path-Attenuation Variability: Maritime Temperate (7b) Climate Over Sea Path ( $10 \leq d_e \leq 100$ km)	15
3.	Look-up Table for Path-Attenuation Variability: Maritime Temperate (7b) Climate Over Sea Path ( $110 \leq d_e \leq 200$ km)	16
4.	Look-up Table for Path-Attenuation Variability: Maritime Temperate (7b) Climate Over Sea Path ( $210 \leq d_e \leq 300$ km)	16
5.	Look-up Table for Galactic Noise: Equivalent Temperature	19
6.	Line-of-Sight Distances $d$ [km] Between Elevated Antennas, Computed for a Curved Earth of Radius $a_e = 8504$ km	22

# Propagation Study for a Tropospheric Transhorizon Radar

## 1. INTRODUCTION

It is of interest to examine the possibility of detecting low-altitude targets beyond and within the line-of-sight. It is postulated that beyond the line-of-sight propagation is achievable by several propagation mechanisms involving the troposphere. The dominant transhorizon propagation mechanism is expected to depend on frequency, distance, climate, terrain, time, effective antenna and target heights. Considering these parameters, a loss-quantity had to be identified that could be incorporated into the radar equation for signal-to-noise ratio estimates for a given set of systems parameters. The desired and appropriate loss quantity was recognized as being the difference in dB between the basic transmission loss and the basic free-space transmission loss. This difference in dB is known as path attenuation. These, and other terms will be defined shortly. Both loss terms refer to isotropic antennas. Estimates of the expected path attenuation,  $A$ , will yield loss-values for which it was assumed that the antennas at both ends of the path had a gain of unity ( $G_t = G_r = 1$ ). Having obtained this estimate, the gain of the receive antenna will conceptually be replaced by an isotropic target ( $G = 1$ ) that possesses a cross section  $\sigma$  which varies with frequency. The two-way loss that accounts for the return signal at the radar transmitter would be  $2A$  if  $A$  is expressed in decibels or  $A^2$  if  $A$  is expressed as a ratio. The two-way loss term will appear in the radar

---

(Received for publication 8 June 1981)

equation containing the expected radar transmit/receive antenna gains such as  $G = 1000$  or  $10 \log 1000 = 30$  dB.

## 2. DEFINITIONS

Basic Free-Space Transmission Loss  $L_{bf}$  - In free space, the transmission loss expected between radio frequency power radiated from an ideal loss-free isotropic ( $G = 1$ ) transmitting antenna and the received power available from an ideal loss-free isotropic receiving antenna.

Basic Transmission Loss  $L_b$  - Transmission loss expected between ideal, loss-free isotropic transmitting and receiving antennas.

Coherence Bandwidth<sup>1</sup> - Of the fluctuation fields of waves at different frequencies, with correlation determined at the same time, that separation frequency at which the correlation function almost disappears or decreases to a specified level (Note: the inverse of coherence bandwidth is the lengthening of a pulse due to a random medium).

Coherence Time<sup>1</sup> - Of the correlation of an output wave at two different times, the time difference at which the correlation practically disappears or decreases to a specified level. (Note: The inverse of coherence time is the "spectrum broadening" of a wave in a random medium).

Path Attenuation A - The difference between basic transmission loss and basic free-space transmission loss:  $A = L_b - L_{bf}$  (dB).

System Loss<sup>2</sup> - Of a radio system, the transmission loss plus the losses in the transmitting and receiving antennas, all expressed in decibel.

Transhorizon Propagation<sup>3</sup> - Propagation over paths extending beyond the normal radio horizon. It may include diffraction, forward scatter, specular and diffuse reflection, and ducting.

Transmission Loss  $L^2$  - Of a radio link, the difference in decibel between the radio frequency power radiated from the transmitting antenna and the resultant radio frequency signal power that would be available from the receiving antenna if there were no circuit losses other than those associated with radiation resistance.

1. Ishimaru, A. (1978) Wave Propagation and Scattering in Random Media, Vol. 1, Academic Press, New York.
2. IEEE Standard Definitions of Terms for Radio Wave Propagation, IEEE Std. 211-1977; IEEE, New York, New York.
3. C. C. I. R. Recommendation 310-3, Definitions of terms relative to propagation in the troposphere, XIIIth Plenary Assembly, Geneva, 1974, Vol. 5 Propagation in Non-ionized Media, p 63-64.

### 3. ESTIMATING PATH ATTENUATION

Although scatter propagation may not be the dominant mode for a particular transhorizon propagation path, transmission loss is frequently associated with scatter propagation. It was claimed that prediction methods for transmission loss due to forward scatter are consistent with that due to incoherent reflections from patchy elevated layers and agree with long-term median values for "all available data".<sup>4</sup> The choice of "all available data" was not restricted to troposcatter propagation but included ducting and partial reflector. This must be kept in mind when using the median scatter loss equation. The use of the latter may be more appropriate the longer the path and the higher the frequency. For VHF and a path length of about 127 km, scatter propagation was dominant for 20% of the time.<sup>5</sup> Path attenuation  $A$  will be used as a loss term in the free-space radar equation to make signal-to-noise ratio estimates for particular targets. This radar equation contains the gains due to directive antennas relative to free space. When expressed in dB, path attenuation is the difference between basic transmission loss,  $L_b$ , and basic free-space transmission loss,  $L_{bf}$ , both defined earlier. Median path attenuation,  $A(50) = L_b - L_{bf}$ , is computed using the following semi-empirical equation<sup>6</sup> for the median loss along tropospheric paths.

$$A(50) = 10 \log_{10} f - 40 \log_{10} d + F(\theta d) - V(d_e) - 32.4 \quad (1)$$

where

$A(50)$  is median path attenuation (dB)

$f$  is frequency (MHz)

$d$  is distance between terminals (km)

$F(\theta d)$  is attenuation function

$$\theta = \frac{d - d_{Lt} - d_{Lr}}{a_e} = \frac{d'}{a_e} \text{ (rad)}$$

$a_e$  is effective earth radius (km)

$$d_{Lt} = (2 a_e h_{te})^{1/2} \text{ (km)}$$

4. Rice, P. L., Longley, A. G., Norton, K. A., and Barsis, A. P. (1966) Transmission Loss Predictions for Tropospheric Communication Circuits, National Bureau of Standards, Technical Note 101, Vol. 1, 9-1, revised May 1966.
5. Toman, K. (1952) An Investigation of Tropospheric Propagation, U. of Illinois, Urbana, Phd Thesis.
6. Hall, M. P. M. (1979) Effects of the Troposphere on Radio Communication, Peter Peregrinus Ltd., IEE London and New York, p. 137.

- $d_{Lr} = (2 a_e h_{tr})^{1/2}$  (km)  
 $h_{te}$  is effective transmitting antenna height (km)  
 $h_{re}$  is effective receiving antenna height (km)  
 $V(d_e)$  is climate function (dB)  
 $d_e$  is effective distance (km).

Both the climatic correction  $V$  for the path attenuation  $A(50)$ , as defined above, as well as percentage levels of variability  $q$  ( $p$ ) relative to the median were linked to effective distance.<sup>4, 6, 7</sup> This effective distance  $d_e$  depends on frequency, distance between terminals, effective antenna heights, effective earth radius. To evaluate the effective distance, an arbitrary reference distance  $d_{ref}$  is introduced. It contains a frequency dependent distance term  $d_{sl}$  which signifies that distance from the radiating source where diffraction and forward 'scatter' transmission loss are approximately equal over a smooth earth. For different frequencies, this equality is achieved at different distances as  $d_{sl} = 300 f^{-1/3}$  [km]. The reference distance  $d_{ref}$  is composed as follows:  $d_{ref} = d_{sl} + d_{Lt} + d_{Lr}$  [km]. If it is found that a terminal distance  $d \leq d_{ref}$ , one computes the effective distance from  $d_e = 130 d / d_{ref}$ . For  $d > d_{ref}$  one uses  $d_e = 130 + d - d_{ref}$ . The values for  $V(d_e)$ , usually published in graphical form, can be inferred from Table 1 for the appropriate climate zone.

### 3.1 Attenuation Function $F(\theta d)$

The attenuation function  $F(\theta d)$ , which appeared in the equation for path attenuation, yields attenuation in dB as a function of the product of the scatter angle  $\theta$  in radians and the distance between terminals in kilometers. The geometry is illustrated in Figure 1. The scatter angle  $\theta = d' / a_e$ , where  $d'$  is the distance between points at which rays from the transmitting and receiving antennas are tangents to the surface of the earth. As illustrated in Figure 2, the attenuation function varies with surface refractivity. Depending on the magnitude of the product  $\theta d$ ,  $F(\theta d)$  can be computed from three mathematical representations valid for a surface refractivity  $N_s = 301$ .<sup>7</sup>

For  $0.01 \leq \theta d \leq 10$ :

$$F(\theta d) = 135.82 + 0.33 \theta d + 30 \log_{10} (\theta d) \quad (2)$$

For  $10 \leq \theta d \leq 70$ :

$$F(\theta d) = 129.5 + 0.212 \theta d + 37.5 \log_{10} (\theta d) \quad (3)$$

7. C. C. I. R. Report 244-1, Estimation of tropospheric-wave transmission loss, Documents of the XIth Plenary Assembly, Oslo, (1966) Vol. 1, Propagation; pp. 143-167.

Figure 1. Curved-earth Geometry for Transhorizon Propagation Between Elevated Antennas

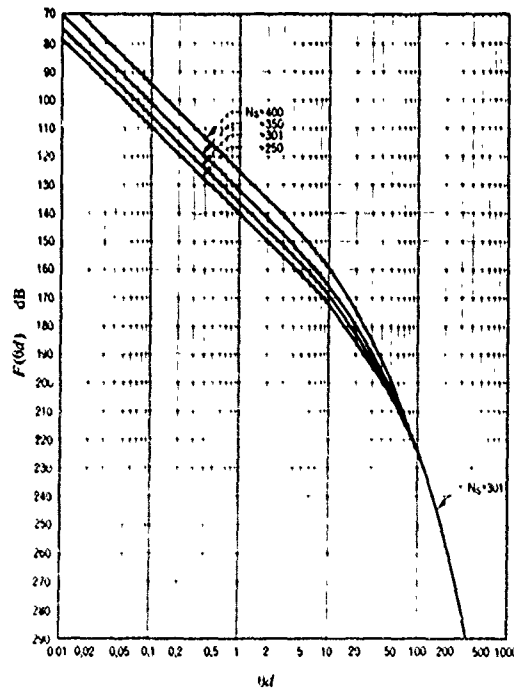
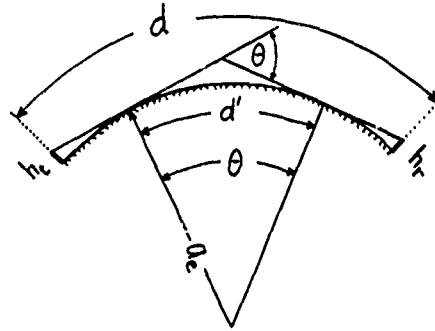


Figure 2. Attenuation Function  $F(\theta d)$ , in dB, Parametric in Surface Refractivity, as a Function of the Product  $\theta d$ .  $\theta$  is the scatter angle in radians and  $d$  is the distance between terminals in kilometers

For  $\theta d > 70$ :

$$F(\theta d) = 119.2 + 0.157 \theta d + 45 \log_{10} (\theta d) \quad (4)$$

For  $N_s \neq 301$ , the function  $F(\theta d)$  may be obtained by a modifying equation

$$F(\theta d, N_s) = F(\theta d, N_s = 301) - [0.1 (N_s - 301) \exp - \theta d / 40] \quad (5)$$

Table 1. Look-up Table for  $V(d_e)^*$

$d_e$ (km)	Effective distance, $d_e$ (km)									
	1 dB	2 dB	3 dB	4 dB	5 dB	6 dB	7a dB	7b dB	Maritime temp. over sea	Maritime temp. over land
0	0	0	0	0	No data	0	0	0	0	0
10	0	0	0	0	0	0	0	0	0	0
20	0	0	0	0	0	0	0	0	0	0
30	0	0	0	0	0	0	0	0	0	0
40	0	0	0	0	0	0	0	0	0	0
50	0	0	0	0	0	0	0	0	0	0
60	0	0	0	0	0	0	0	0	0	0
70	0	0	0.2	0	0	0	0	0	0	0
80	0	0.4	0.5	0	0	0	0	0	0	0
90	0.2	0.7	0.7	-0.1	0	0.4	0	0	0	0.1
100	0.4	1.0	1.3	-0.4	0	0.7	0	0	0	0.5
110	0.6	1.2	2.0	-0.6	0	1.0	0	0	0	1.0
120	0.8	1.5	2.5	-0.7	0	1.2	0.1	0.1	0.1	1.8
130	1.0	1.7	3.0	-1.0	0	1.5	0.2	0.2	0.2	2.5
140	1.2	2.0	3.5	-1.2	0	1.7	0.3	0.3	0.3	3.0
150	1.4	2.3	4.0	-1.5	0	2.0	0.4	0.4	0.4	3.5
160	1.5	2.7	4.5	-1.8	0	2.3	0.5	0.5	0.5	4.2
170	1.6	3.0	5.0	-2.2	0	2.7	0.6	0.6	0.6	5.0
180	1.7	3.2	5.3	-2.5	0	3.0	0.7	0.7	0.7	6.0
190	1.7	3.4	5.6	-3.0	0	3.2	0.8	0.8	0.8	6.5
200	1.7	3.5	6.0	-3.5	0	3.4	0.9	0.9	0.9	6.6
210	1.6	3.6	6.0	-4.0	0	3.5	1.0	1.0	1.0	6.7
220	1.5	3.8	6.0	-4.5	0	3.6	1.1	1.1	1.1	7.0
230	1.3	3.9	6.0	-5.0	0	3.8	1.2	1.2	1.2	7.2
240	0.9	4.0	5.9	-5.3	0	3.9	1.3	1.3	1.3	7.4
250	0.5	4.1	5.8	-5.7	0	4.0	1.4	1.4	1.4	7.4
260	0.25	4.1	5.7	-6.0	0	4.1	1.5	1.5	1.5	7.5
270	0	4.0	5.7	-6.3	0	4.1	1.6	1.6	1.6	7.5
280	-0.4	3.9	5.4	-6.7	0	4.0	1.7	1.7	1.7	7.5
290	-0.8	3.8	5.2	-7.0	0	3.9	1.8	1.8	1.8	7.4
300	-1.2	3.7	5.0	-7.5	0	3.8	1.9	1.9	1.9	7.3
						3.7	2.0	2.0	2.0	7.2

\* From: C. C. I. R. report 238-2, Vol. 5, Geneva 1974.

Eq. (2) is useful for all values of the asymmetry parameter  $s = \alpha_0/\beta_0$  illustrated in Figure 3. For  $\theta d > 10$ , Eq. (3) is limited to  $0.7 \leq s \leq 1.0$ .

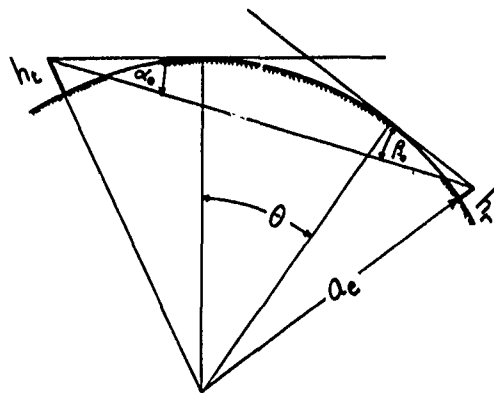


Figure 3. Geometry for the Asymmetry Parameter  $s = \alpha_0/\beta_0$

The  $F(\theta d)$  functions were said to be useful for 'most land-based scatter links'.<sup>8</sup> Some of the following computations were made for a continental temperate climate (#6) over a land path. Others were made for a maritime temperate climate over a sea path (#7b) using the above  $F(\theta d)$  equations. For the latter type of propagation path, a frequency dependent  $g(f)$  - factor that modifies the variability estimates appears to be lacking.<sup>9</sup> In these computations it was assumed for climate #7b that  $g(f) = 1$ .

Figure 4 illustrates the two-way median path attenuation in dB relative to free space for a continental temperate climate (#6) as a function of frequency (10 to 1000 MHz) and distance (100, 200, 300, 1000 km). For  $d = 100$  km, a 38 dB height gain is achieved by elevating both antennas from  $h_t = h_r = 0$  to 100 m.

The expected path-attenuation variability relative to  $A(50)$  depends on effective distance and climate. The variability of transmission loss and its variation with effective distance is usually plotted as a family of curves for selected percentages of  $q$  which indicates the percentage in time that a particular level relative to the median is exceeded. For a range of effective distances  $10 \leq d_e \leq 300$  km, Tables 2, 3, and 4 were prepared from curves<sup>9</sup> for a maritime temperate climate #7b.

8. Rice, P. L., Longley, A. G., Norton, K. A., and Barsis, A. P. (1966) Transmission Loss Predictions for Tropospheric Communication Circuits, National Bureau of Standards, Technical Note 101, Vol. 2, III-24, revised May 1966.

9. C. C. I. R. Report 238-2, Propagation data required for trans-horizon radio-relay systems, XIII Plenary Assembly, Geneva, (1974) Vol. V, Propagation in Non-Ionized Media, pp 209-229.

Over a sea path, the range of variation between the 1% and 99% level can amount to 24 dB at  $d = 100$  km and 54 dB at  $d = 200$  km.

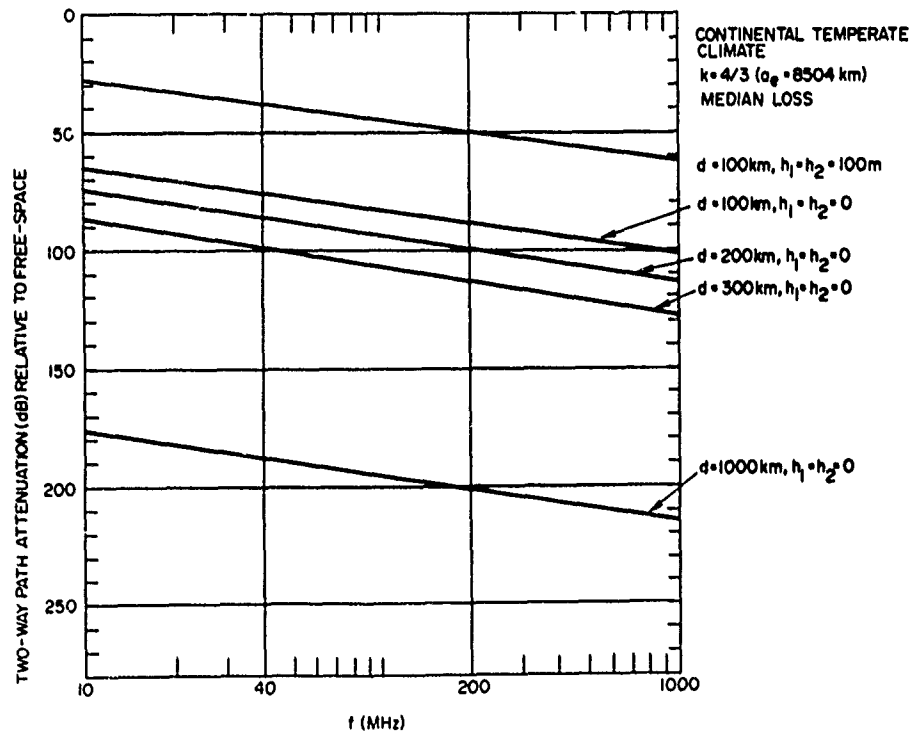


Figure 4. For Tropospheric Transhorizon Propagation, the Two-way Median Path Attenuation, in dB, Relative to Free Space as a Function of Frequency, Parametric With Distance for Pairs of Equal Antenna Heights, Standard Refraction, and Continental Temperate Climate

Figure 5 illustrates the effects of attenuation variability for a maritime temperate climate on signal-to-noise ratios for a ground-based radar ( $h_t = 0$ ) looking at a ground-based target ( $h_p = 0$ ) 100 km away that has a constant scatter cross section  $\sigma = 17$  m<sup>2</sup>. Although details of Figure 5 will be discussed in the following section, the signal-to-noise ratio percentage contours of availability in time suggest, for example, that on the 99% level, more than 18 dB increase in S/N is needed at 40 MHz to detect a 17 m<sup>2</sup> target at  $d = 100$  km 99% of the time.

In Appendix A, a computer produced set of five plots illustrates for distances of 100, 150, 200, 250, 300 km, the two-way loss in dB as a function of frequency for a maritime climate over sea water (#7b). Each curve corresponds to pairs of equal antenna heights  $h_t = h_r = 0.001, 0.1, 1.0$  km with symbols  $\Delta, X, \nabla$ , respectively. The effective earth radius is  $a_e = 8504$  km, referring to a surface refractivity of  $N_s = 301$ . Missing curves for  $h_t = h_r = 1.0$  km indicate line-of-sight condition.

In Appendix B, a computer produced set of three plots illustrates the two-way loss in dB as a function of distance for climate #7b, parametric in frequency  $f = 10, 40, 100, 200, 500, 1000$  MHz.

Table 2. Look-up Table for Path-Attenuation Variability: Maritime Temperate (7b) Climate Over Sea Path ( $10 \leq d_e \leq 100$  km)

A (q) = A (50) - Y <sub>0</sub> (q)										
d <sub>e</sub> (km)	10	20	30	40	50	60	70	80	90	100
q %	These numbers represent Y <sub>0</sub> (q) in dB									
0.01	0.5	1.2	2.4	3.8	5.5	8.5	10	14	17	22
0.1	0.3	1	2	3	4	6	9	11	14	17
1	0.2	0.5	1.5	2.3	3.0	5	7	8.5	10	13
10	0.1	0.2	0.5	1	1.2	2	3.5	4	5	6
50	0	0	0	0	0	0	0	0	0	0
90	-0.05	-0.15	-0.2	-0.5	-0.8	-1.1	-1.9	-2.5	-4	-5.5
99	-0.07	-0.2	-0.5	-1	-2	-3	-5	-7	-9	-11
99.9	-0.09	-0.3	-0.8	-1.5	-3	-4.5	-6	-10	-13	-16
99.99	-0.1	-0.5	-1	-2	-4	-6	-9	-13	-17	-20

Table 3. Look-up Table for Path-Attenuation Variability: Maritime Temperate (7b) Climate Over Sea Path ( $110 \leq d_e \leq 200$  km)

$A(q) = A(50) - Y_o(q)$										
$d_e$ (km)	110	120	130	140	150	160	170	180	190	200
$q$ %	These numbers represent $Y_o(q)$ in dB									
0.01	25	29	33	37	41	45	48	50	52	53
0.1	20	23	26	29	32	35	38	41	43	45
1	16	19	22	24	26	27	28	29	30	31
10	7.5	9	10	10.5	11	11.5	12	13	14	14.5
50	0	0	0	0	0	0	0	0	0	0
90	-7.5	-9	-10	-10.8	-11.5	-11.8	-12.2	-12.6	-13	-13.5
99	-14	-17	-18	-19.5	-20.5	-21	-21.5	-22.3	-22.8	-23.5
99.9	-19	-22	-25	-26.2	-27.3	-28	-29	-30	-30.6	-31
99.99	-22.5	-25	-28	-31	-33	-33	-34.6	-35.5	-36	-37

Table 4. Look-up Table for Path-Attenuation Variability: Maritime Temperate (7b) Climate Over Sea Path ( $210 \leq d_e \leq 300$  km)

$A(q) = A(50) - Y_o(q)$										
$d_e$ (km)	210	220	230	240	250	260	270	280	290	300
$q$ %	These numbers represent $Y_o(q)$ in dB									
0.01	54	54.4	54.8	55.2	55.5	55.5	55.2	54.8	54.4	54
0.1	45.2	45.4	45.6	45.8	46	45.8	45.6	45.4	45.2	45
1	31.2	31.4	31.6	31.8	32	31.9	31.6	31.2	30.9	30.5
10	14.6	14.7	14.8	14.9	15	15	14.8	14.5	14.2	13.8
50	0	0	0	0	0	0	0	0	0	0
90	-13.8	-14	-14	-13.8	-13.5	-13.4	-13.3	-13.2	-13.1	-13
99	-23.9	-24.3	-24.6	-25	-25	-24.6	-24.1	-23.7	-23.3	-23.2
99.9	-31.3	-31.6	-31.9	-32.2	-32.5	-32.3	-31.8	-31.5	-31.2	-31
99.99	-38	-39.2	-39.2	-39.1	-39	-38.5	-38	-37.6	-37.3	-37

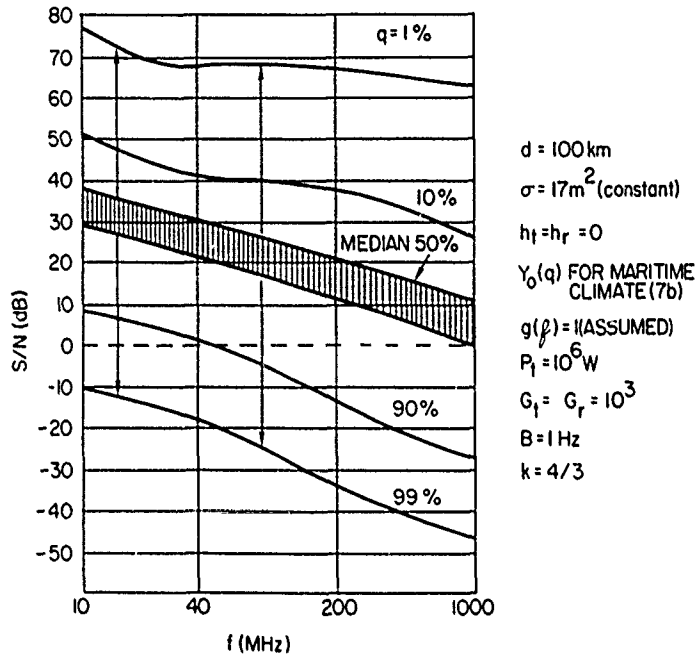


Figure 5. For Tropospheric Transhorizon Propagation, the Signal-to-Noise Ratio, in dB, Available at a Monostatic Radar From a Target, as a Function of Frequency, With Frequency Independent Scattering Cross Section.  $\sigma = 17 \text{ m}^2$  assuming median (50%) loss and 1, 10, 90, 99% predicted variability with indication of the effect of equivalent maximum and minimum galactic noise temperature (shaded).  $d = 100 \text{ km}$ ,  $h_t = h_r = 0$ , variability for maritime climate (#7b) assuming  $g(f) = 1$ , transmitted power  $P_t = 10^6 \text{ W}$ ,  $G_t = G_r = 10^3$ ,  $B = 1 \text{ Hz}$ , standard refraction ( $k = 4/3$ ;  $a_e = 8504 \text{ km}$ )

#### 4. SIGNAL-TO-NOISE RATIO

In the free-space radar equation, the received power  $P_r$ , which is synonymous to a signal  $S$ , is the result of a product of three terms. The first term yields the power density at a distance  $d$  from the radar transmitter where a target is encountered with a scattering cross section  $\sigma$ . In the second term, the gain of the scatterer is assumed as unity; the scattered power is then radiated isotropically and yields the power density at a receiving location  $d$  kilometers from the target. The third term signifies the effective area of the receiving antenna.

$$P_r = S = \left( \frac{P_t G_t}{4\pi d^2} \right) \left( \frac{\sigma}{4\pi d^2} \right) \frac{G_r \lambda^2}{4\pi} \quad (6)$$

A tropospheric transhorizon detection capability is related to tropospheric inhomogeneities which deflect the incident signal. In the process of deflection, the signal encounters a loss. In the radar equation, the square of a loss term A is introduced. A is called path attenuation and its assessment was described above.

Noise power depends on the effective temperature T (°K) of an antenna receiving galactic noise, the receiver bandwidth B(Hz) and the receiver noise figure F.<sup>10</sup> If signal detection within the receiver is achievable when the signal power is twice the noise power, it follows that F = 2, which corresponds to a noise figure of 3 dB. For a receiver noise figure of 10 dB, the signal power has to be ten-times the noise power for detection. Based on the above, the equation for the signal-to-noise ratio can be written as follows:

$$S/N = \frac{P_t G_t G_r \sigma \lambda^2}{(4\pi)^3 d^4 A^2 k T B (F-1)} \quad (7)$$

where

- $P_t$  is transmitter power (W)
- $G_t$  is transmitting antenna gain
- $G_r$  is receiving antenna gain
- $\sigma$  is scattering cross section of target (m<sup>2</sup>)
- $\lambda$  is wavelength (m)
- d is distance between terminals (m)
- $A^2$  is two-way path attenuation
- k is Boltzmann's constant ( $1.38 \times 10^{-23}$  J/°K/Hz)
- T is effective temperature of an antenna receiving galactic noise (°K)
- B is receiver bandwidth (Hz)
- F is receiver noise figure

Regarding the numerical values to be used for the equivalent temperature in the equation for S/N, it was assumed that the controlling influence is due to galactic noise.<sup>11, 12, 13</sup> This assumption is probably reasonable in the VHF band if man-made noise can be minimized when siting a radar. At frequencies above 0.7 GHz, noise due to radiation from the atmosphere is likely to exceed the galactic noise level<sup>10</sup> particularly for low elevation angles for which the equivalent atmospheric temperatures could be larger than galactic temperatures by a factor of 3 at 1 GHz and 100 at 4 GHz. For selected frequencies of interest, Table 5 provides look-up values for galactic noise equivalent maximum and minimum temperatures.

(Due to the large number of references cited above, they will not be listed here. See References, page 29.)

Table 5. Look-up Table for Galactic Noise: Equivalent Temperature (Effective temperature of an antenna receiving galactic noise)

Frequency	Wavelength	Temperature	
		Minimum	Maximum
f (MHz)	$\lambda$ (m)	$T_{\min}$ °K	$T_{\max}$ °K
10	30	$10^5$	$5 \times 10^5$
40	7.5	7000	$5 \times 10^4$
100	3.0	800	7000
200	1.5	125	1600
500	0.6	8	190
1000	0.3	3	35

Sources: Baghdady 1961  
 David & Voge 1969  
 C. C. I. R. Rep. 342-2  
 Kraus & Ko (May 1957)

For a median path attenuation typical of a continental temperate climate (#6), the S/N equation was used to illustrate in Figure 6 the effect of three different target characteristics and min/max noise temperatures on the behavior of S/N with frequency. The following values were used: Distance between terminals  $d = 100$  km; effective antenna heights  $h_t = h_r = 0$ ; transmitter power  $P_t = 1$  MW; antenna gains  $G_t = G_r = 1000$ ; receiver bandwidth  $B = 1$  Hz, effective earth radius  $a_e = 8504$  km corresponding to a surface refractivity of  $N_s = 301$ .<sup>14</sup> Computations were performed for min/max noise temperatures of Table 5 and for three types of target cross section  $\sigma$ : (a)  $\sigma = 17 \text{ m}^2$  is independent of frequency, (b)  $\sigma$  is due to a metal sphere with a diameter of 2.4 m which is resonant at 40 MHz when  $\sigma = 17 \text{ m}^2$ , (c) the target is represented by a resonant dipole with a scatter cross section  $\sigma = 0.7 \lambda^2$ . In this particular example a systems parameter ratio can be computed as  $\text{SPR} = \frac{P_t G_t G_r}{B (F-1)} = 10^{12}$ . If different systems parameters are used resulting, for example, in a ratio of  $10^7$ , the curves of Figure 6 could simply be lowered by 50 dB ( $10 \log 10^{12}/10^7$ ), or the dashed line for S/N = 0 could be raised to 50 dB. For this case, all targets would be undetectable for maximum galactic noise over the displayed frequency band.

14. Panter, P. F. (1972) Communication Systems Design, Line-of-Sight and Troposcatter Systems, McGraw-Hill Book Co., New York.

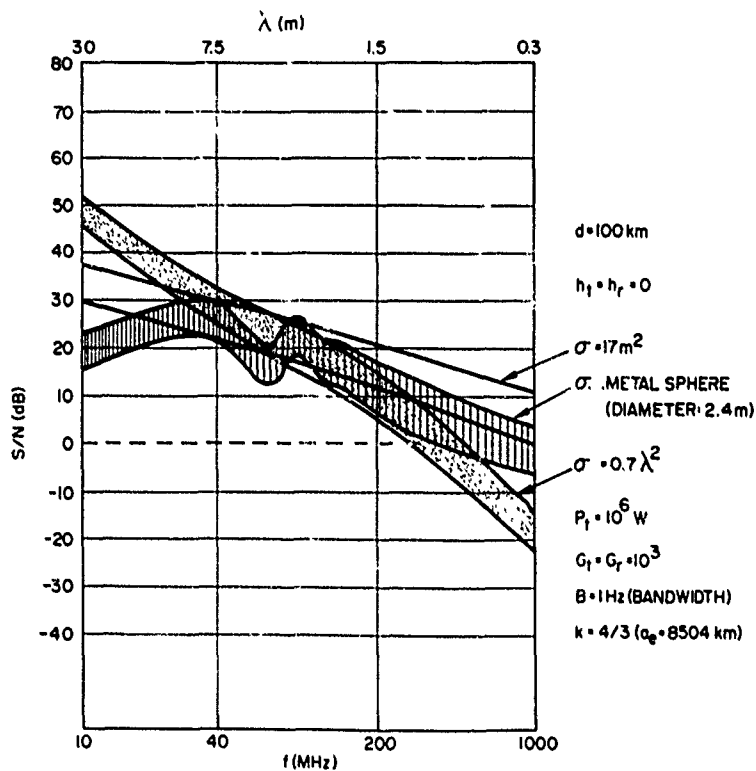


Figure 6. For Tropospheric Transhorizon Propagation, the Signal-to-Noise Ratio, in dB, Available at a Mono-static Radar From Three Different Types of Targets, as a Function of Frequency. (a)  $\sigma = 17 \text{ m}^2$ , (b)  $\sigma$  due to metal sphere of 2.4 m diameter, (c)  $\sigma = 0.7 \lambda^2$ ;  $d = 100 \text{ km}$ ,  $h_t = h_r = 0$ , median loss for temperate climate #6;  $P_t = 10^6 \text{ W}$ ,  $G_t = G_r = 10^3$ ,  $B = 1 \text{ Hz}$ , standard refraction ( $k = 4/3$ ;  $a_e = 8504 \text{ km}$ ); maximum and minimum galactic noise temperature

For the same systems parameter ratio of  $10^{12}$ , climate #6 and min/max galactic noise, but for a composite scatter cross section with  $\sigma = 17 \text{ m}^2$  (constant) for  $f \geq 40 \text{ MHz}$  and an assumed  $\lambda^{-4}$  dependence to estimate  $\sigma$  at 10 MHz, Figure 7, illustrates for median path attenuation the signal-to-noise ratio variation with frequency, for three distances and several effective transmitting and receiving antenna height combinations. The computations were made at 10, 40, 200 and 1000 MHz. Intermediate values were visually interpolated. If, at  $d = 100 \text{ km}$ , both antenna heights are elevated from  $h_t = h_r = 0$  to  $h_t = h_r = 100 \text{ m}$ , a gain of 35 dB is achieved. The height gain would be only 15 dB if one antenna remains at  $h = 0$ .

This is illustrated for  $d = 100$  km at  $f = 40$  MHz where, starting at the S/N value for the cosmic noise minimum,  $h_t$  remains zero while  $h_r = 0, 20, 50, 100, 200$  m.

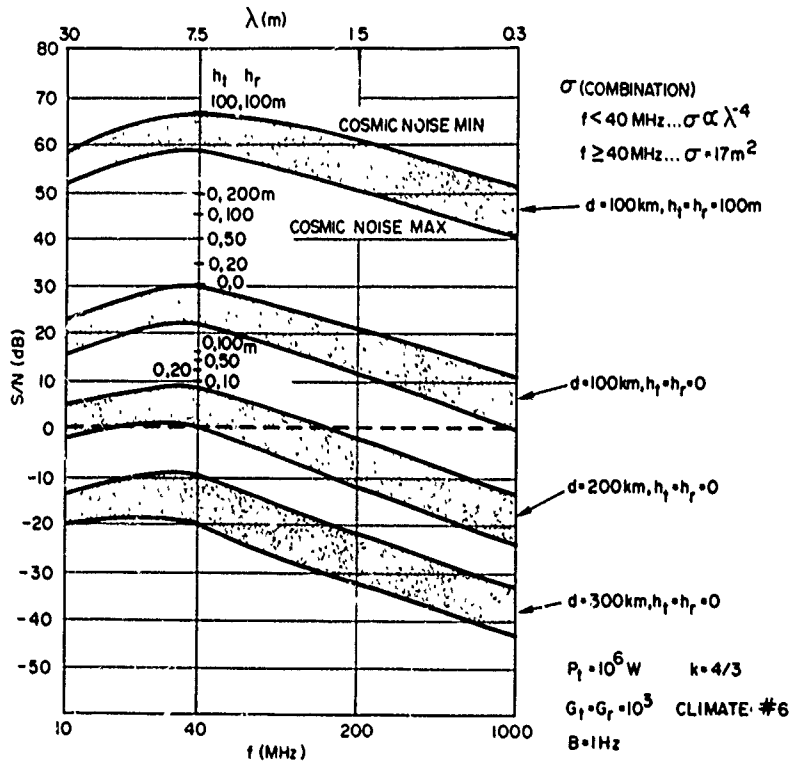


Figure 7. For Tropospheric Transhorizon Propagation, the Signal-to-Noise Ratio, in dB, Available at a Mono-static Radar From a Composite Target. Target is with  $\sigma \propto \lambda^{-4}$  for  $f < 40$  MHz and  $\sigma = 17 \text{ m}^2$  (constant) for  $f \geq 40$  MHz, parametric in distance, height including asymmetry conditions; median loss for temperate climate #6; the shaded width of curves signifies minimum and maximum noise temperature.  $P_t = 10^6 \text{ W}$ ,  $G_t = G_r = 10^3$ ,  $B = 1 \text{ Hz}$ , standard refraction ( $k = 4/3$ ;  $a_e = 8504 \text{ km}$ )

While these computations were performed on a desk calculator, a comprehensive set of computer produced plots is given in Appendices C to F. These computer generated results were obtained for a maritime temperate climate #7b. To avoid an overcrowding of curves, results were plotted only for maximum galactic noise temperatures. The minimum noise temperature raises S/N by about 10 dB

above that for  $T_{\max}$ . Distances range from 100 to 300 km in 50 km increments. Transmitting antenna heights were judiciously limited to 0.001, 0.1, and 1.0 km. Eleven receiving antenna heights were chosen in 0.05 km height increments starting at zero. The missing of data points for large antenna heights is related to approaching or achieving line-of-sight propagation which makes the scattering angle small, zero or negative. Table 6 illustrates the line-of-sight distances between elevated antennas computed for an effective earth radius  $a_e = 8504$  km. These distances may be compared with the combinations of antenna heights and distance of the computations. In Appendix C, using the median loss A (50) in the radar equation, the signal-to-noise ratio (dB) is plotted as a function of frequency for fixed distances, transmitting antenna heights, and a combination of receiving antenna heights.

Table 6. Line-of-Sight Distances  $d$  [km] Between Elevated Antennas, Computed for a Curved Earth of Radius  $a_e = 8504$  km.

$$(d = d_{Lt} + d_{Lr} = (2 a_e h_t)^{1/2} + (2 a_e h_r)^{1/2})$$

		$h_r$ (km)											
		0	0.001	0.01	0.1	0.5	1.0	2.0	3.0	4.0	5.0	6.0	10.0
$h_t$ [km]	0	0	4	13	41	92	130	184	225	260	291	319	412
	0.001	4	8	17	45	96	134	188	229	264	295	323	416
	0.01	13	17	26	54	105	143	197	238	273	302	330	423
	0.1	41	45	54	82	133	171	225	266	301	332	360	453
	0.5	92	96	105	133	184	222	276	317	352	383	411	504
	1.0	130	134	143	171	222	260	314	355	390	421	449	542
	2.0	184	188	197	225	276	314	368	409	444	475	503	596
	3.0	225	229	238	266	317	355	409	450	483	516	544	637
	4.0	260	264	273	301	352	390	444	485	520	551	579	672
	5.0	291	295	302	332	383	421	475	516	551	582	610	703
	6.0	319	323	330	360	411	449	503	544	579	610	638	731
10.0	412	416	423	453	504	542	596	637	672	703	731	824	

In Appendix D, the variability in S/N is illustrated for similar conditions as were employed before, except  $h_t$  and  $h_r$  were made to be equal in pairs of values 0.001, 0.1, 1.0 km, while  $q$  values varied from 1, 10, 50, 90, 99% of signal-to-noise level availability. The extent of variability was found to vary with distance. Increased availability of a detectable signal in percent of time requires system parameter adjustments. If for example, at 40 MHz and for  $d = 250$  km, a 50% availability of a detectable signal is to be raised to a 99% availability, the system parameter ratio would need to be increased by 50 dB.

For the indicated system parameters, scattering cross-sections, antenna heights, and median loss for a maritime climate, Appendix E displays the variation of S/N with distance parametric in frequency. For  $f \geq 40$  MHz, the scattering cross section varies with wavelength as  $\sigma = 0.7 \lambda^2$ . For  $f < 40$  MHz,  $\sigma$  is assumed to vary approximately with  $\lambda^{-4}$ . Because of this choice for  $\sigma(f)$ , the signal-to-noise ratio is largest at 40 MHz.

In Appendix F the set of plots for probabilities  $q(1, 10, 50, 90, 99\%)$  is similar to those of Appendix D except the signal-to-noise ratio is plotted as a function of distance instead of frequency. Each set of curves corresponds to one frequency. This frequency is identified in the Input Data underneath the transmitter power  $P_t$ .

## 5. AVAILABLE BANDWIDTH AND COHERENCE TIME

Over a tropospheric propagation path, signal fading may be correlated with movements in the atmosphere. These movements may be due to a mean wind velocity, especially when the fading rate is fast. While the fading period may intermittently limit the duration of signal reception, bandwidth limitations are imposed by path delay times which when received by an FM receiver, will introduce in the output from the receiver baseband an intermodulation noise. The level of this noise depends not only on actual delay involved but also on the width of the transmitted spectrum. The maximum baseband width  $f_m(\max) = 0.22/\tau$  where  $\tau$  is the echo time delay.<sup>14</sup> Since path delays on troposcatter circuits are larger for broader antenna beams, the longest path delays can be reduced and the available bandwidth be increased by using high-gain, narrow-beam antennas.<sup>6</sup> Tentative estimates for the usable frequency band as a function of range and free-space antenna gains ( $25 \text{ dB} \leq G \leq 55 \text{ dB}$ ) were derived from 1 to 2 GHz test links<sup>15</sup> as illustrated in Figure 8. Bandwidth formulas for very narrow and broad antenna beams have been derived.<sup>16</sup> Using the formula for a broad antenna beamwidth of  $5^\circ$  and assuming  $d = 300$  km for a tropospheric scattering circuit, an available bandwidth of 4 MHz is obtained. This bandwidth implies a differential delay in transmission of about 1 microsecond. Relatively large values for bandwidth are also predicted in Figure 8.

While the differential delay limits the rate of data transmission, the coherence time of a transmission, which may differ from the fading period, places limits on phase coherent integration which may be needed if the signal requires enhancement

15. Picquenard, A. (1974) Radio Wave Propagation, A Halstead Press Book, John Wiley & Sons, New York, p. 298.

16. Gerks, I. H. (1955) Factors affecting spacings of radio terminals in a UHF link, Proc. IRE 43(10):1290-1297.

for detection. For a tropospheric transhorizon transmission, the coherence time could be estimated from backscatter observations of turbulence in the troposphere and stratosphere made with the sunset radar.<sup>17</sup> This coherence time is likely to vary with meteorological conditions along a propagation path. The 40.76 MHz backscatter radar observations of atmospheric irregularities between 4 and 19 km altitude showed Doppler velocity spectral widths ranging from 1 to 2 Hz which could be interpreted in terms of a 1/2- to 1-sec coherence time. For oblique transmissions, coherence times may be of the same order of magnitude. They may vary with time, depending on the meteorological condition and the propagation mechanism.

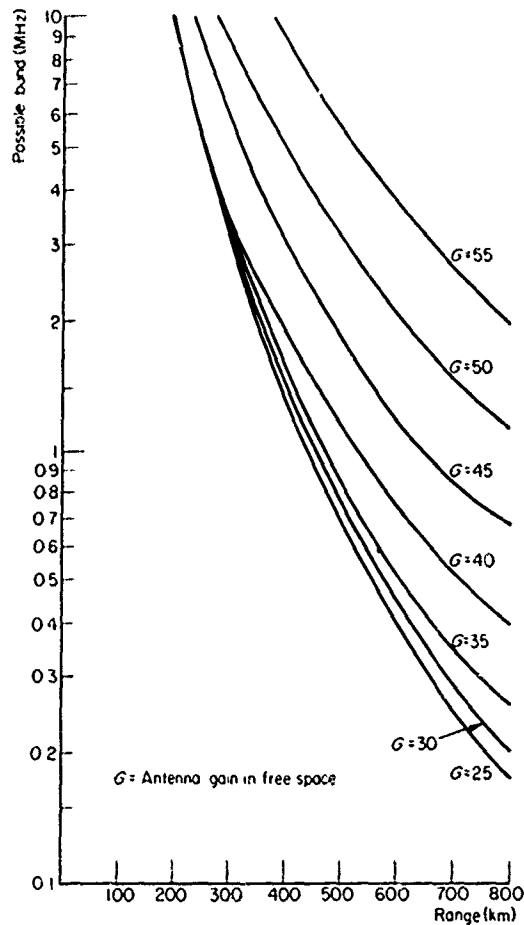


Figure 8. Tentative Estimate of the Usable Frequency Band of a Tropospheric Transhorizon Propagation Link as a Function of Range for Several Values of Free-space Antenna Gains. (Source: A. Picquenard "Radio Wave Propagation" John Wiley & Sons, New York, 1974)

17. Gage, K.S., and Balsley, B.B. (1978) Doppler radar probing of the clear atmosphere, Bulletin, American Meteorological Society, 59(9):1074-1093.

## 6. CLUTTER FACTOR

The clutter factor method appears to be used in the equation for the transmission factor applicable to terrestrial line-of-sight paths.<sup>6</sup> The equation for the transmission factor K is:

$$K = \frac{1}{L} \cdot \frac{P_r}{P_t} = G_t G_r \left( \frac{h_t h_r}{d^2} \right)^2 \beta \quad (8)$$

where

- L is transmission loss
- $h_t, h_r$  is antenna heights
- $G_t, G_r$  is antenna gains
- $P_r$  is received power
- $P_t$  is transmitted power
- d is distance
- $\beta$  is clutter factor ( $\beta < 1$ ).

The clutter factor  $\beta$  includes the losses relative to a smooth plane earth due to terrain irregularities, buildings and trees causing shadowings, absorption and scattering of the radio energy. Figure 9 shows the clutter factor dependence on frequency.<sup>6</sup> For a rural area, the clutter factor  $\beta$  approaches unity at 40 MHz.

## 7. CONCLUSION

Losses due to path attenuation along tropospheric transhorizon propagation paths have been estimated using prediction methods available in the open literature. Some of the estimates were made for a continental temperate climate over a land path and for a maritime temperate climate over a sea path. The product of distance and scatter angle was the input for computing the attenuation function for a particular value of surface refractivity. Combined with other terms including distance and frequency, the two-way path attenuation was evaluated. This value was entered into the radar equation. Effective antenna noise temperatures were assumed to be of galactic origin. For selected system parameters of radiated power, antenna gains, bandwidth, receiver noise figure, and specified target cross-sections, signal-to-noise ratios were computed and plotted for up to six frequencies (10 to 1000 MHz), nine distances (50 to 1000 km), a combination of three transmitting antenna heights (0.001, 0.1, 1.0 km) and up to eleven receiving antenna (target) heights (zero to

0.5 km in 0.05 km increments). In these computations, the lowest possible elevation angle of a ray originating from the transmitting antenna was used, thus minimizing the loss rate in dB/km of distance. If the elevation angle of an antenna beam above horizontal adds to 1° or 2°, an increase in the loss rate by about 0.05 dB/km can be expected. For the signal-to-noise ratio computations contained in Appendices C to F, a systems parameter ratio (SPR) =  $(P_t G_t G_r / B(F-1))$  was chosen as  $10^{12}$ .

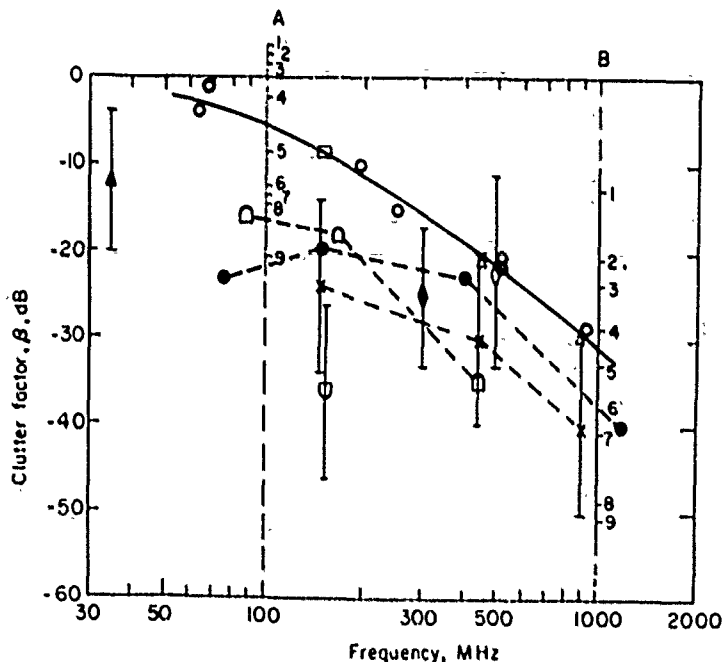


Figure 9. Variation of Clutter Factor  $\beta$  With Frequency Derived From Experimental Studies and From C. C. I. R. (Comité Consultatif International des Radiocommunications) Predictions. (Source: M. P. M. Hall, "Effects of the Troposphere on Radio Communication", Peter Peregrinus, Ltd. IEE London and New York, 1979)

Under the assumptions made, the ordinate scale characterizes the detectability of a target for the specified frequency dependent cross-section. Thus, for other values of SPR (or of the product of SPR and  $\sigma$ ) a simple scale adjustment can be made by computing the ratio of the new SPR to  $10^{12}$ , taking the  $\log_{10}$  of this ratio, multiplying by 10. If the resulting number is negative (for example - 50 dB), the dashed line corresponding to  $S/N = 0$  dB is moved in the direction of positive dB values (for example, to + 50 dB). The charts lend themselves also to the selection

of other information such as maximum range of detection as a function of SPR,  $\sigma$ ,  $h_t$ ,  $h_r$ ,  $d$ ,  $a_e$ ,  $V(d_e)$ , depending on the choices appropriate for the terrain, climate, receiver noise figure, man-made noise level, antenna beam widths, and so on. It is also possible to infer the expected loss rate in dB/km or dB/MHz as a function of distance and antenna heights. Height-gain effects are distance dependent. At larger distances, the rate of change of height-gain tends to increase more markedly at larger heights, whereas, at shorter distances from the transmitting antenna, it increases more markedly at lower heights. It should be remembered that the lines connecting the computed points represent interpolations.

## 8. RECOMMENDATIONS

S/N ratio computations were made for the lowest possible elevation angle over a smooth earth. In practice, elevation angles may be several degrees above the horizontal. If scatter is the dominant propagation mode, the scatter angle would increase and with it the path attenuation. Terrain features, which necessitate the use of several degrees in elevation angle of the antenna beam, should be avoided.

Since the loss prediction method used in this report was derived from trans-horizon data involving all possible propagation mechanisms, a large variability in signal strength is to be expected. If scattering from tropospheric irregularities is the preferred mode of propagation, perhaps because of a possibly permanent presence of such irregularities in the troposphere, and if this particular type of mode is to be further exploited because of this permanence, some thought should be given to the planning of an experiment that maximizes the scatter mode. Then, it may be possible to relate theoretical predictions for scatter propagation to the experimental data which maximize the mode predicted by this theory. On the other hand, one may also wish to consider utilizing for the detection of targets any mode that happens to be dominant.

From the point of view of a large data rate and available bandwidth of which the latter is controlled by the differential delay of the transmission incurred in scatter propagation, it may be advantageous to search for optimum frequencies making a compromise between bandwidth and loss. Extremely high antenna gains which minimize the differential delay and maximize the available bandwidth, are best achieved for the highest frequency. Propagation losses are minimized, however, the lower the frequency. Other limiting factors will be the temperature of the atmosphere at the upper UHF frequencies, and the electromagnetic noise power at lower HF/VHF. Moreover, the frequency characteristic of the cross section of targets may also be a determining factor in the optimal choice of operating frequency.

## References

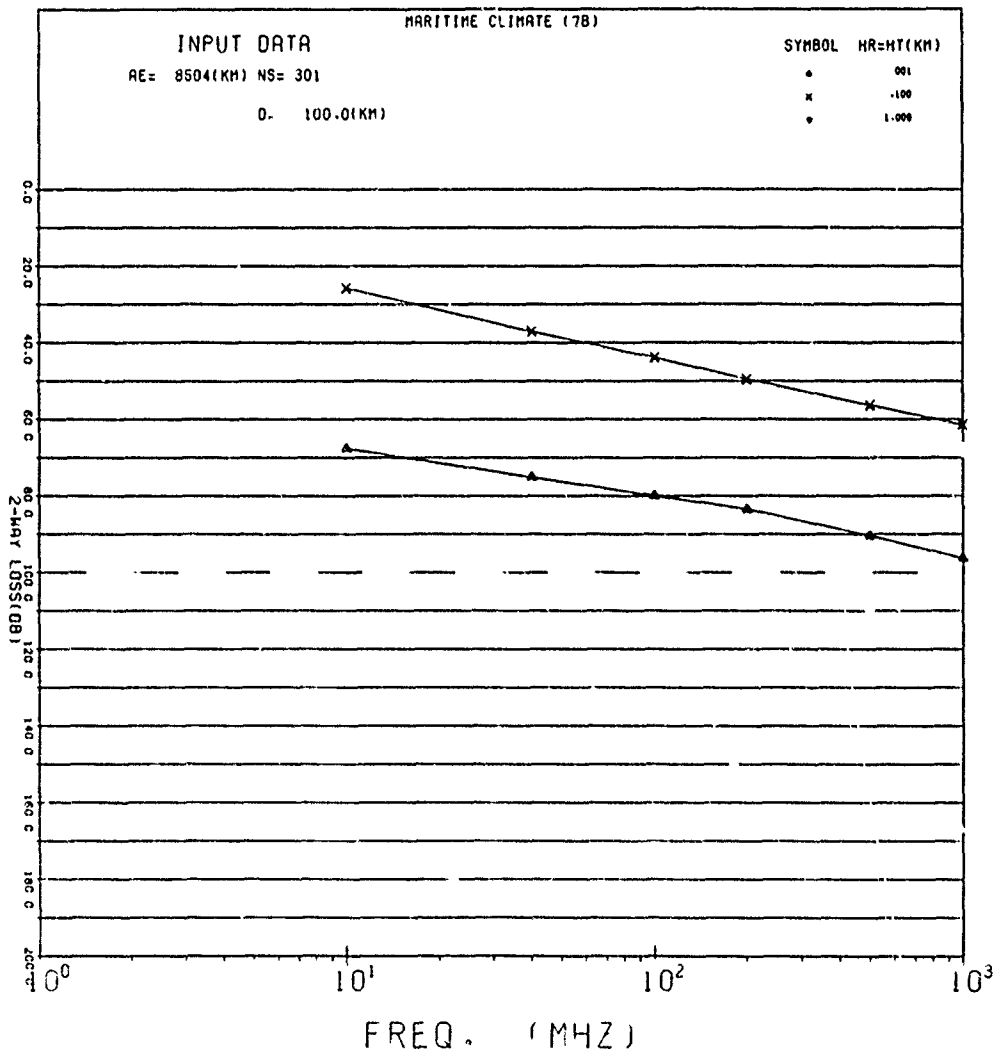
1. Ishimaru, A. (1978) Wave Propagation and Scattering in Random Media, Vol. 1, Academic Press, New York.
2. IEEE Standard Definitions of Terms for Radio Wave Propagation, IEEE Std. 211-1977; IEEE, New York, New York.
3. C. C. I. R. Recommendation 310-3, Definitions of terms relation to propagation in the troposphere, XIIIth Plenary Assembly, Geneva, 1974, Vol. 5 Propagation in Non-ionized Media, p 63-64.
4. Rice, P. L., Longley, A. G., Norton, K. A., and Barsis, A. P. (1966) Transmission-Loss Predictions for Tropospheric Communication Circuits, National Bureau of Standards, Technical Note 101, Vol. 1, 9-1, revised May 1966.
5. Toman, K. (1952) An Investigation of Tropospheric Propagation, U. of Illinois, Urbana, Phd Thesis.
6. Hall, M. P. M. (1979) Effects of the Troposphere on Radio Communication, Peter Peregrinus Ltd., IEE London and New York, p. 137.
7. C. C. I. R. Report 244-1, Estimation of tropospheric-wave transmission loss, Documents of the XIth Plenary Assembly, Oslo, (1966) Vol. 1, Propagation; pp. 143-167.
8. Rice, P. L., Longley, A. G., Norton, K. A., and Barsis, A. P. (1966) Transmission Loss Predictions for Tropospheric Communication Circuits, National Bureau of Standards, Technical Note 101, Vol. 2, III-24, revised May 1966.
9. C. C. I. R. Report 238-2, Propagation data required for trans-horizon radio-relay systems, XIII Plenary Assembly, Geneva, (1974) Vol. V, Propagation in Non-ionized Media, pp 209-229.
10. David, P., and Voge, F. (1969) Propagation of Waves, Pergamon Press Ltd., London.
11. Baghdady, E. J. (1961) Communication System Theory, McGraw-Hill Book Co., Inc., New York, p 587.

## References

12. Kraus, J. D., and Ko, H. C. (1957) Celestial radio radiation, RF Project 673, Scientific Report No. 1, The Ohio State University Research Foundation, Columbus, Ohio, May, p: 51.
13. C. C. I. R. Report 342-3, Radio noise within and above the ionosphere, Documents of the XIVth Plenary Assembly, Kyoto, (1978) Vol. 6, Propagation in Ionized Media, pp. 103-114.
14. Panter, P. F. (1972) Communication Systems Design, Line-of-Sight and Troposcatter Systems, McGraw-Hill Book Co., New York.
15. Picquenard, A. (1974) Radio Wave Propagation, A Halstead Press Book, John Wiley & Sons, New York, p. 298.
16. Gerks, I. H. (1955) Factors affecting spacings of radio terminals in a UHF link, Proc. IRE 43(10):1290-1297.
17. Gage, K. S., and Balsley, B. B. (1978) Doppler radar probing of the clear atmosphere, Bulletin, American Meteorological Society, 59(9):1074-1093.

## Appendix A

Five Plots of Two-way Loss (dB) vs Frequency (MHz)



MARITIME CLIMATE (7B)

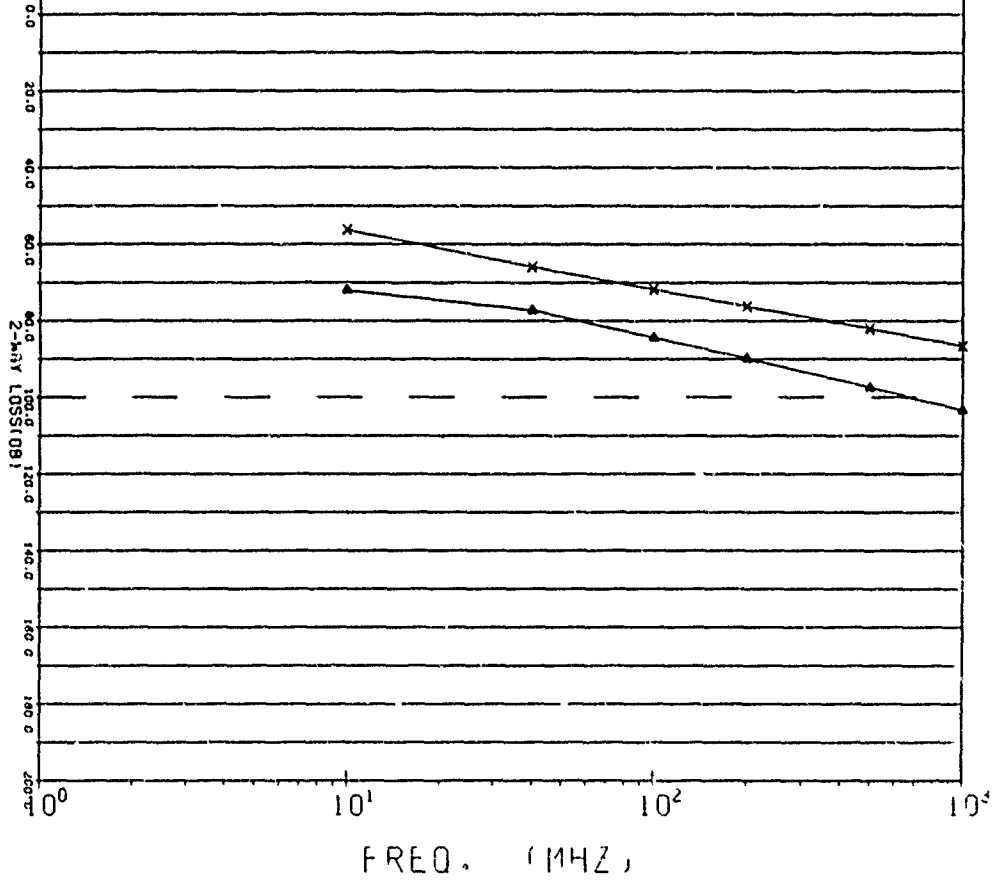
INPUT DATA

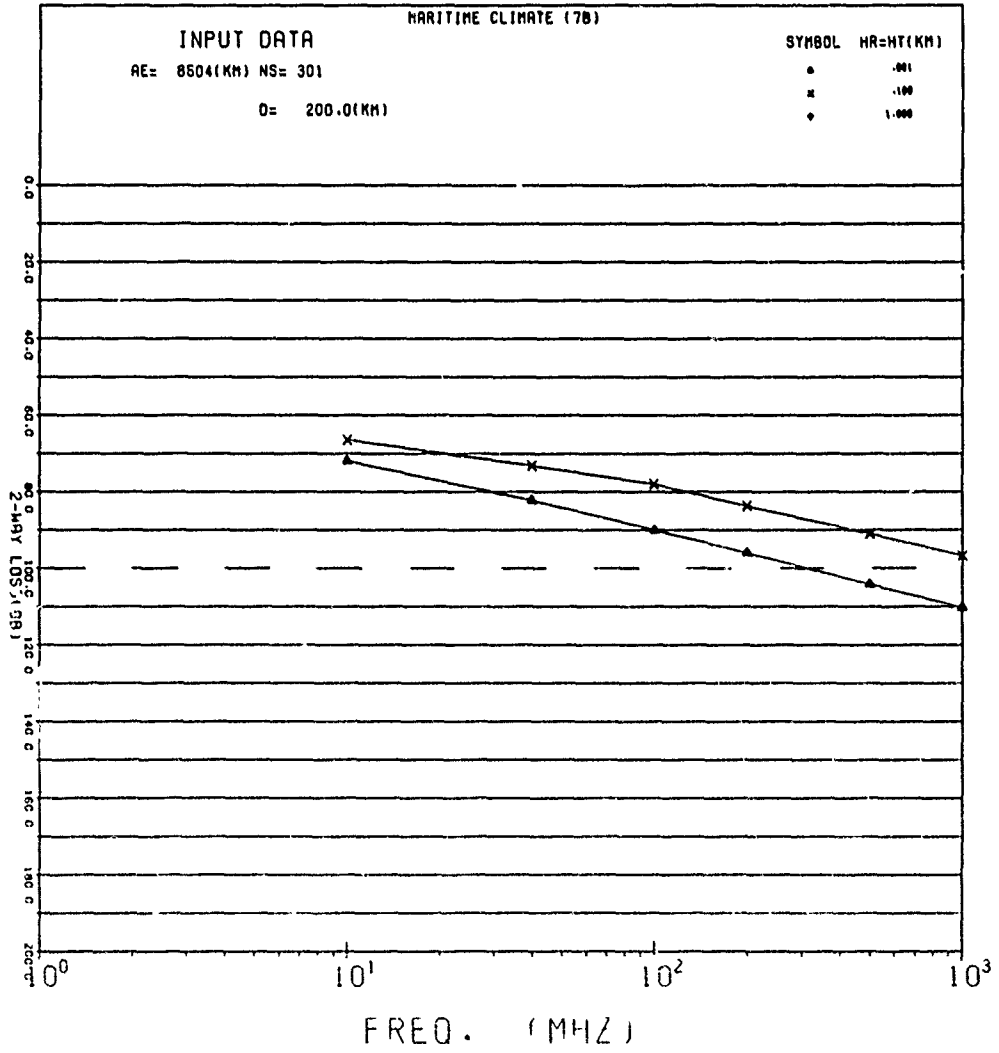
RE= 8504(KM) NS= 301

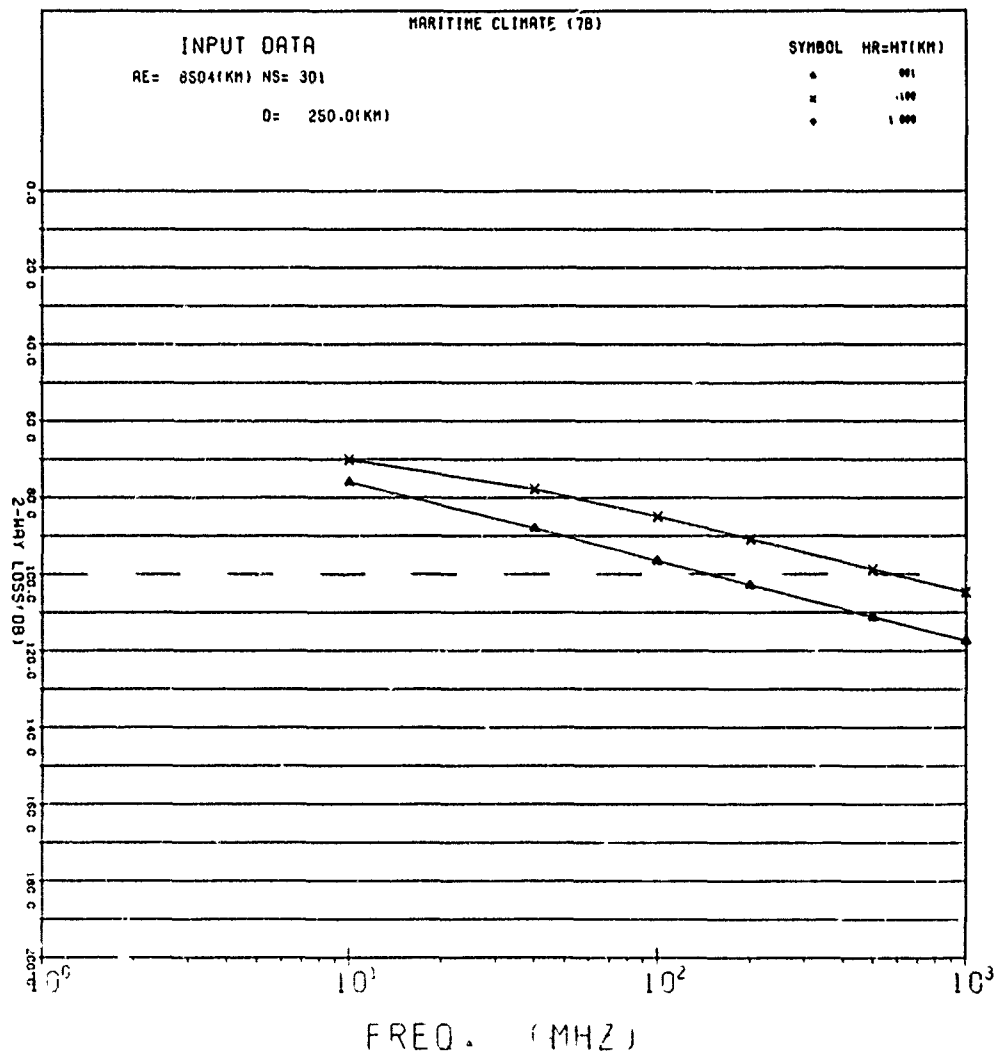
D= 150.0(KM)

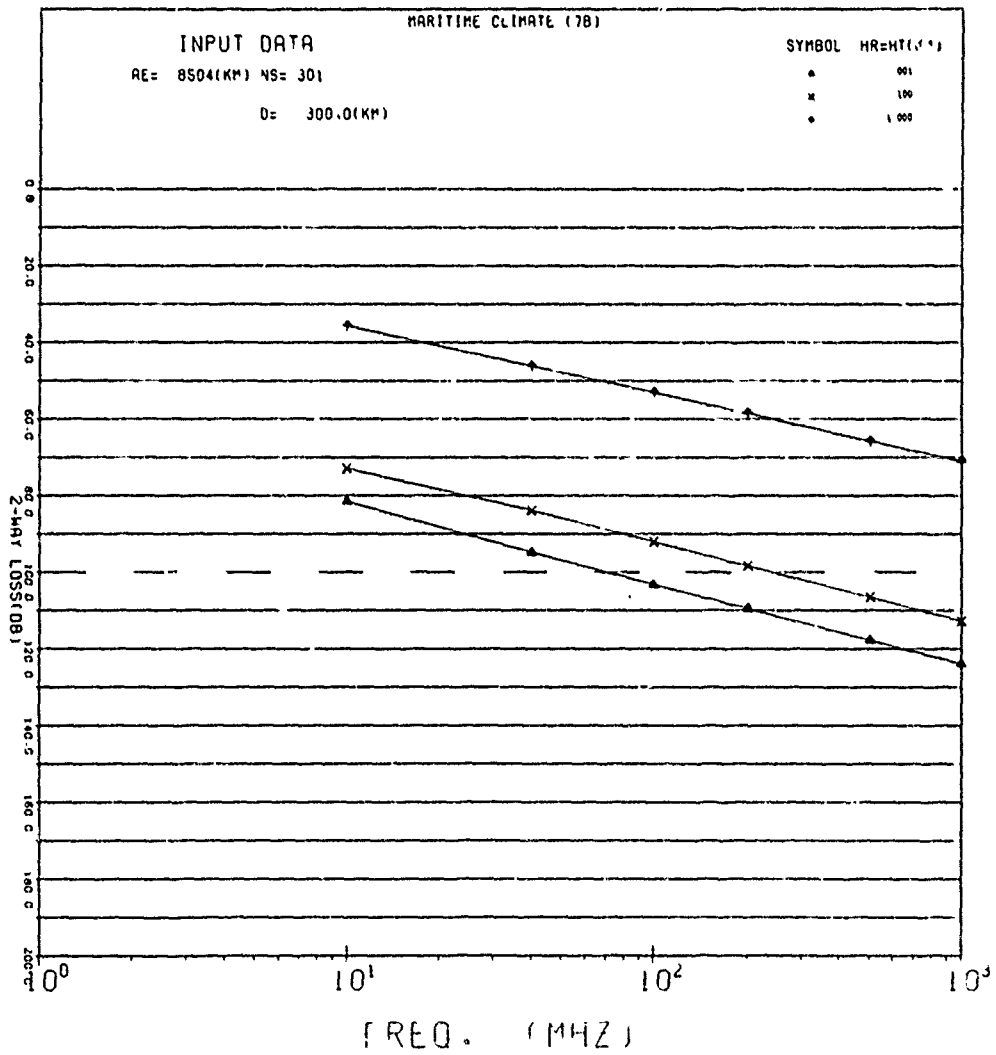
SYMBOL HA=HT(KM)

• .001  
 x .100  
 ◊ 1.000



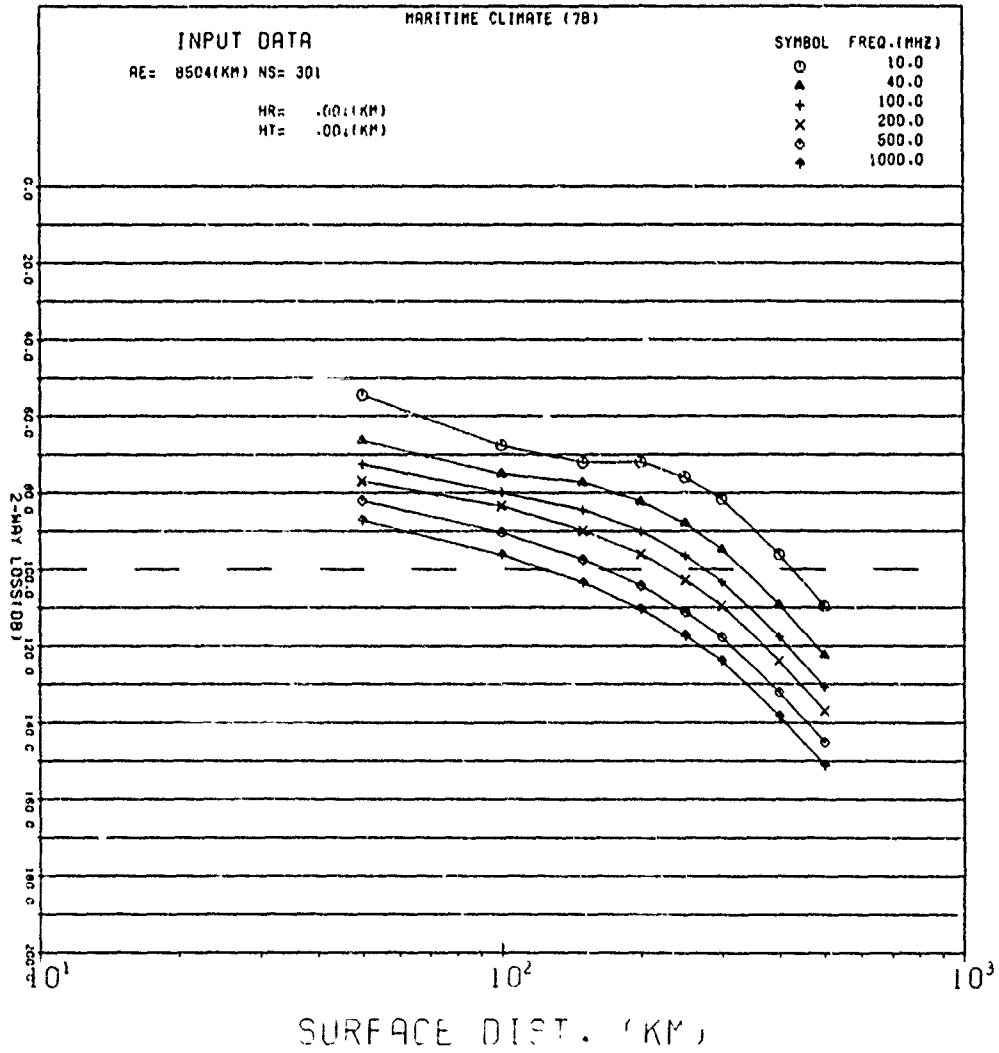


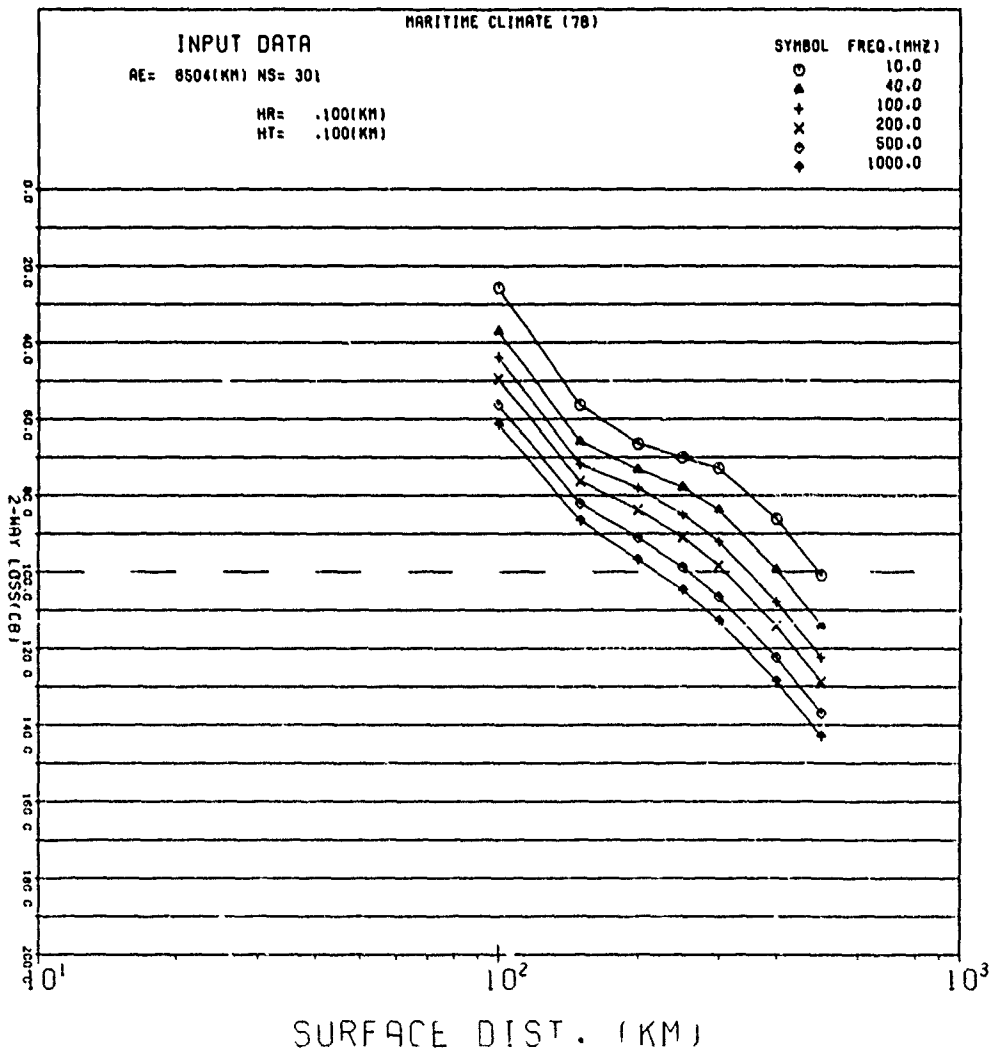


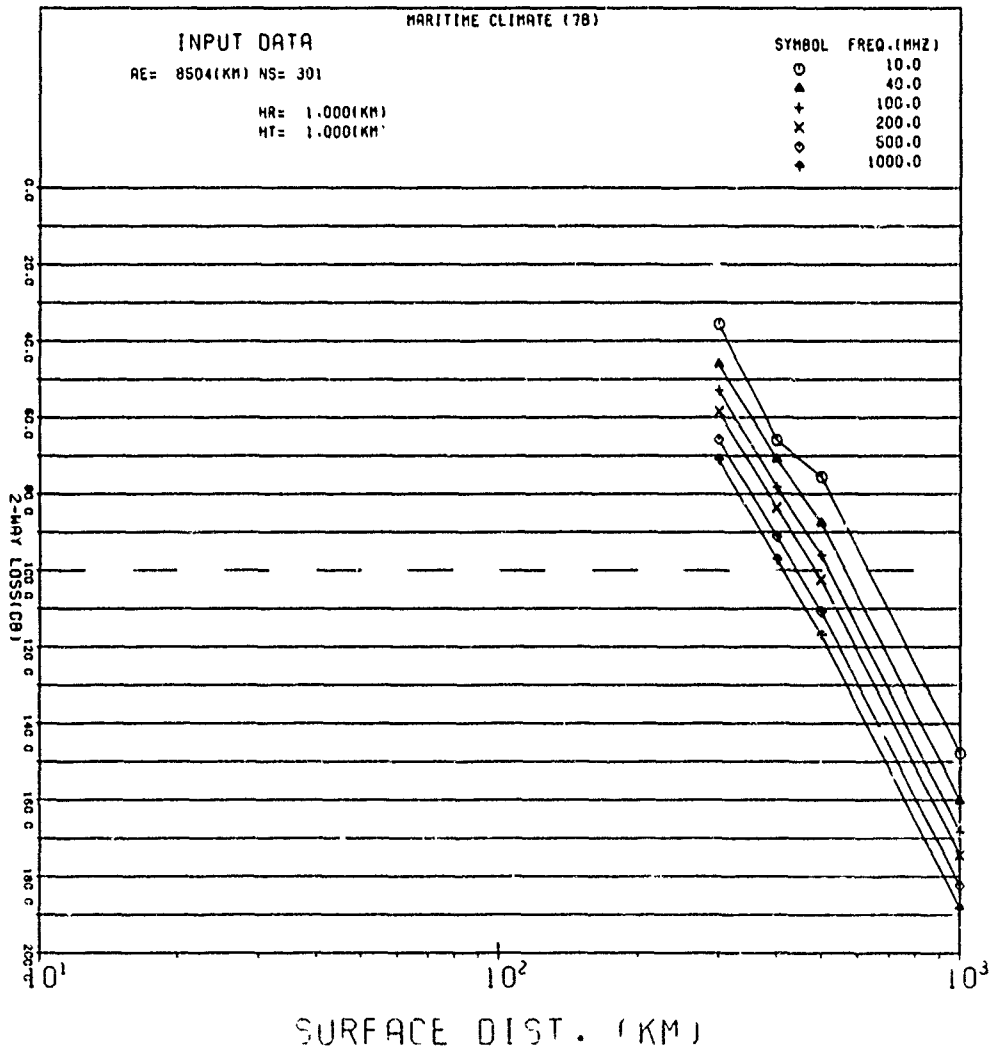


**Appendix B**

**Three Plots of Two-way Loss (dB) vs Distance (km)**

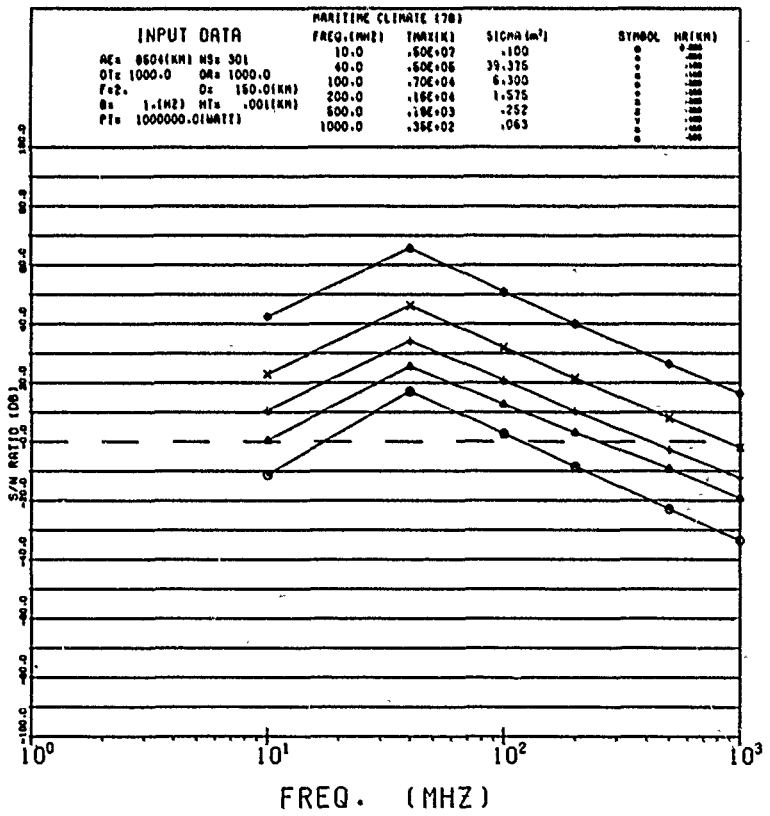
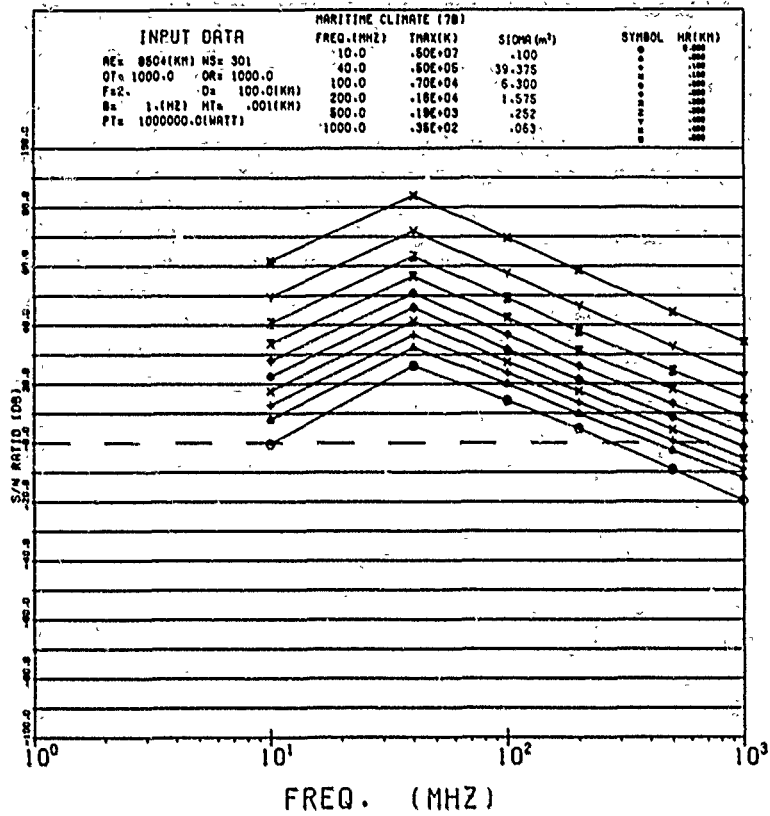


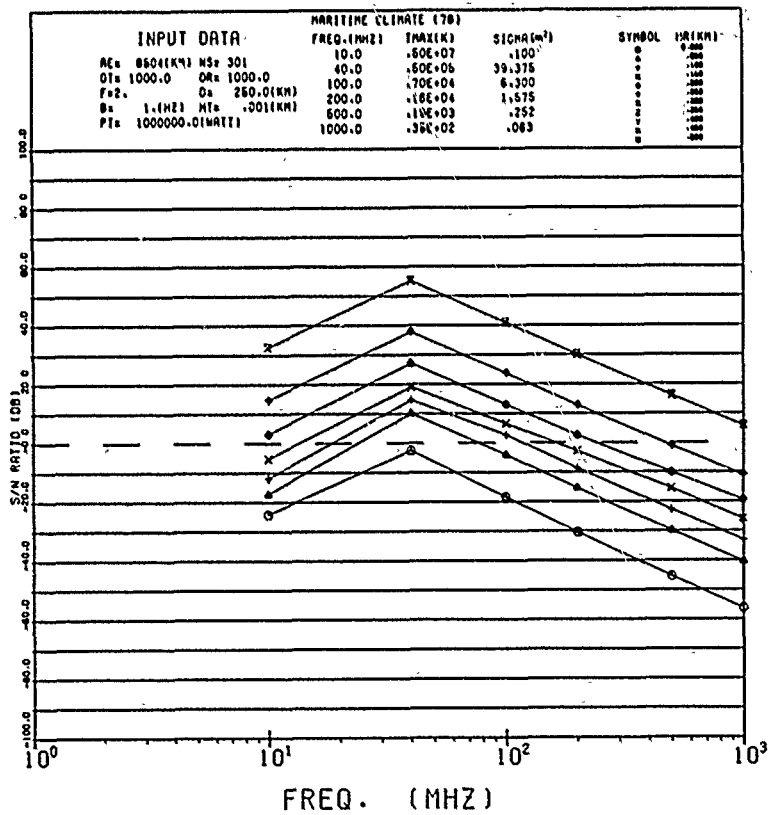
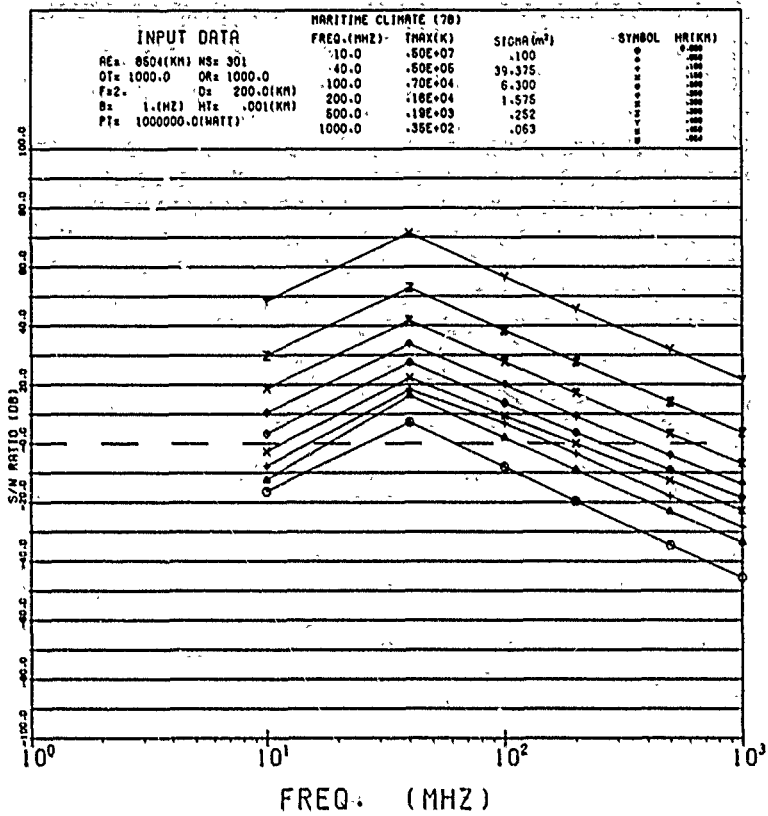


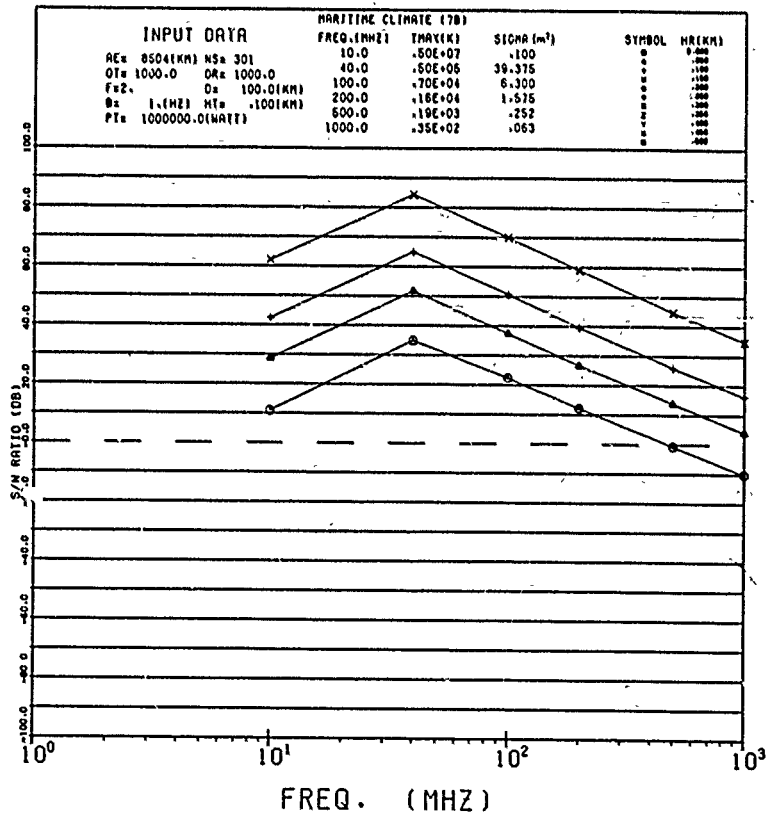
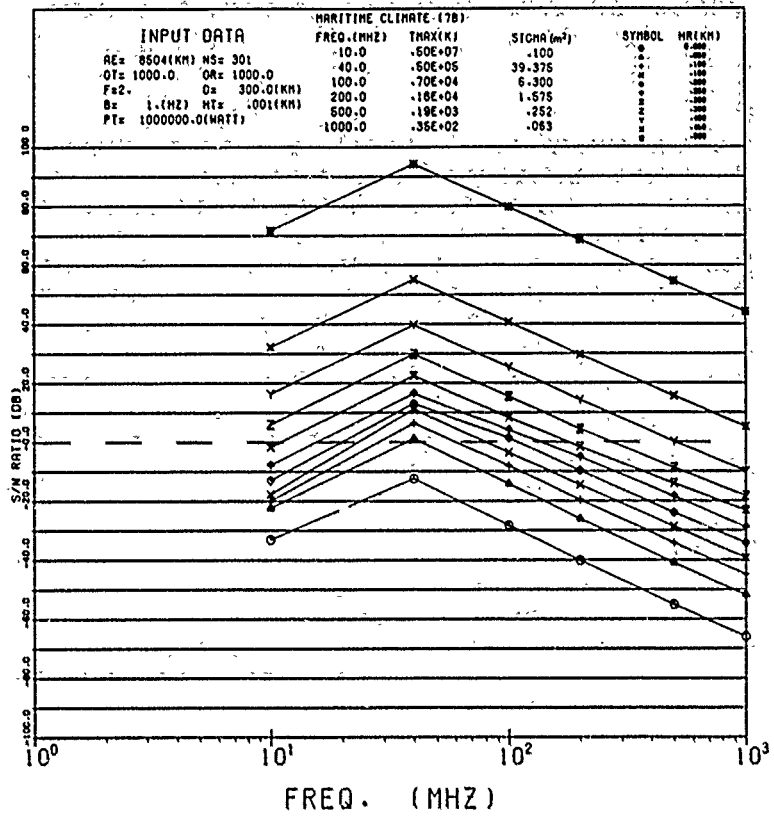


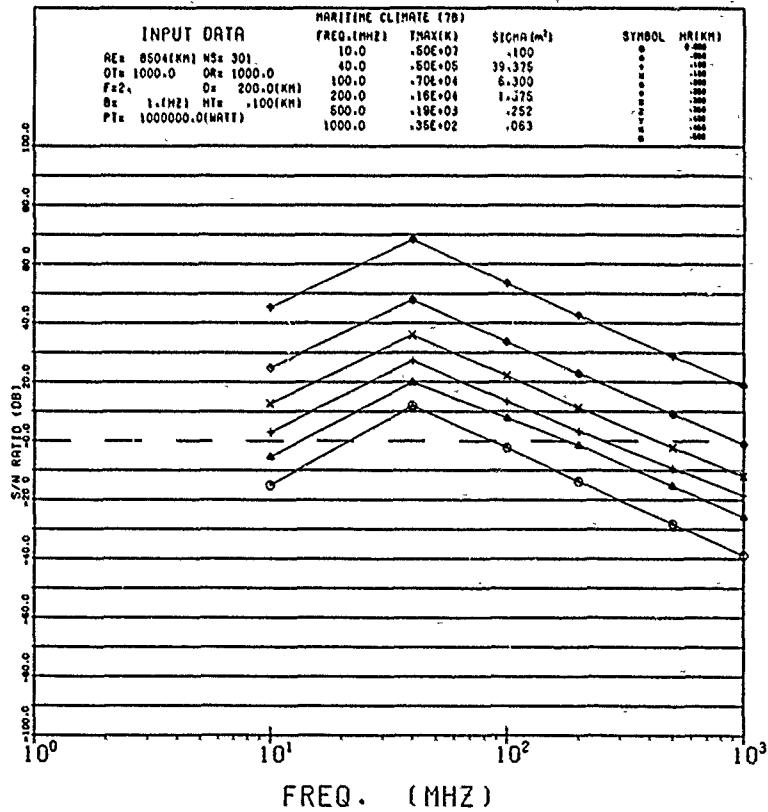
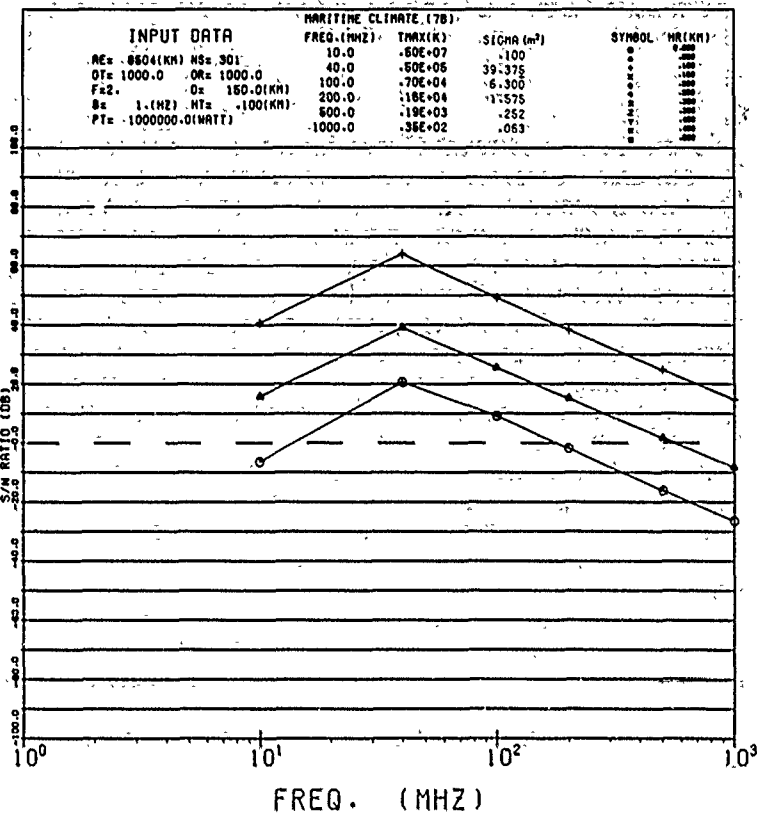
## Appendix C

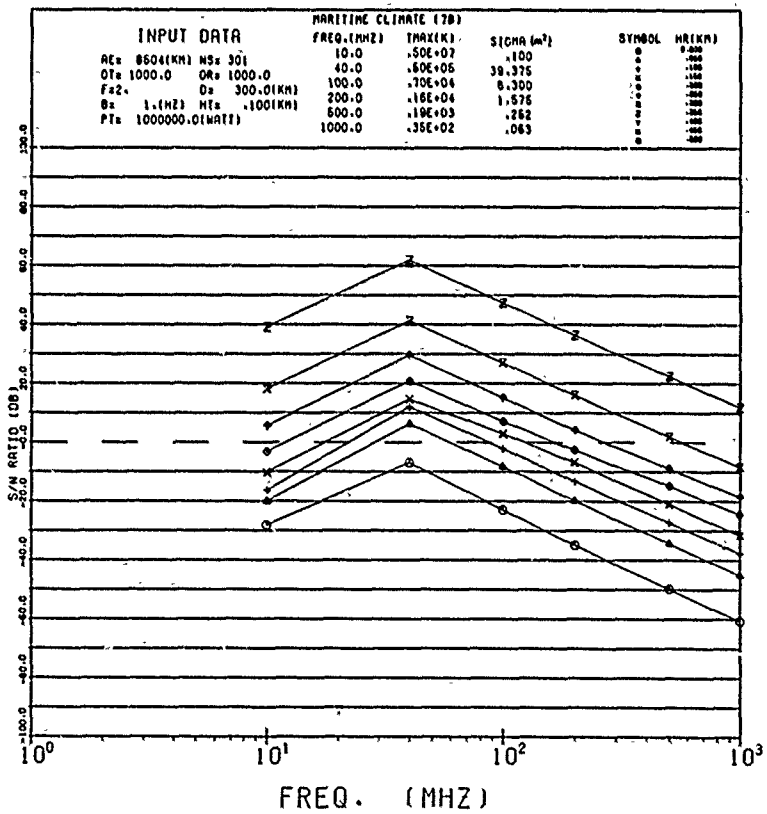
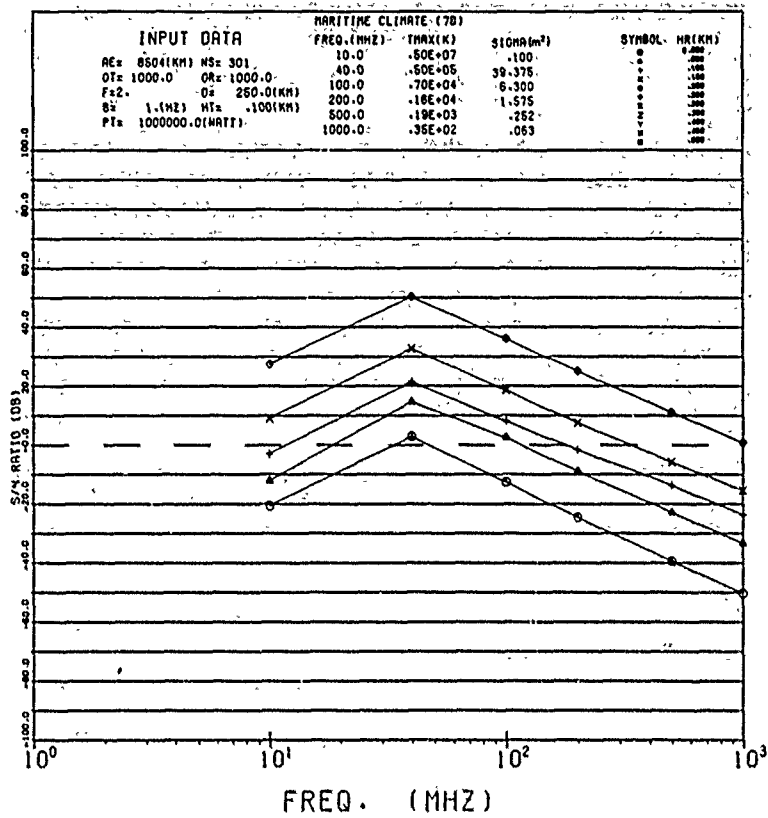
Fourteen Plots of Signal-to-Noise Ratio (dB)  
vs Frequency (MHz) for Median Loss

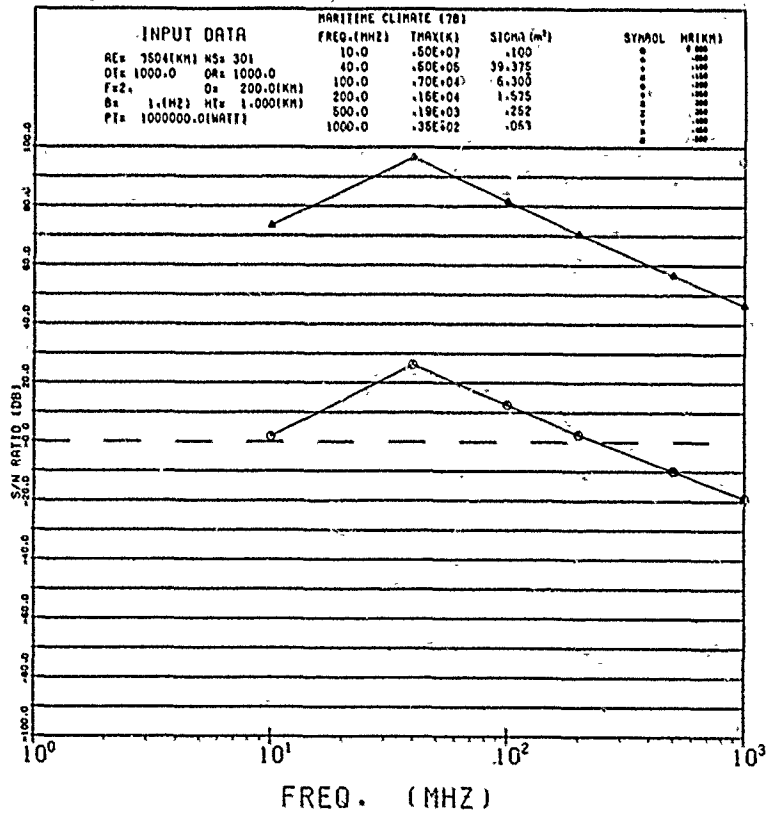
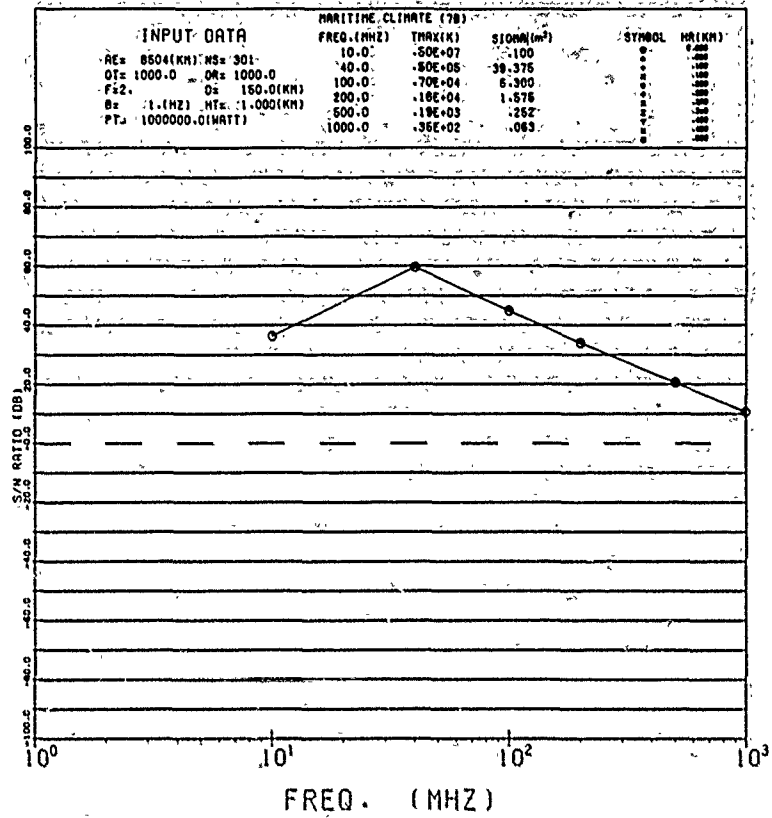


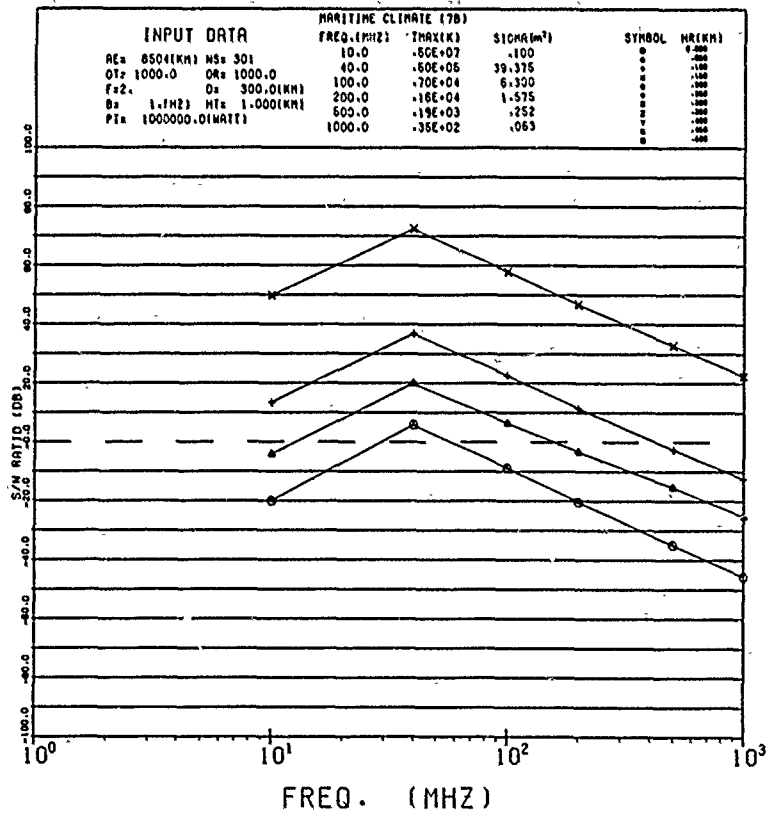
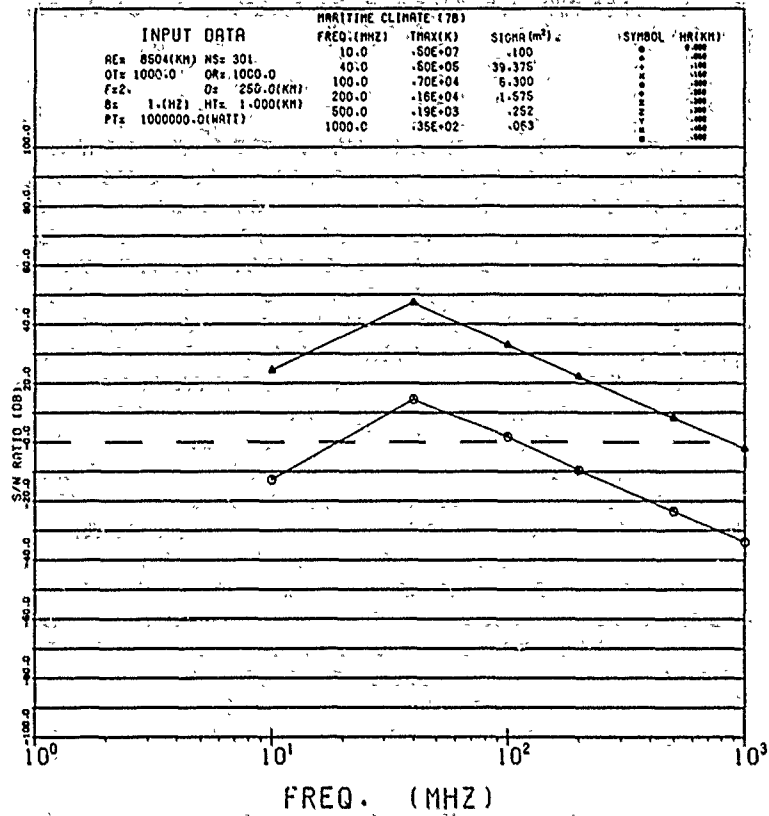






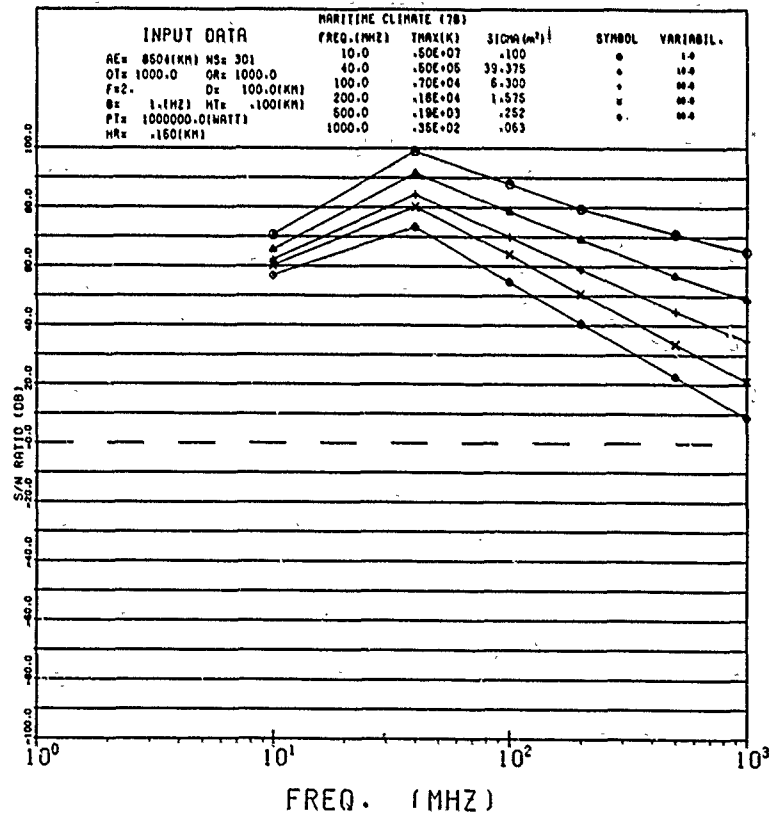
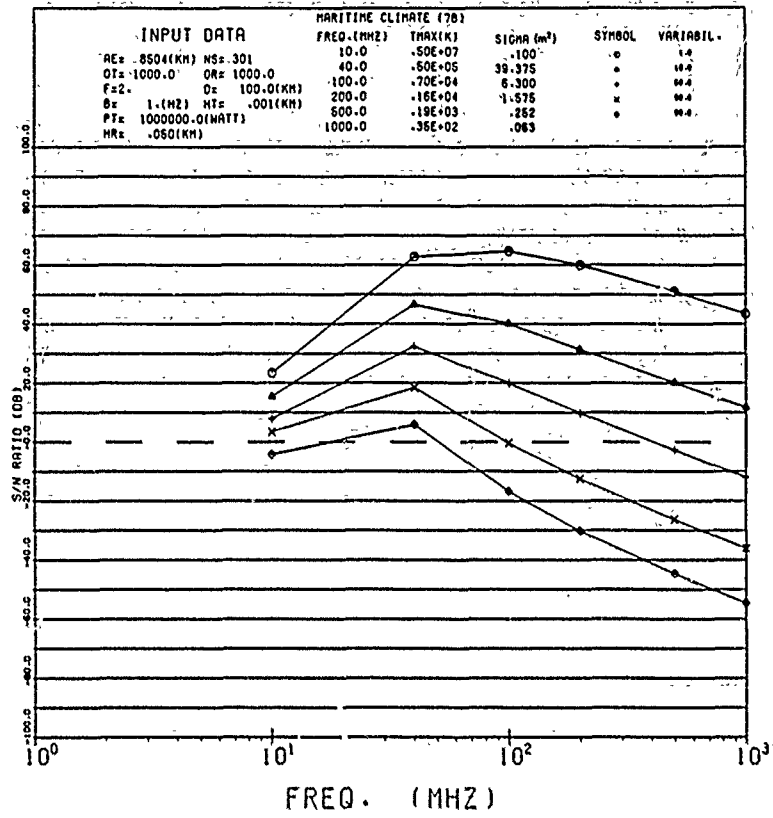


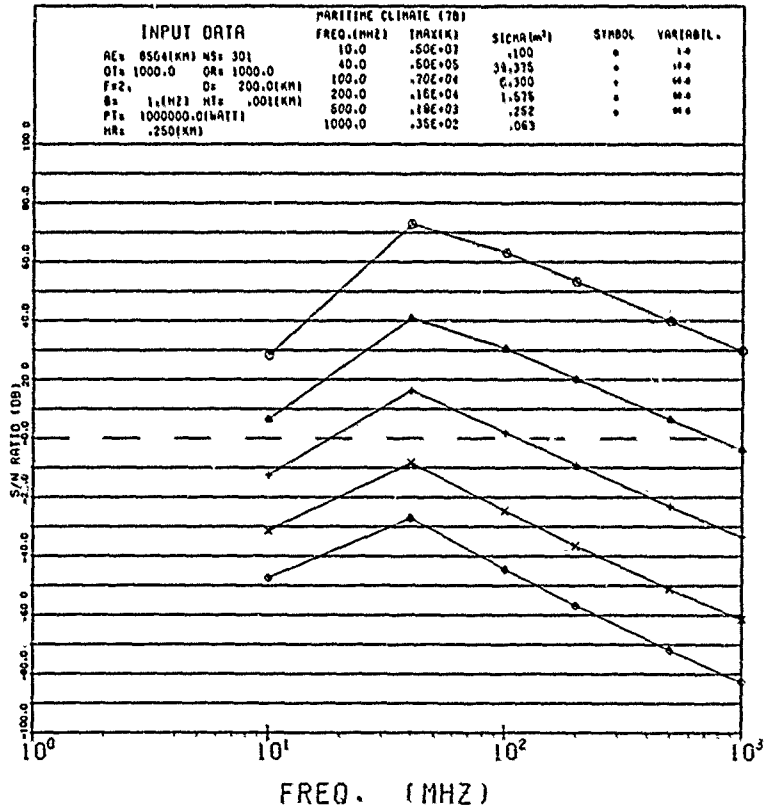
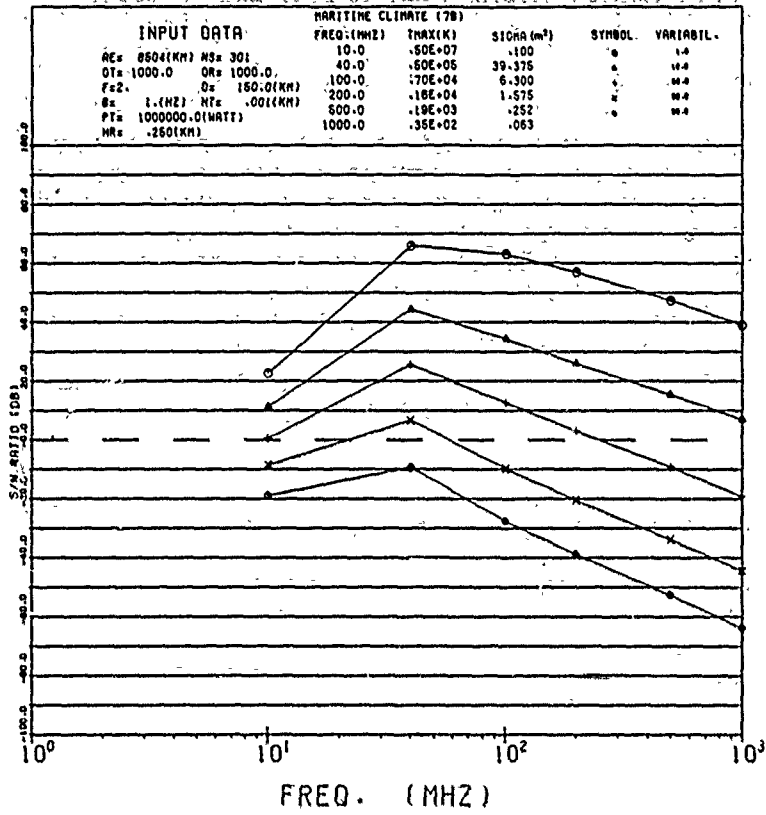


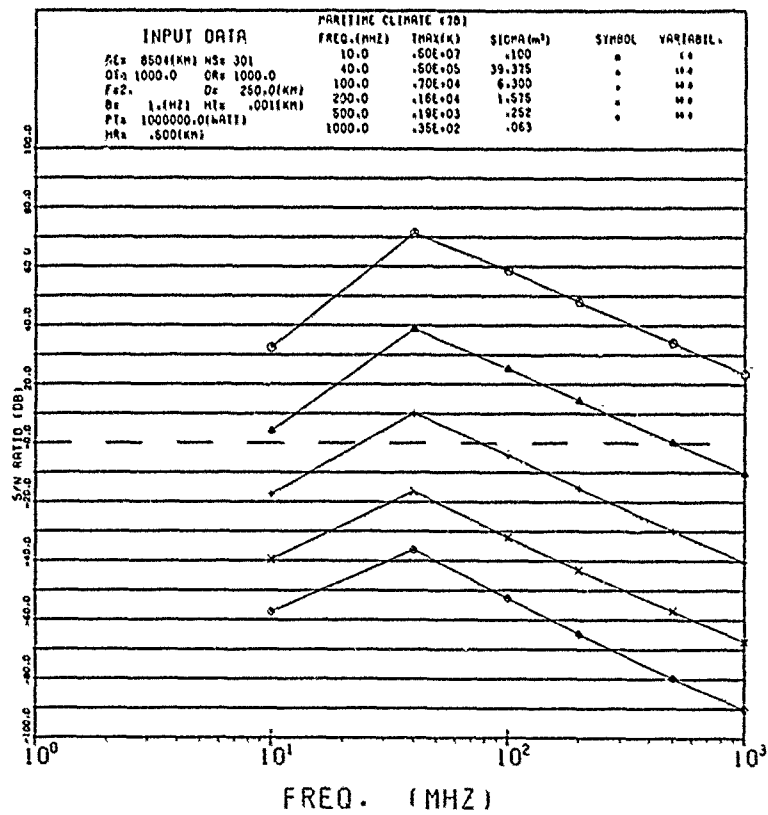
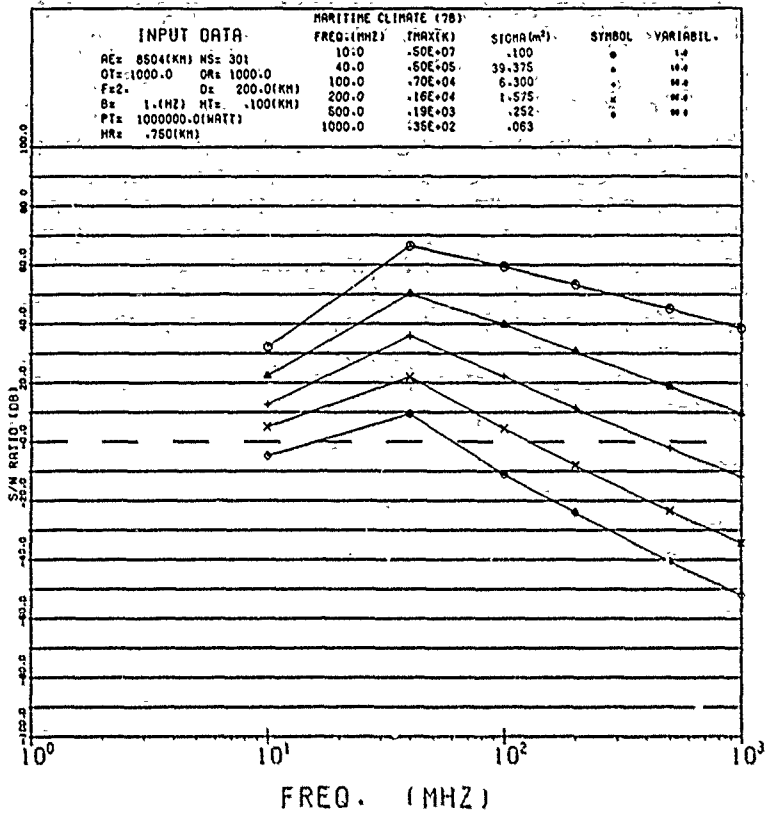


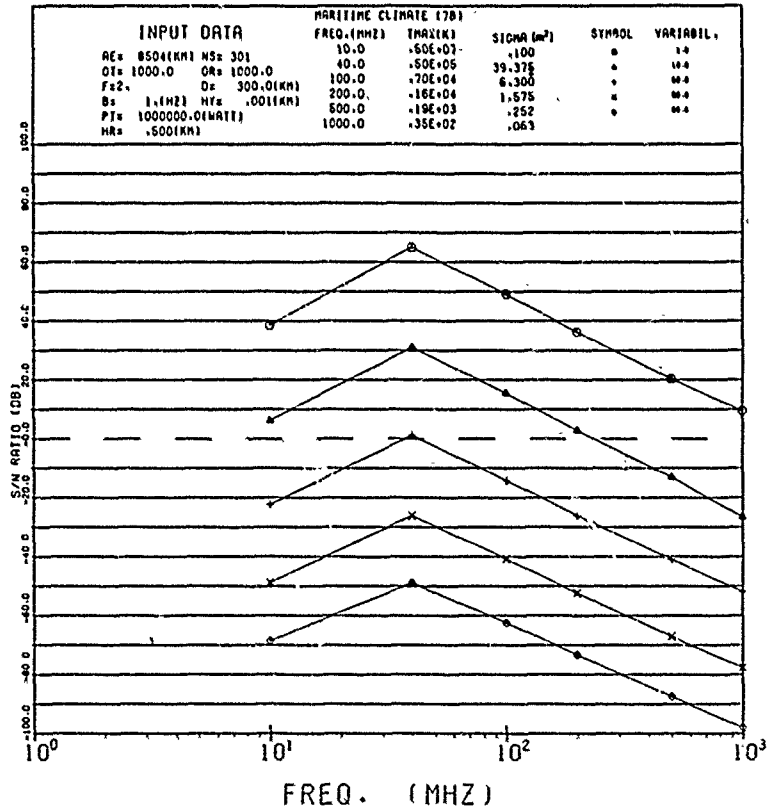
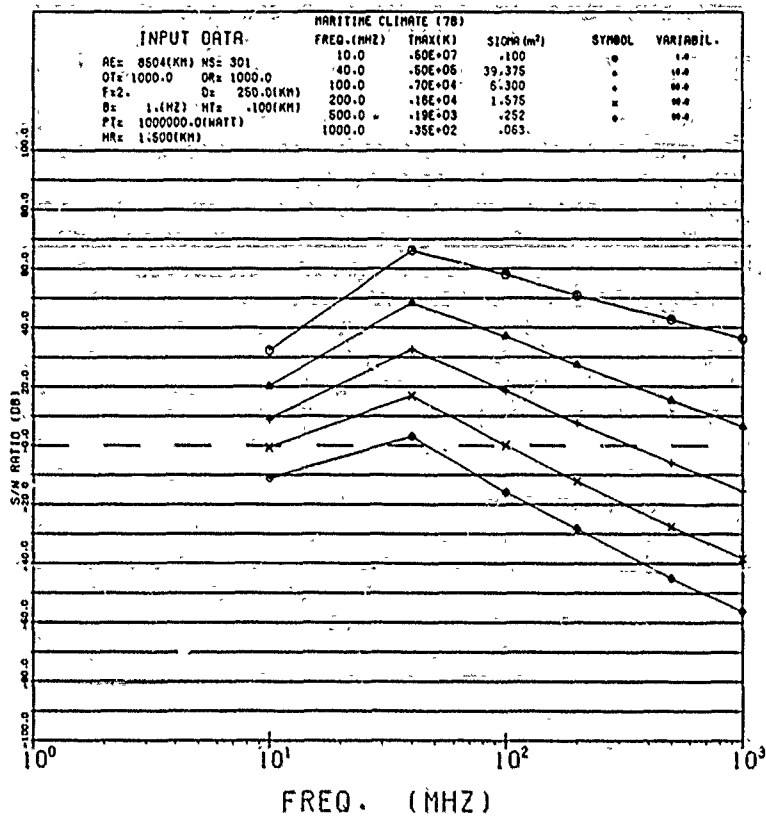
## Appendix D

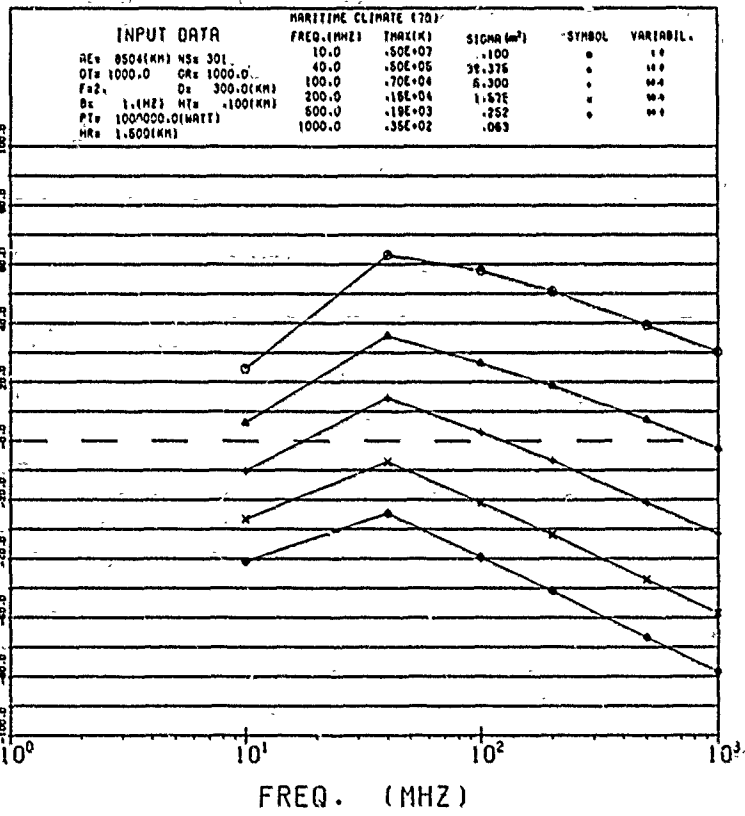
Nine Plots of Signal-to-Noise Ratio (dB)  
vs Frequency (MHz) for 1 to 99% Loss Variability





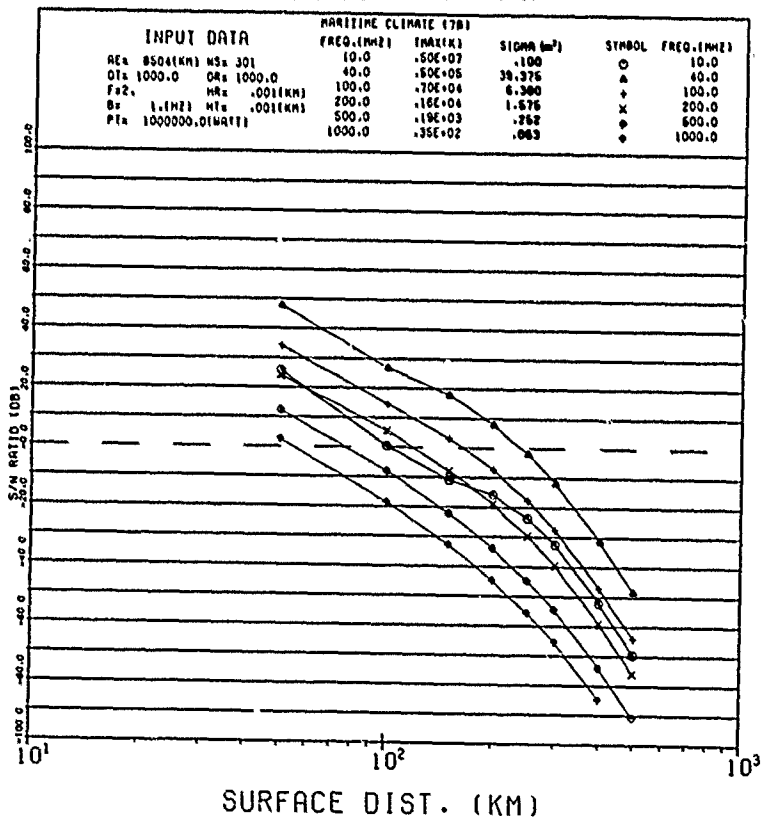
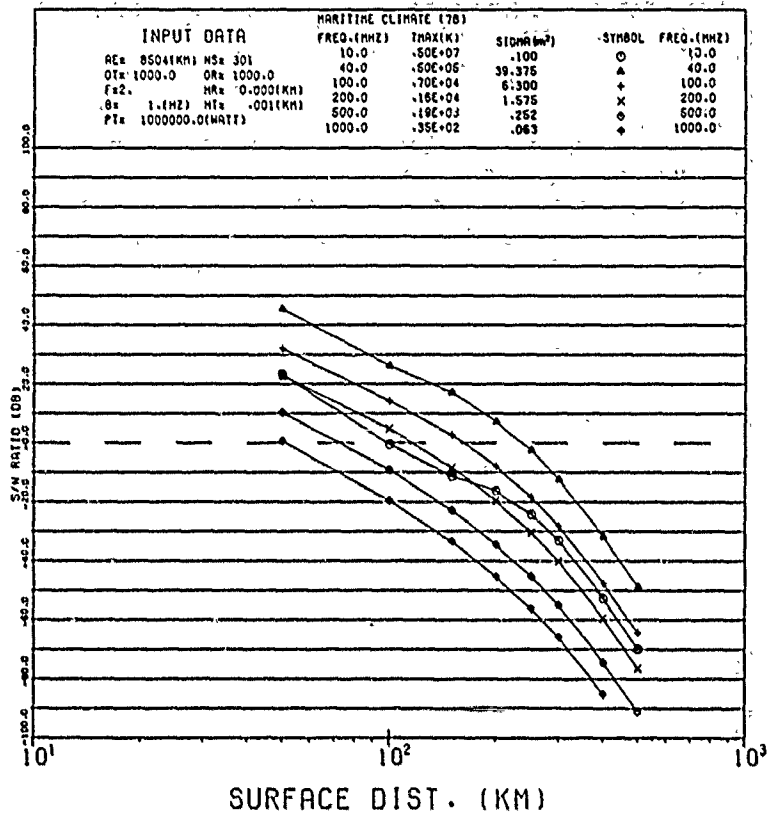


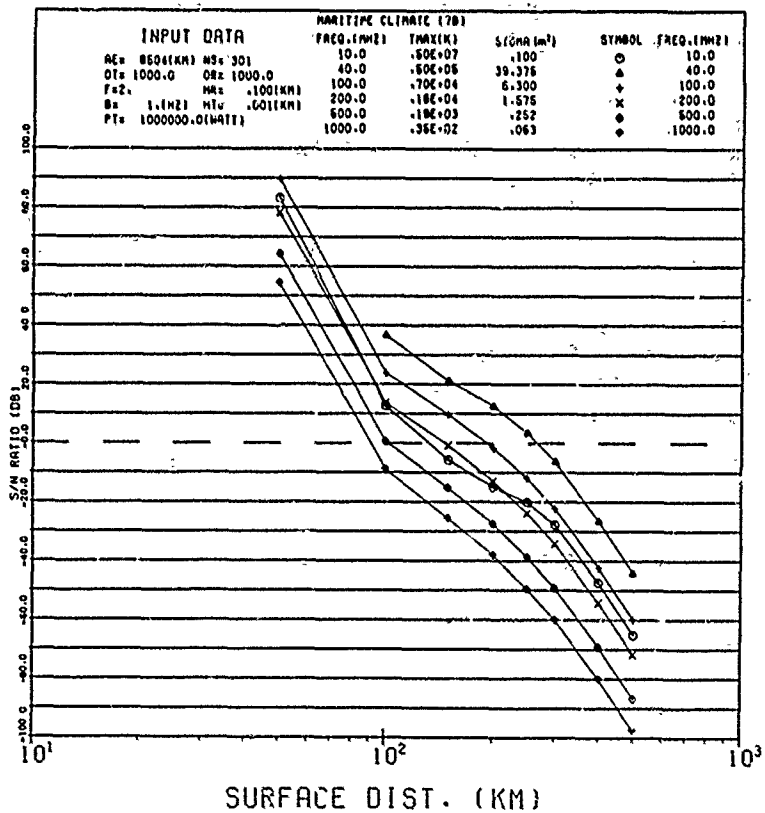
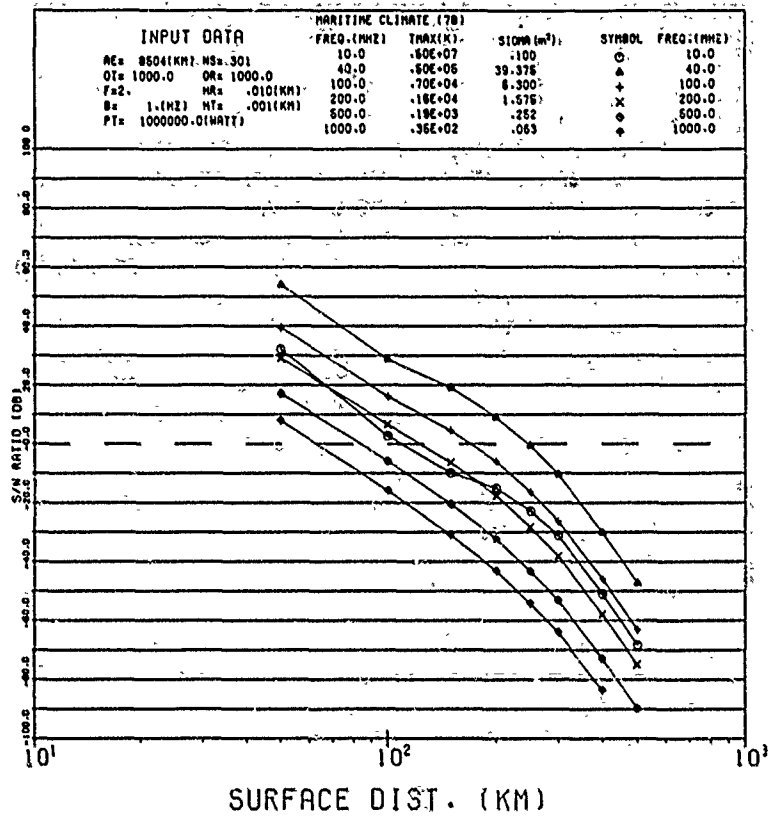


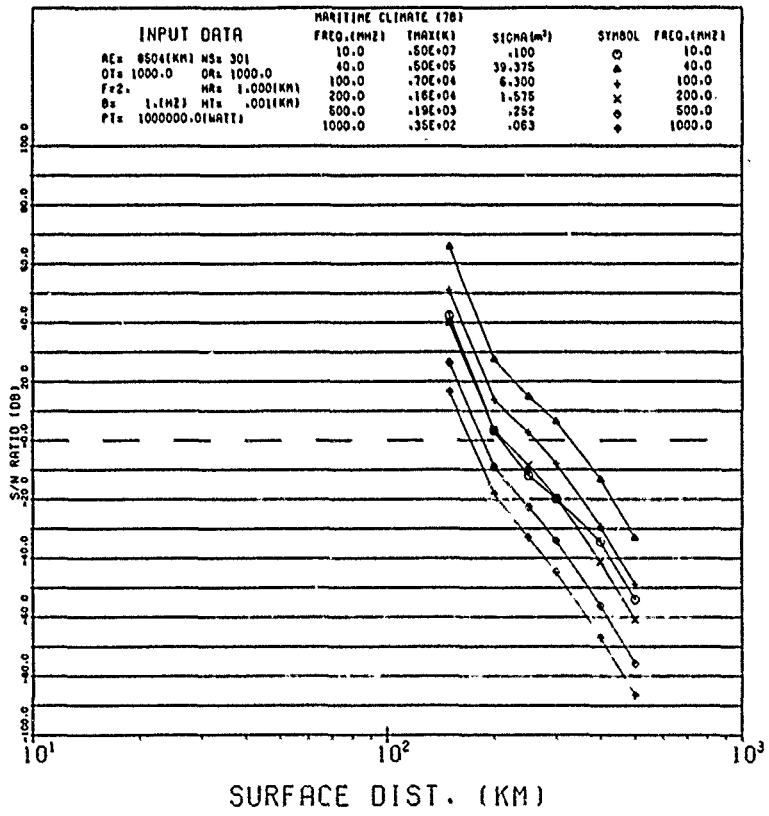
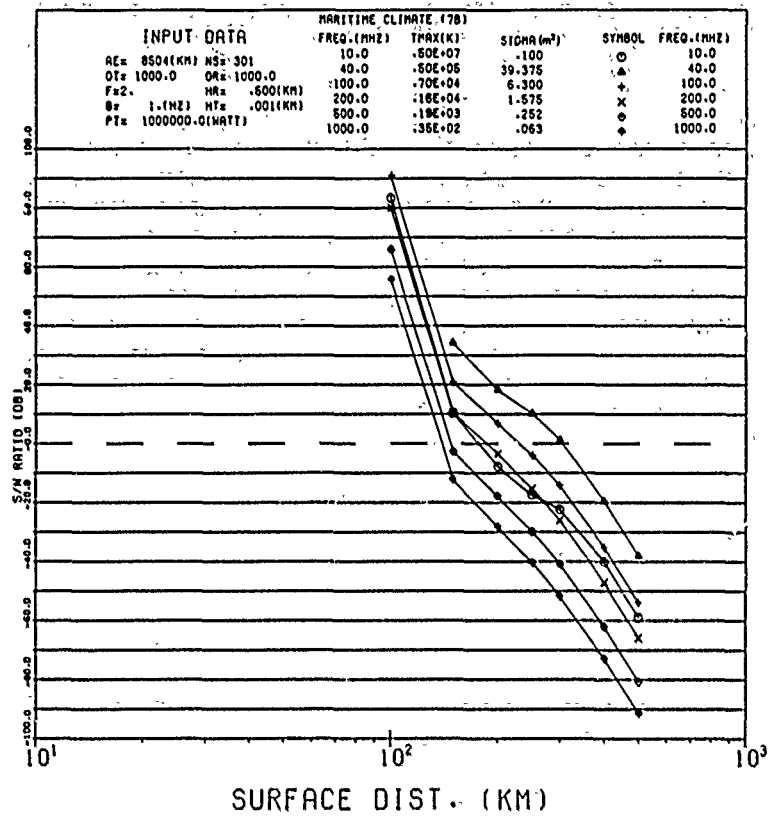


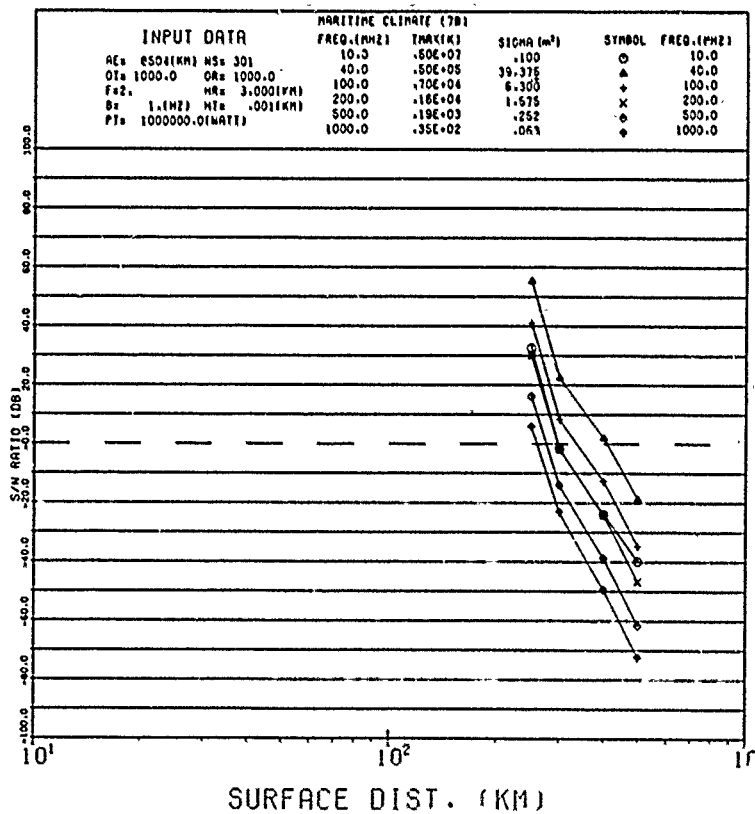
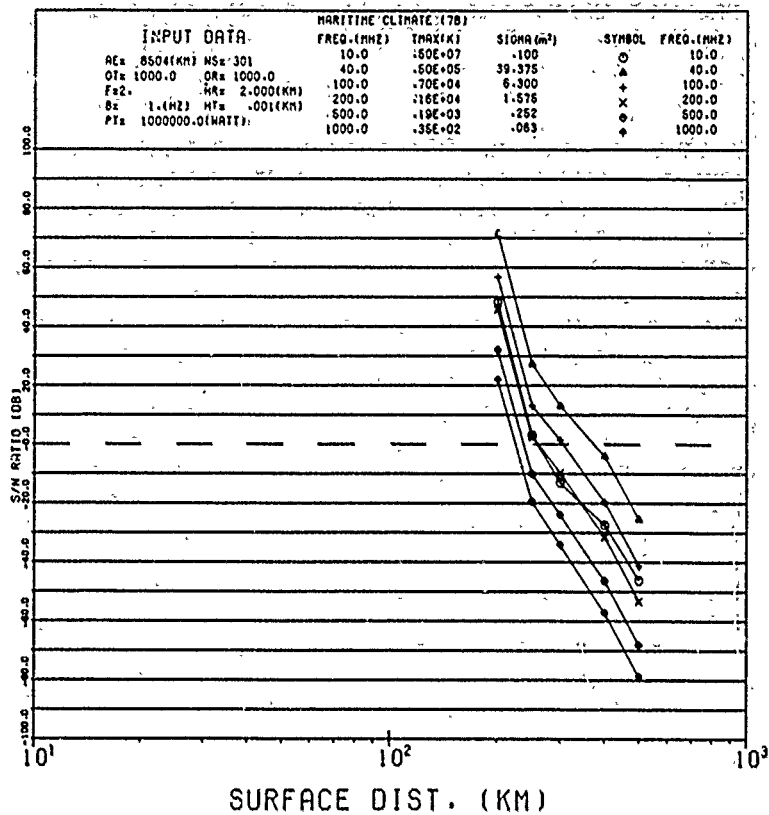
## Appendix E

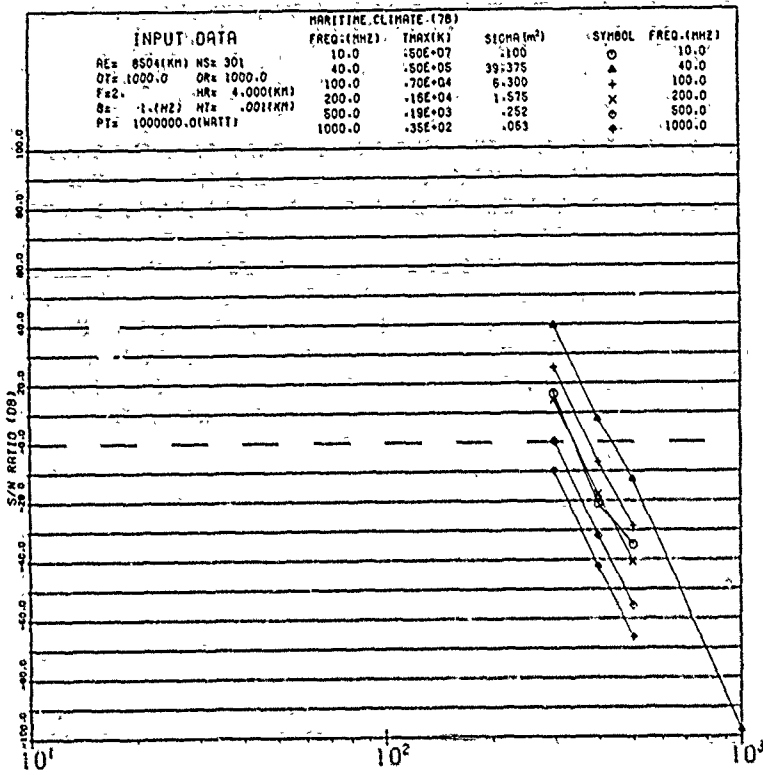
Thirty-three Plots of Signal-to-Noise Ratio (dB)  
vs Distance (km) for Median Loss



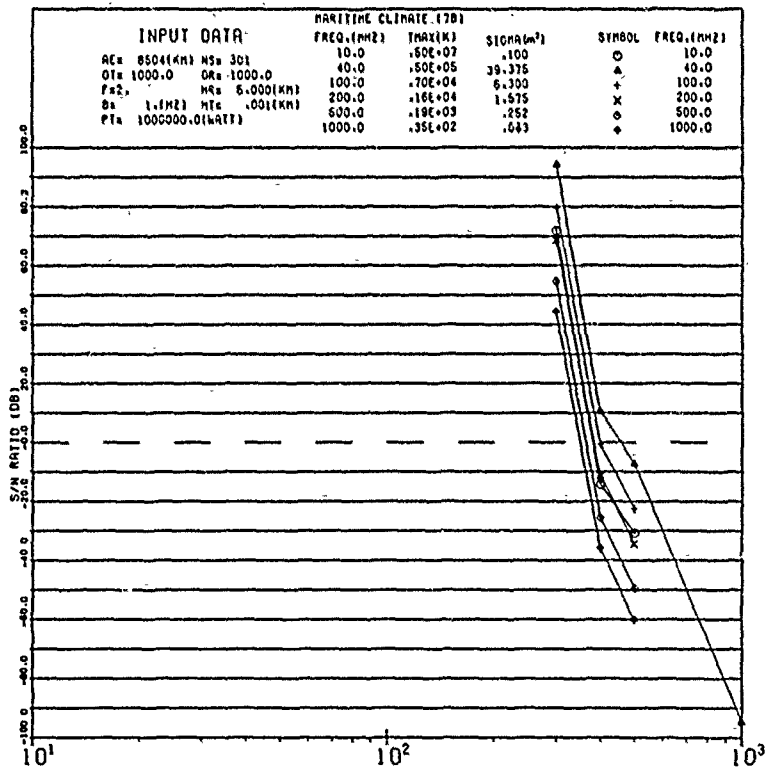




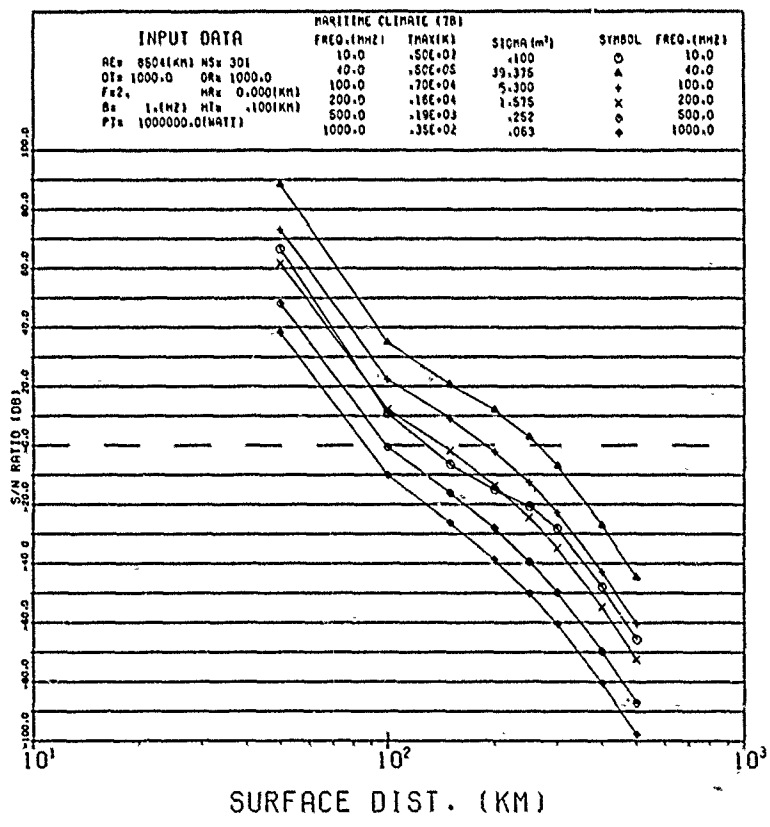
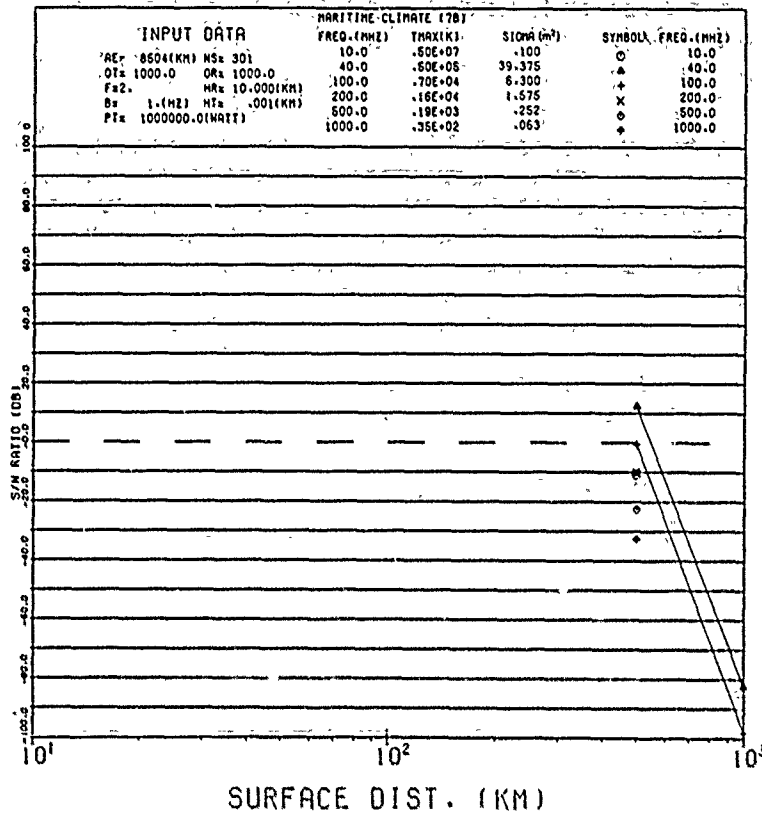


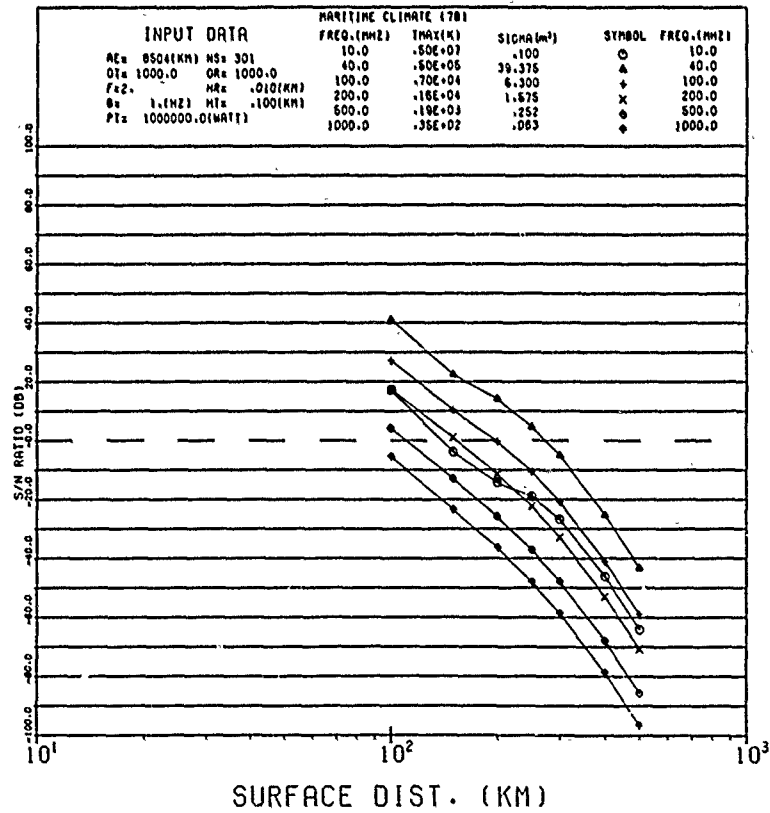
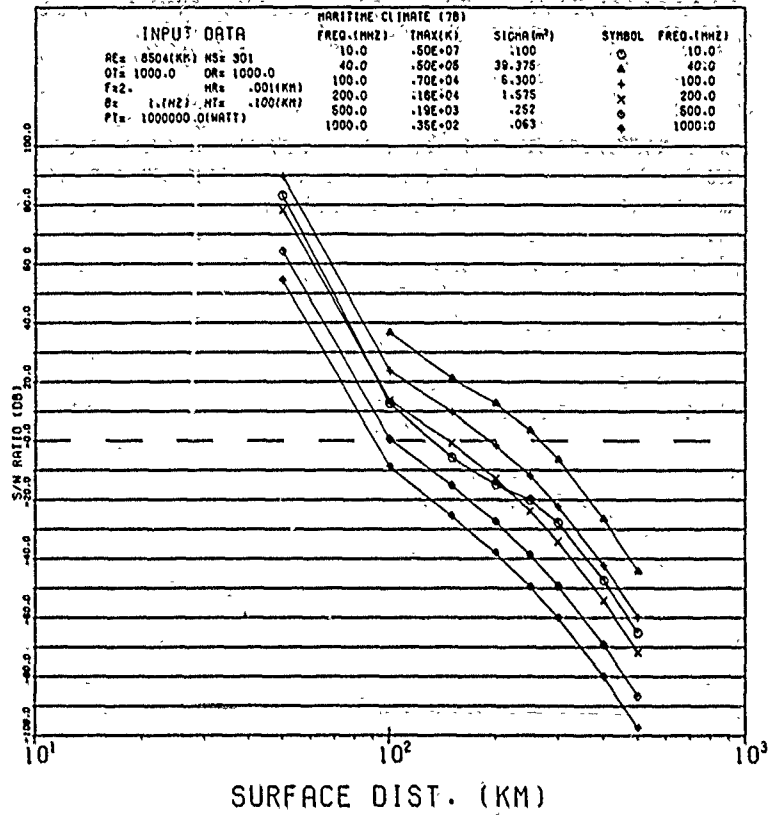


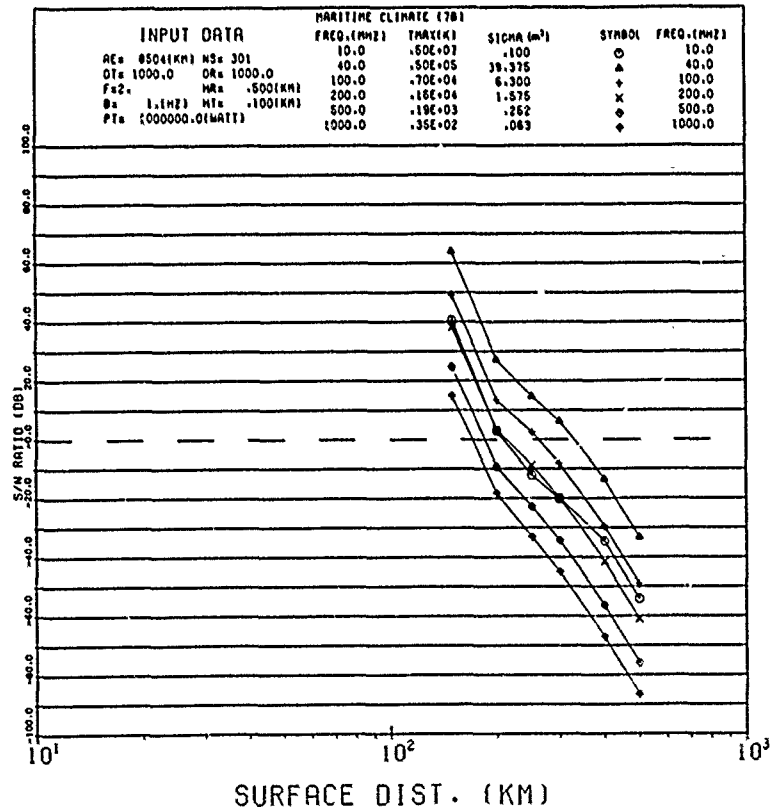
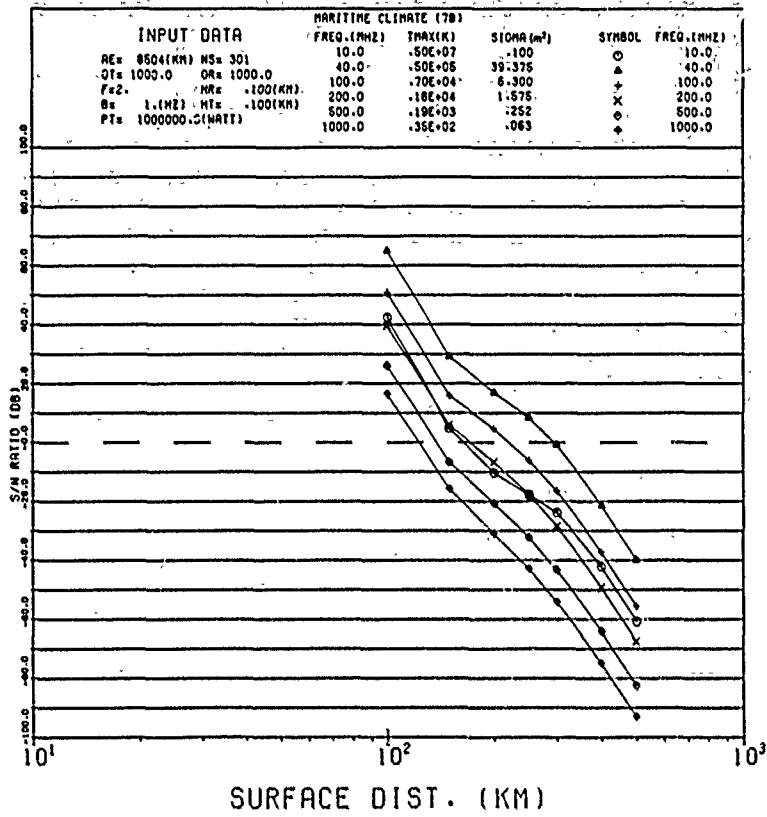
SURFACE DIST. (KM)

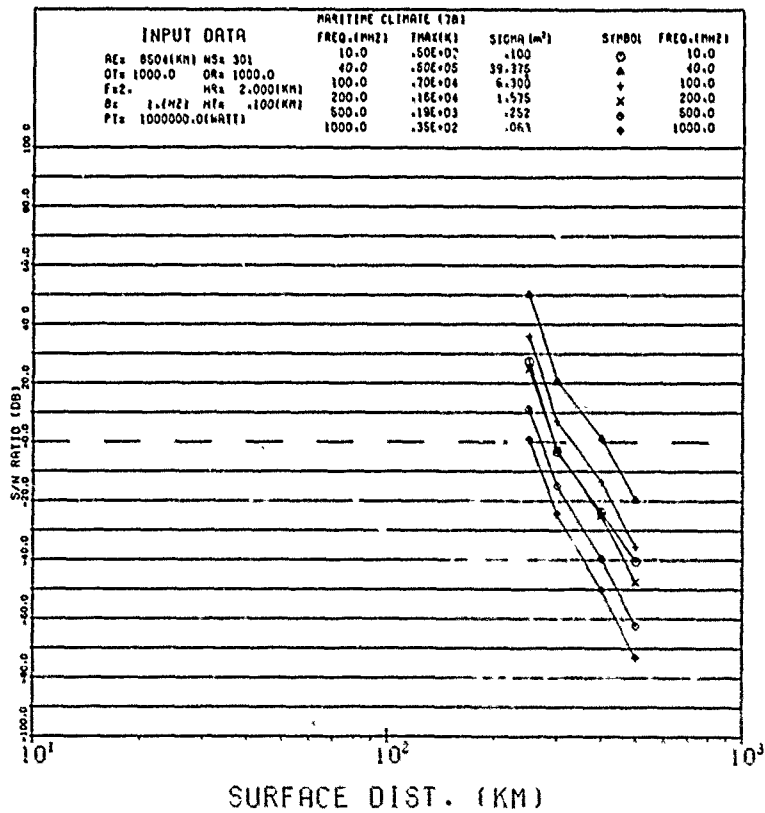
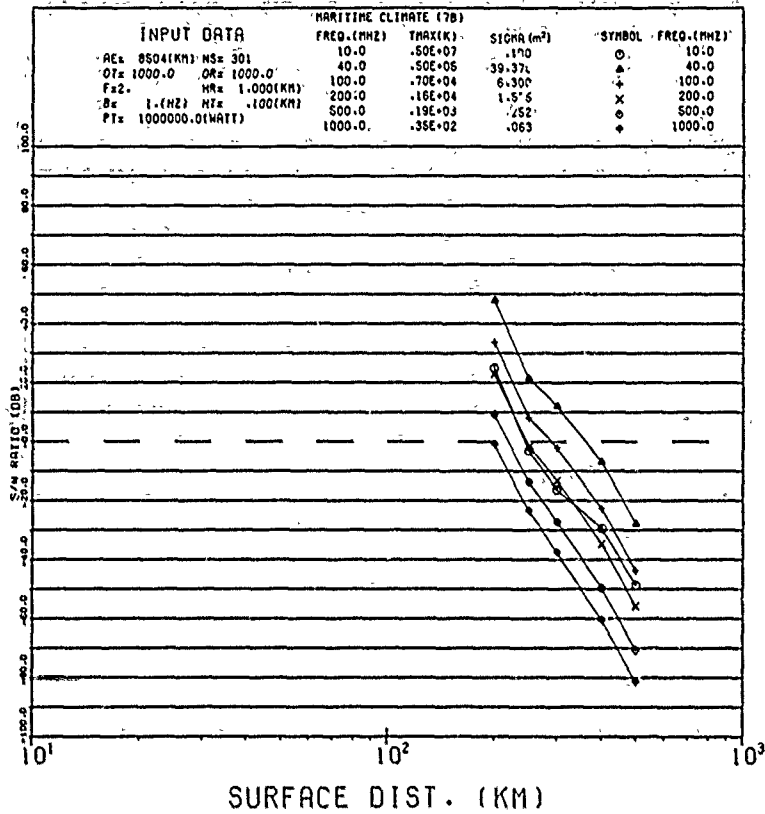


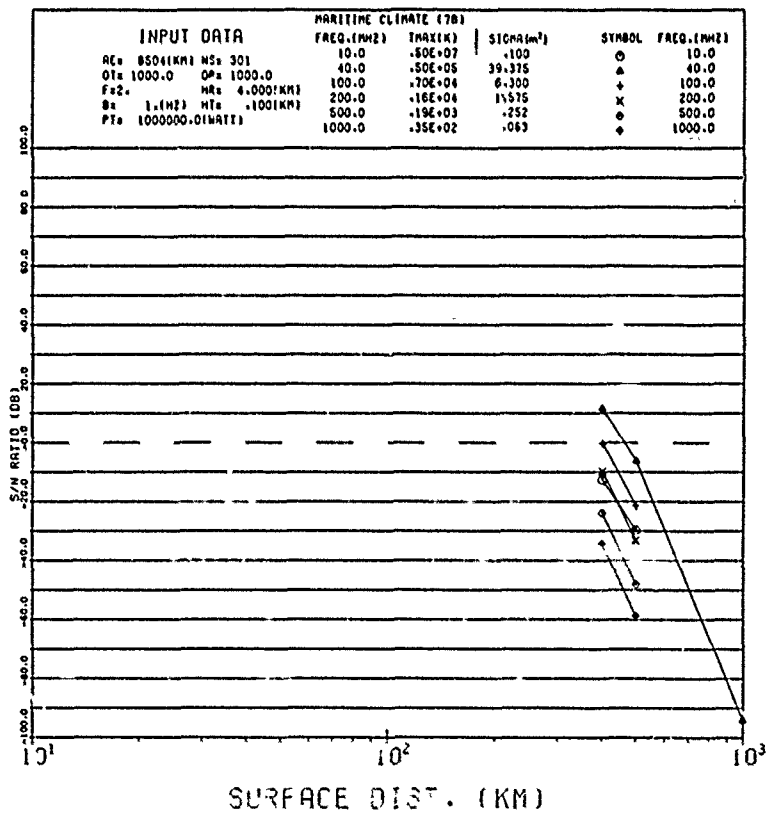
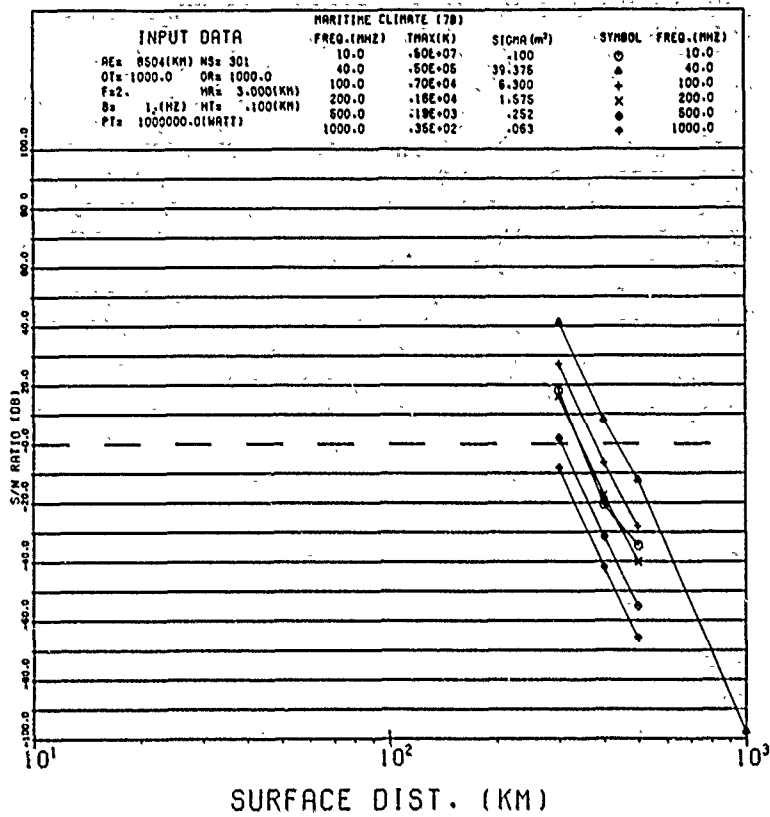
SURFACE DIST. (KM)

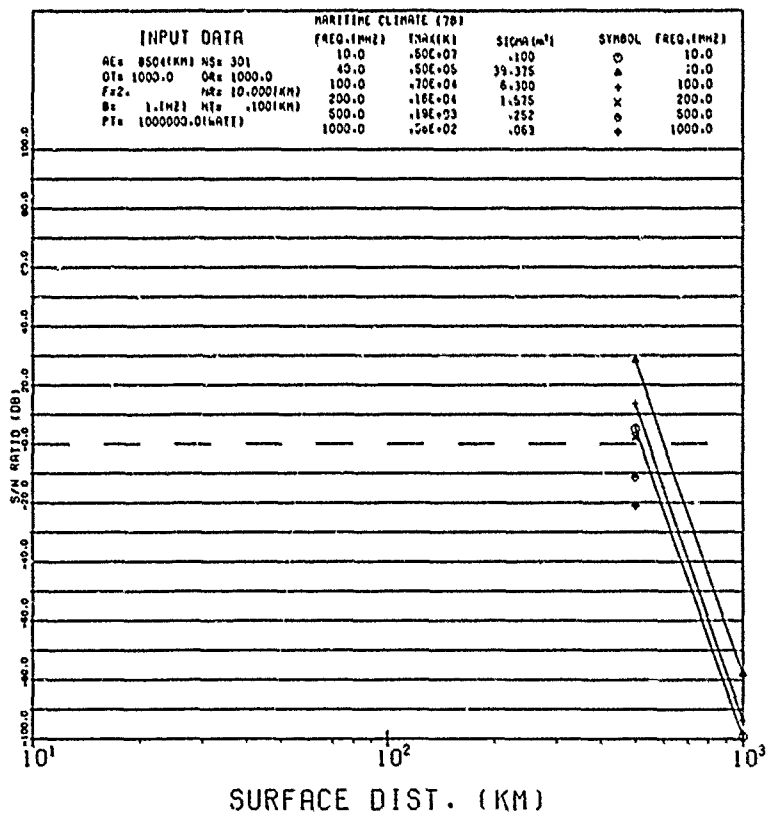
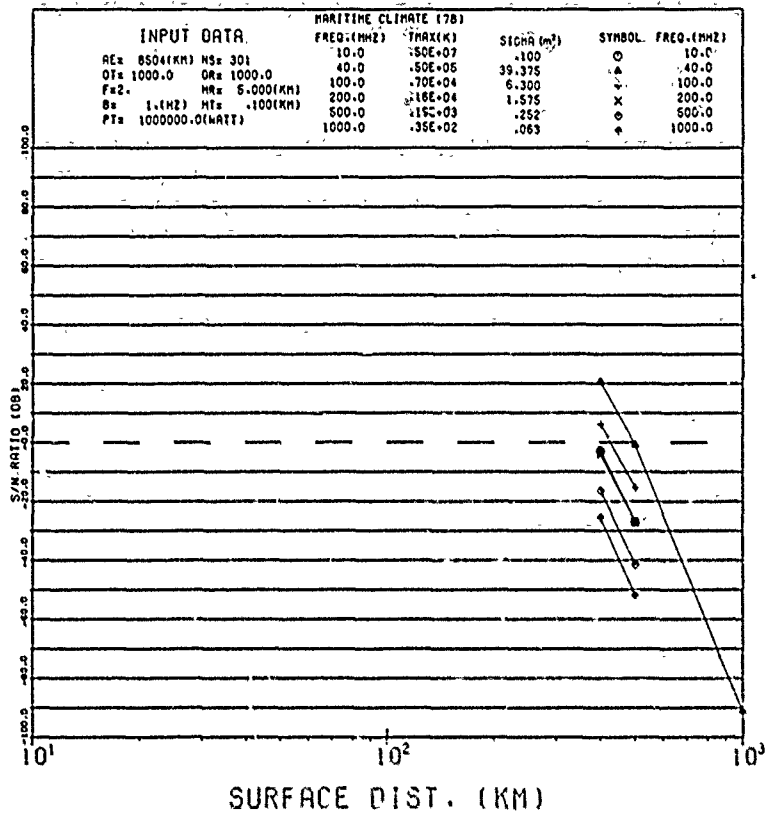


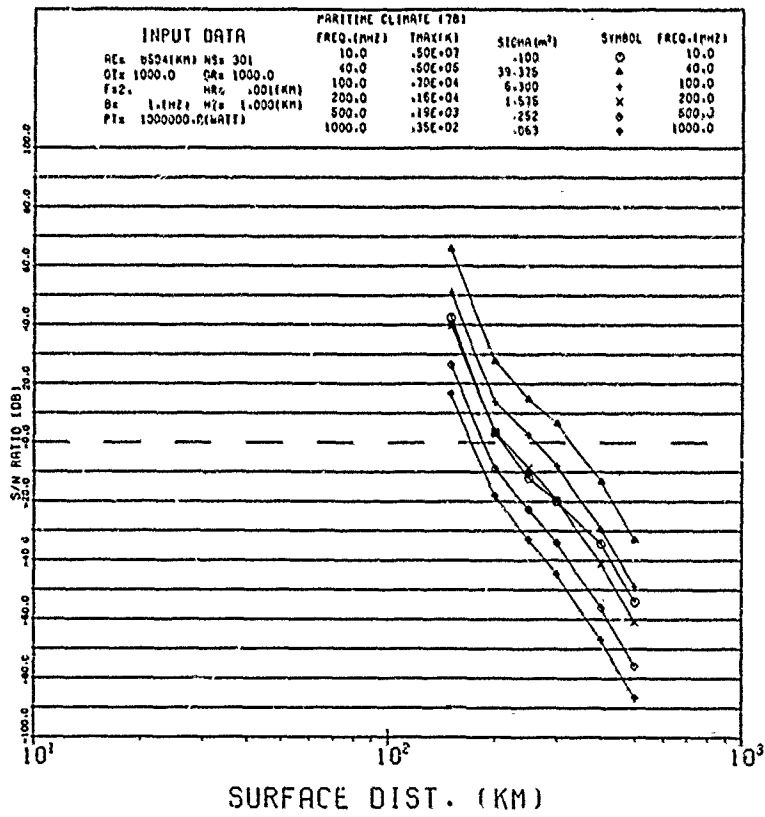
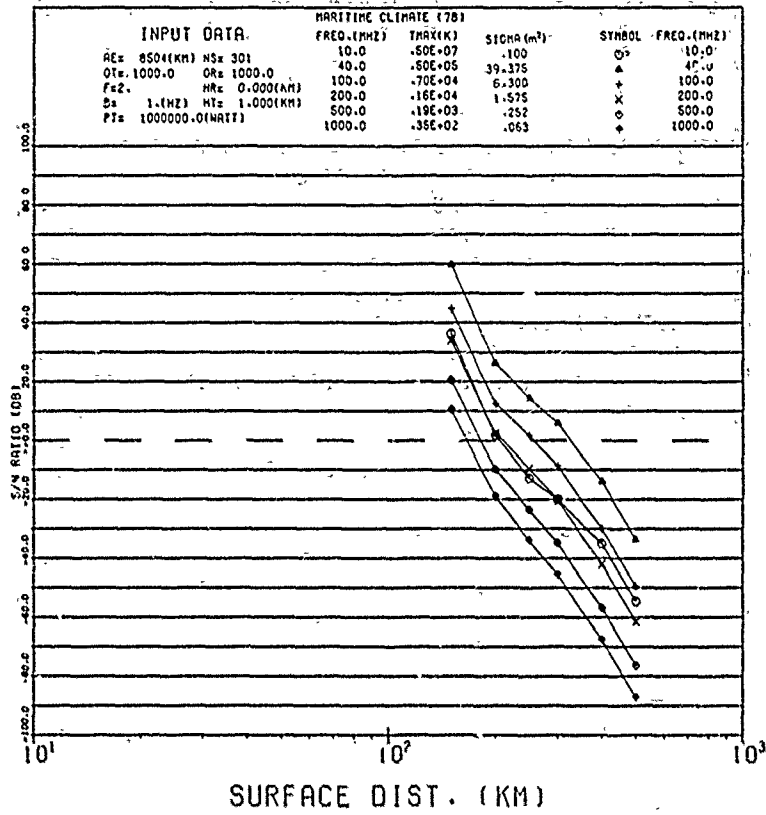


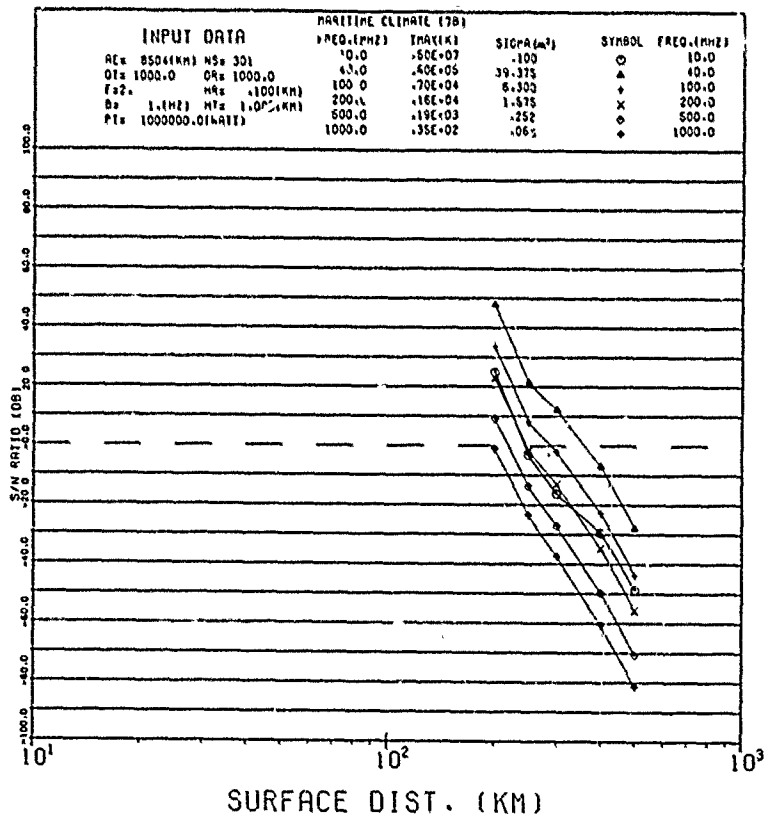
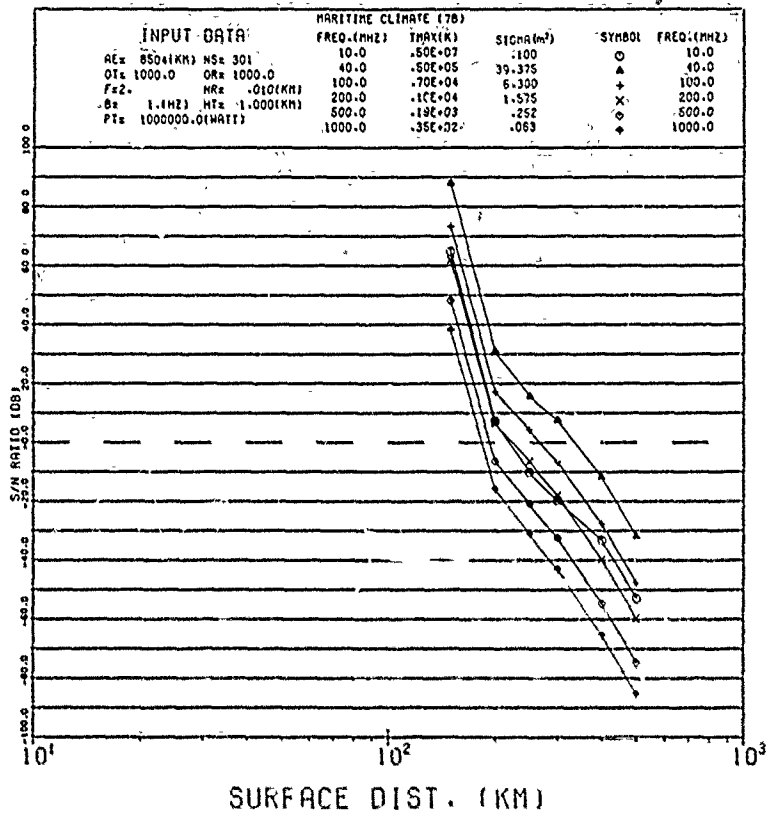


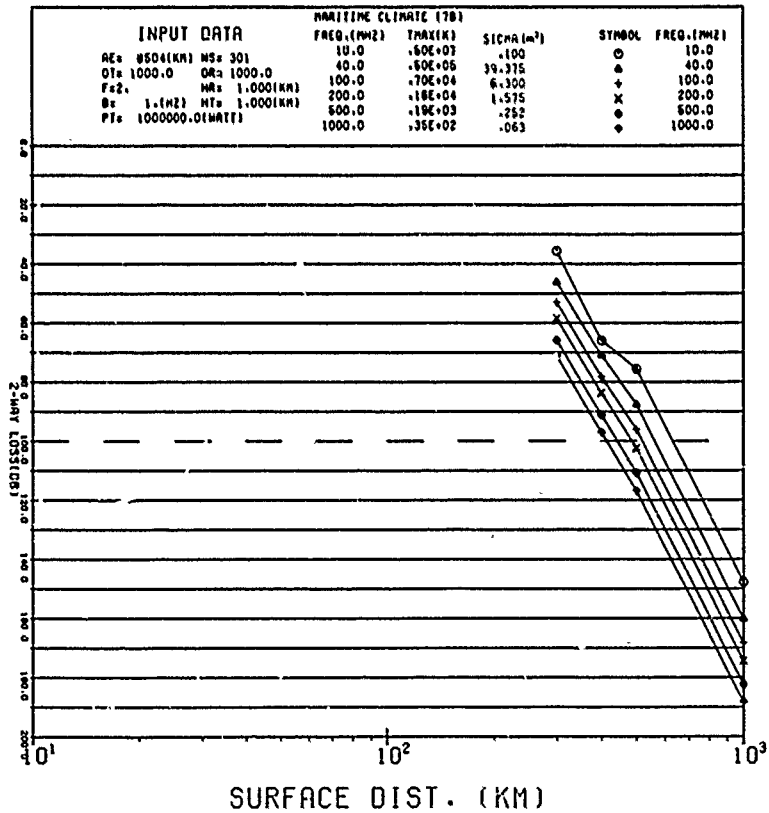
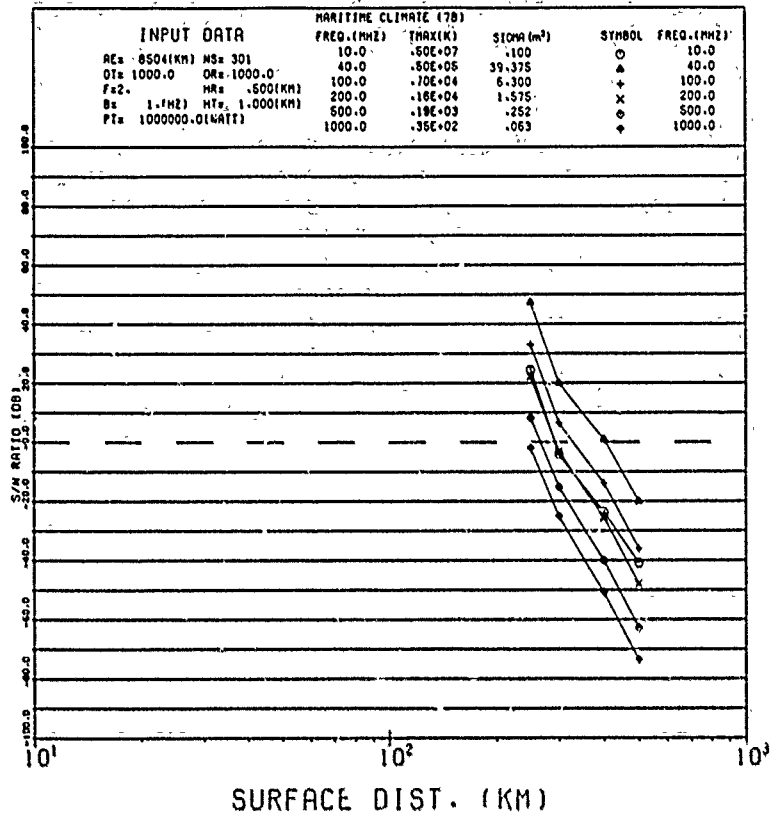


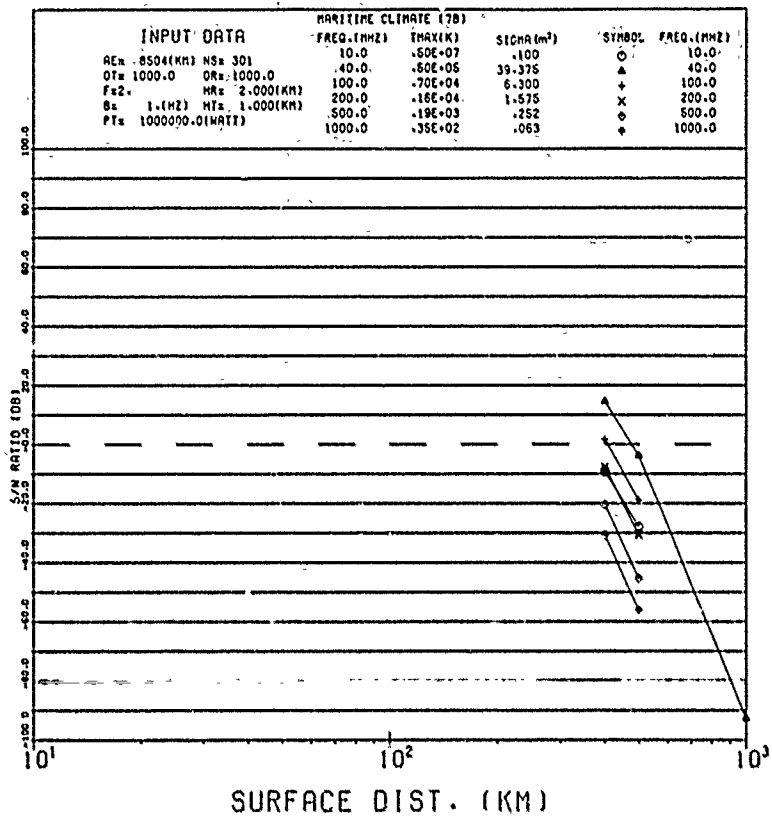




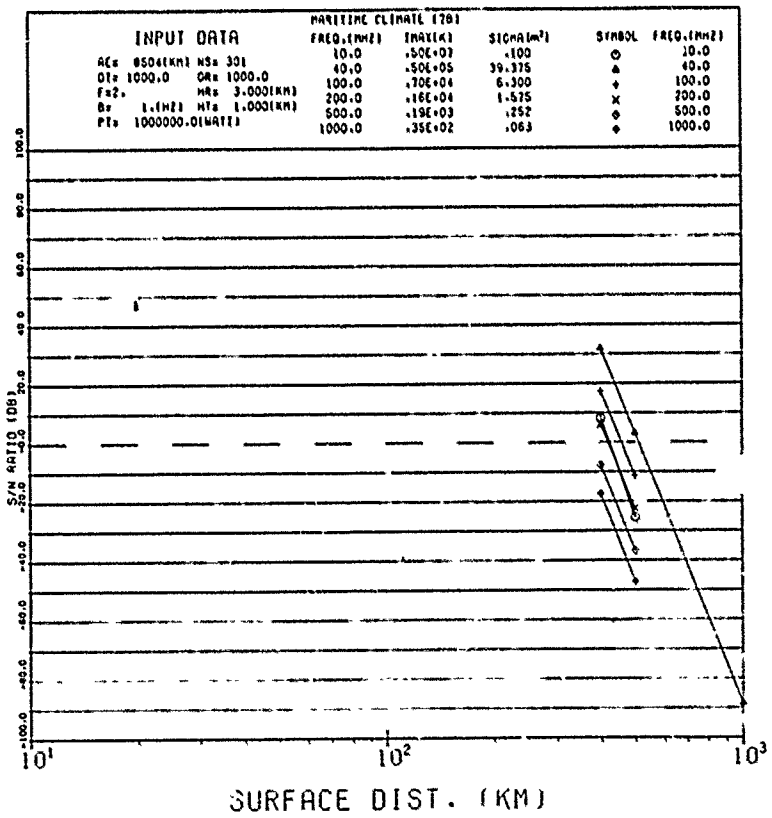




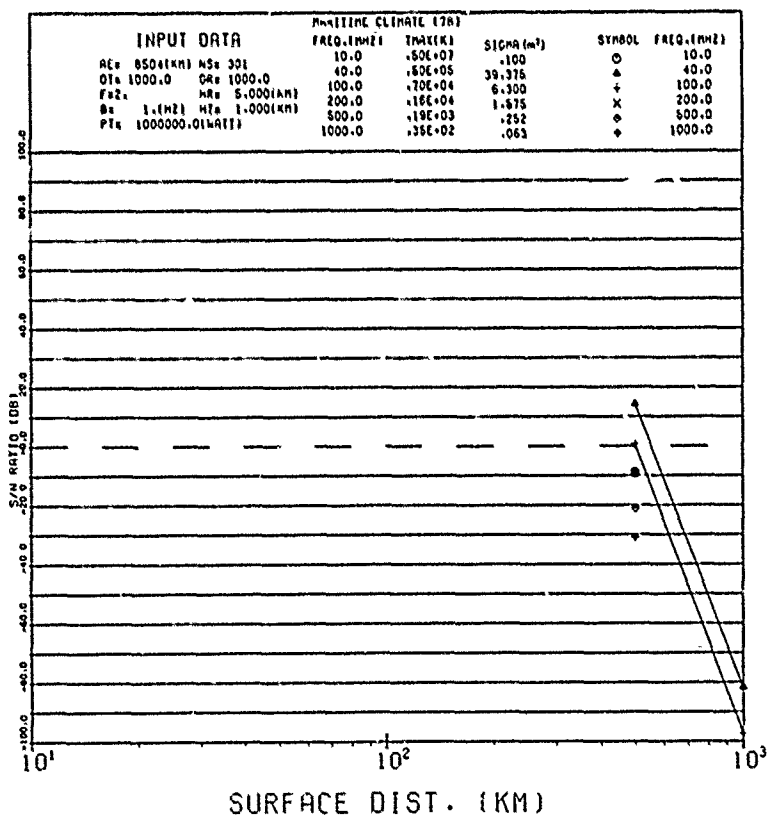
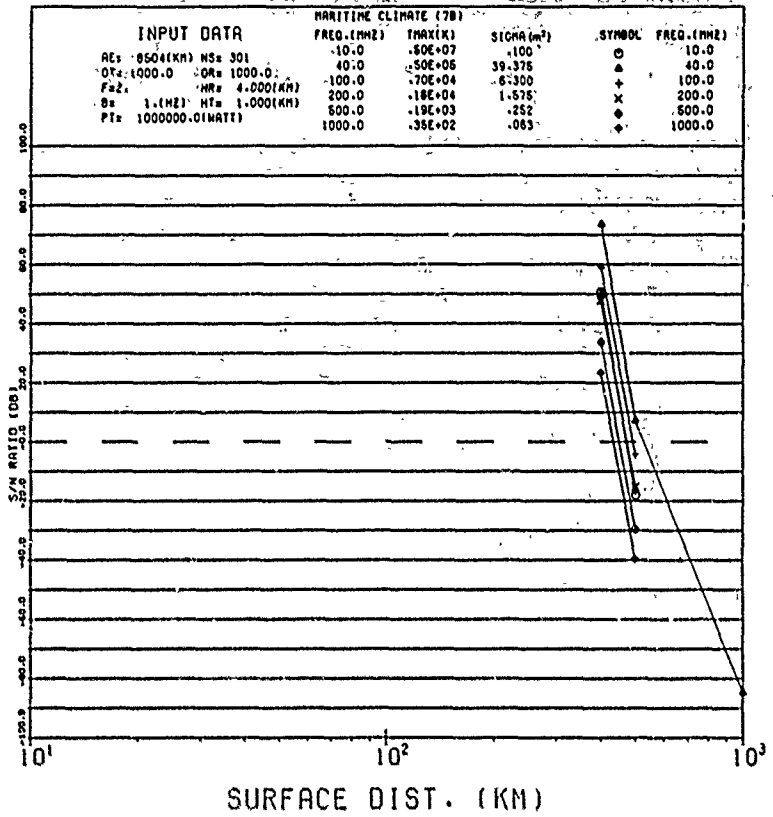


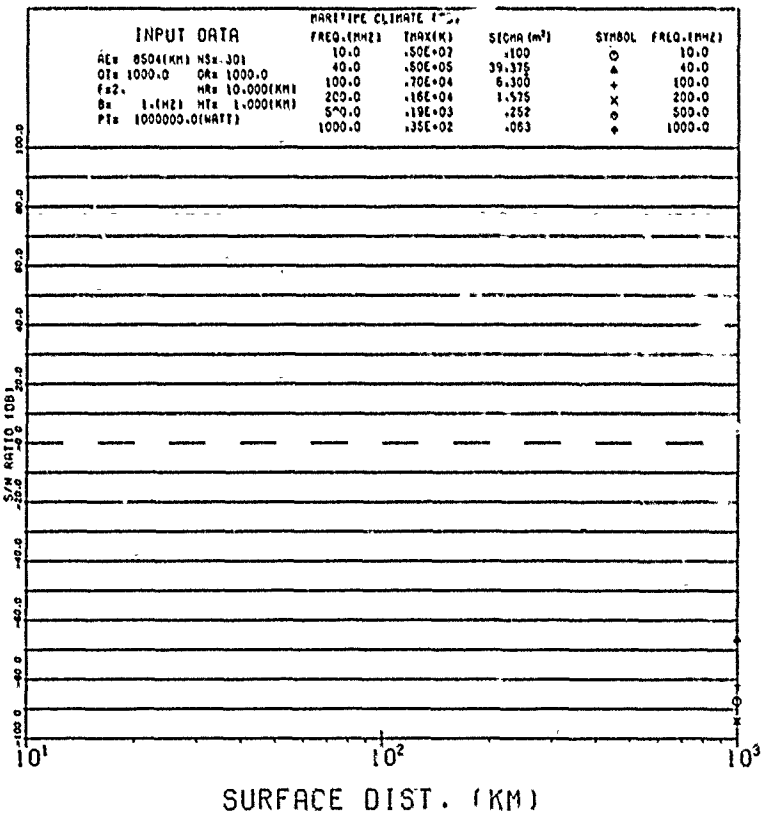


SURFACE DIST. (KM)



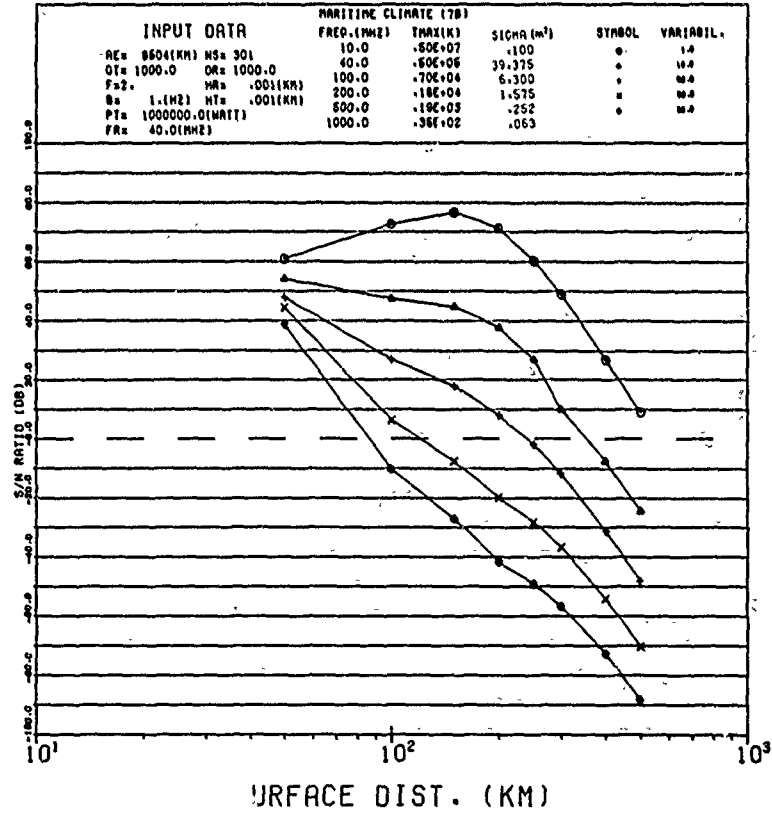
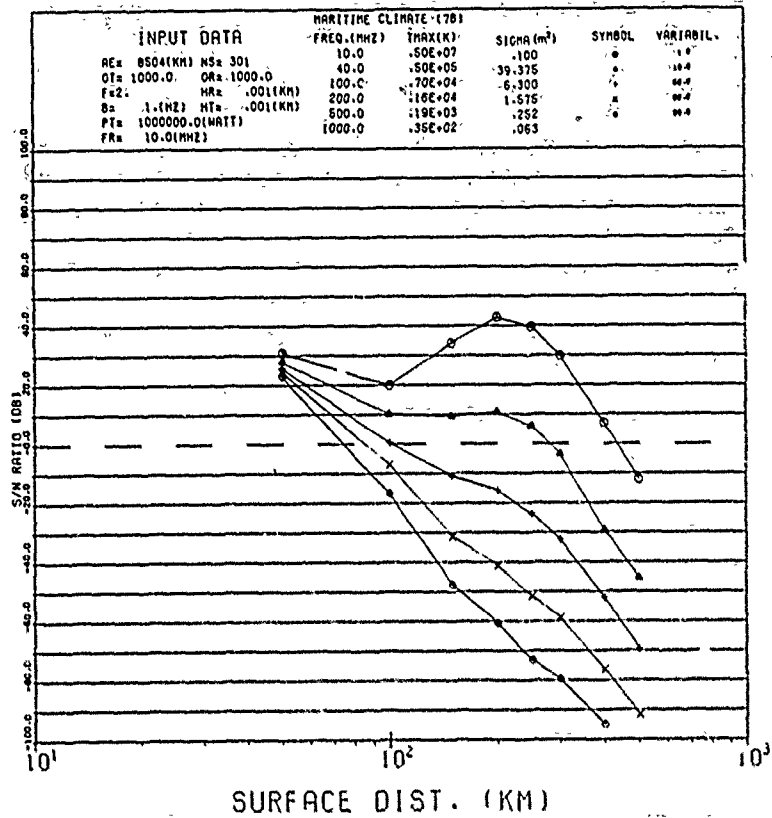
SURFACE DIST. (KM)

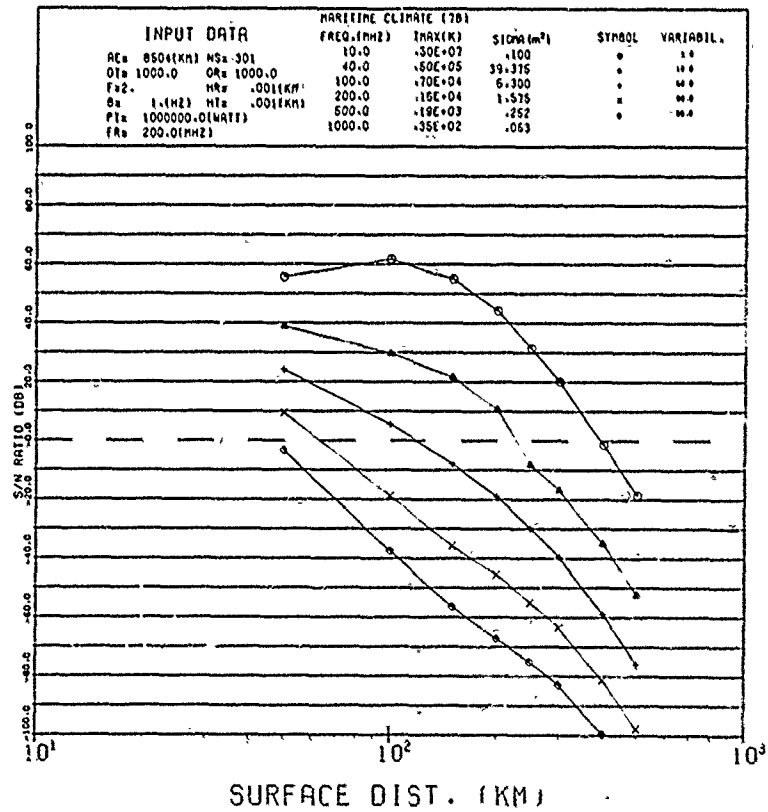
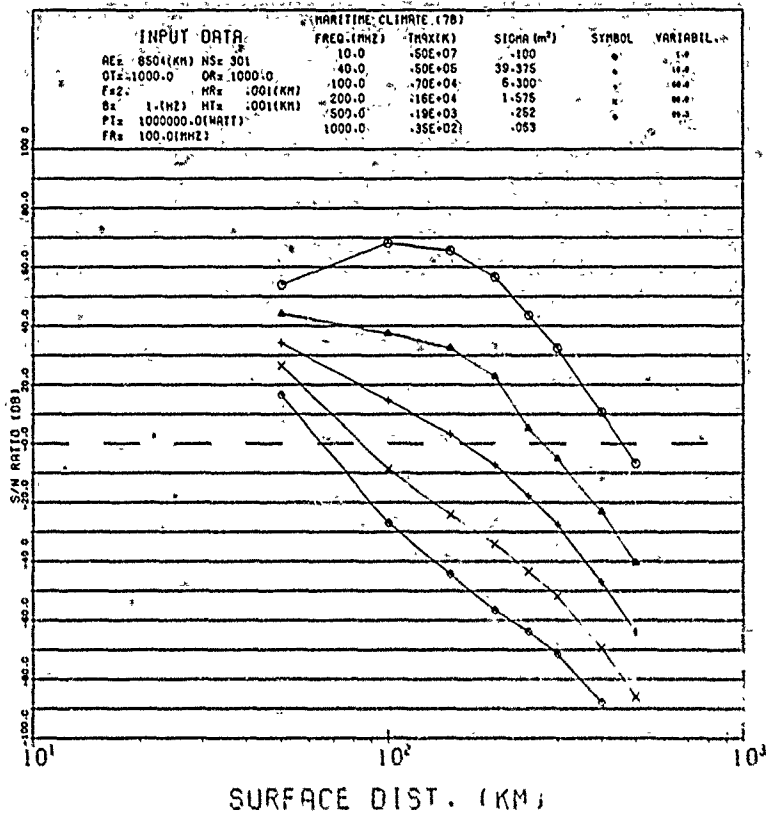


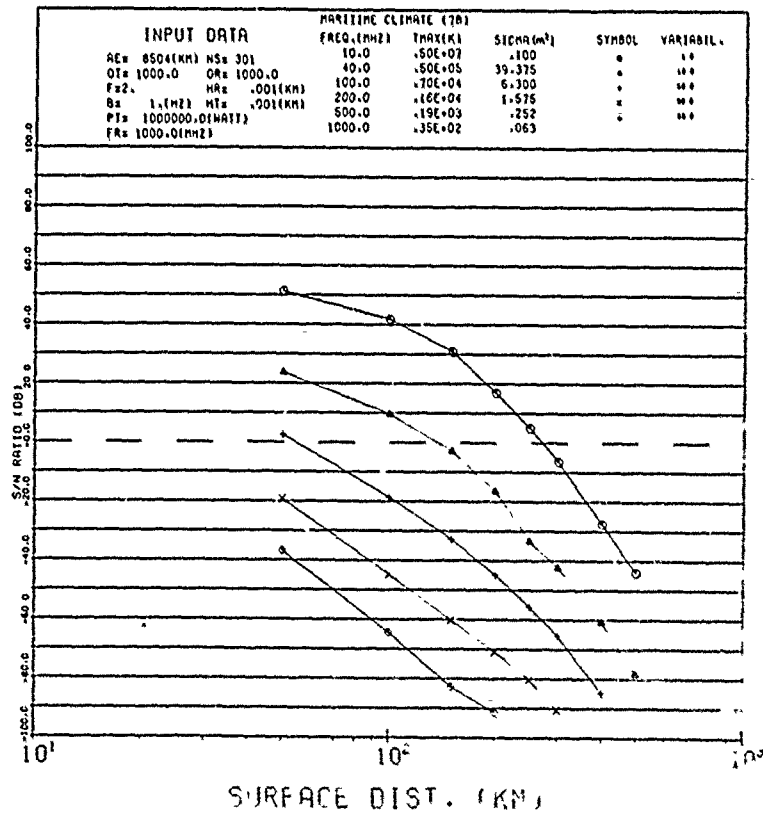
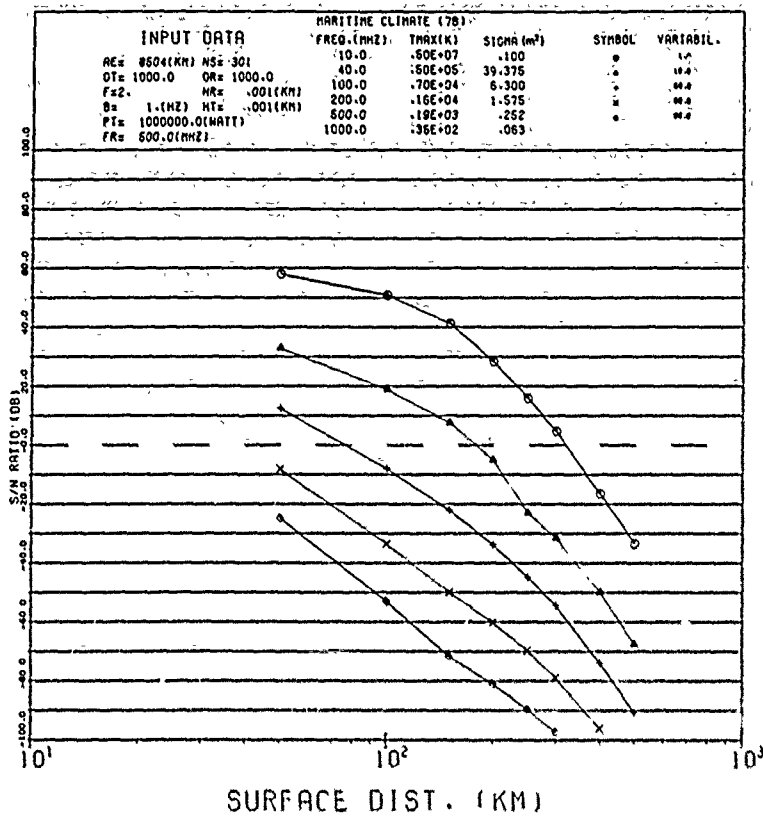


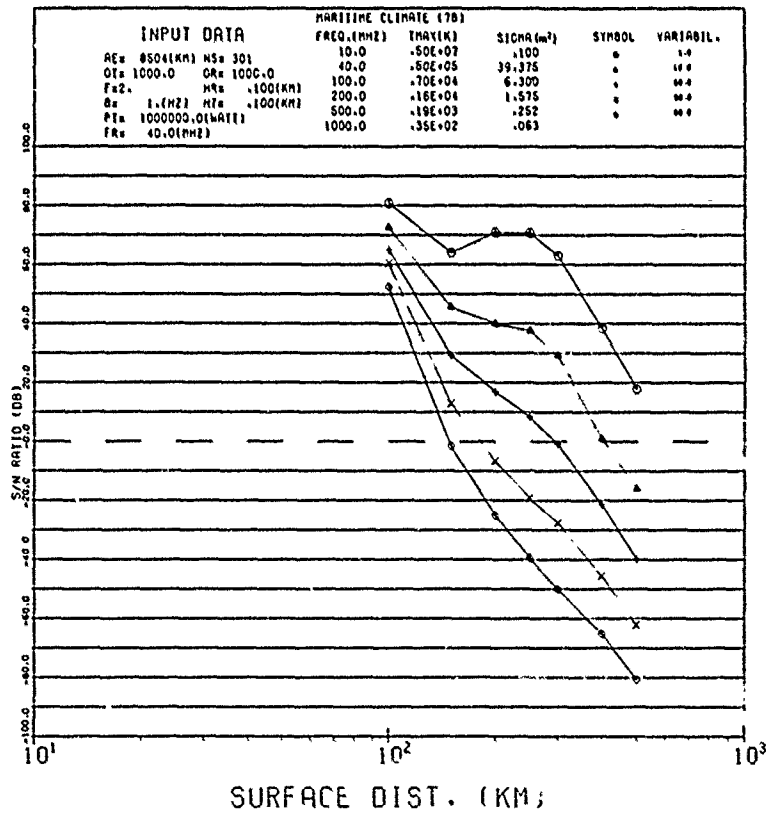
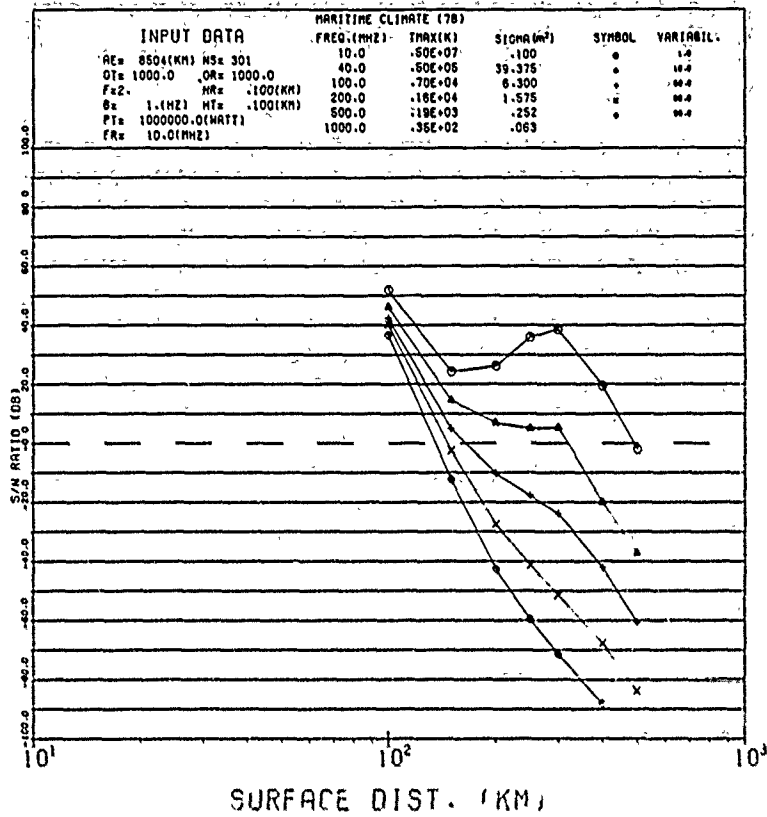
**Appendix F**

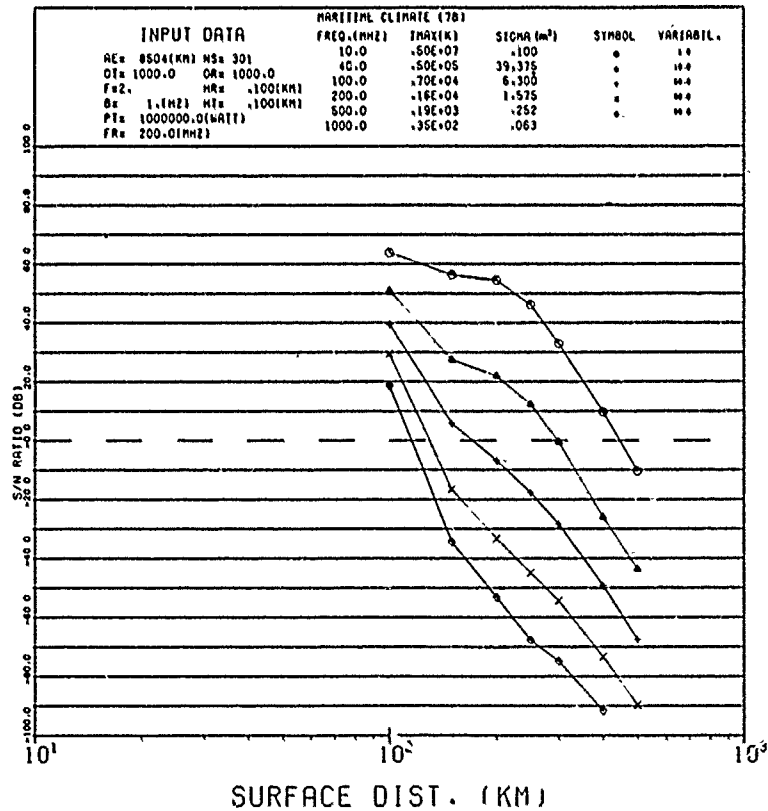
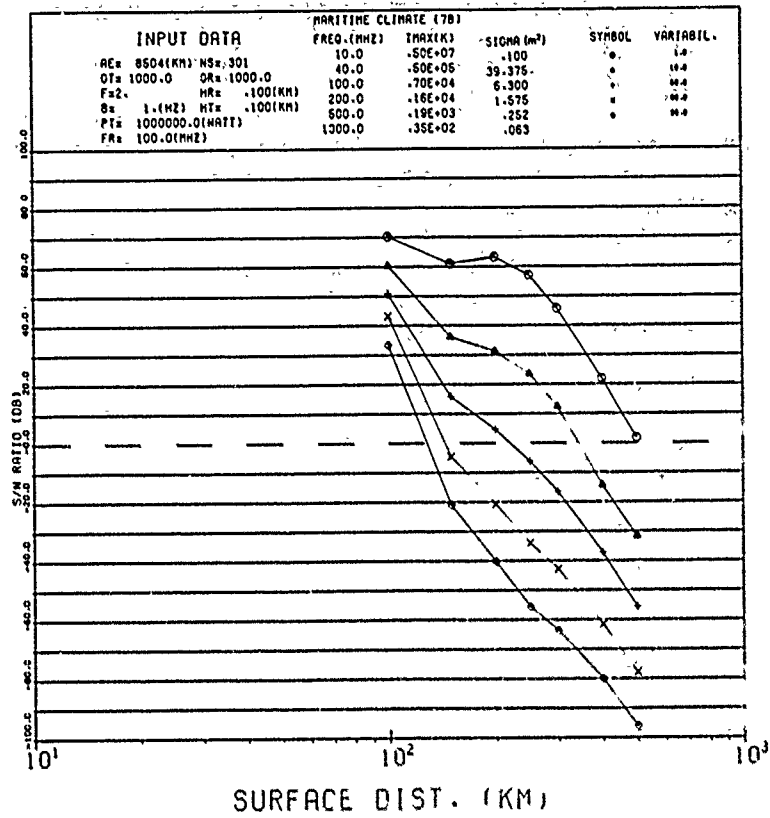
**Eighteen Plots of Signal-to-Noise Ratio (dB)  
vs Distance (km) for 1 to 99% Loss Variability**

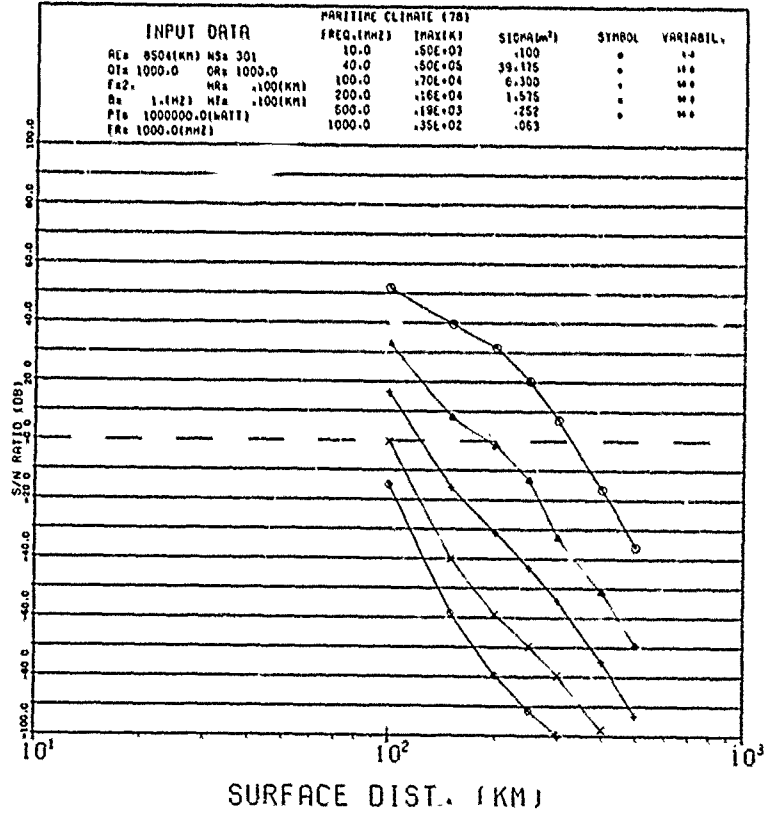
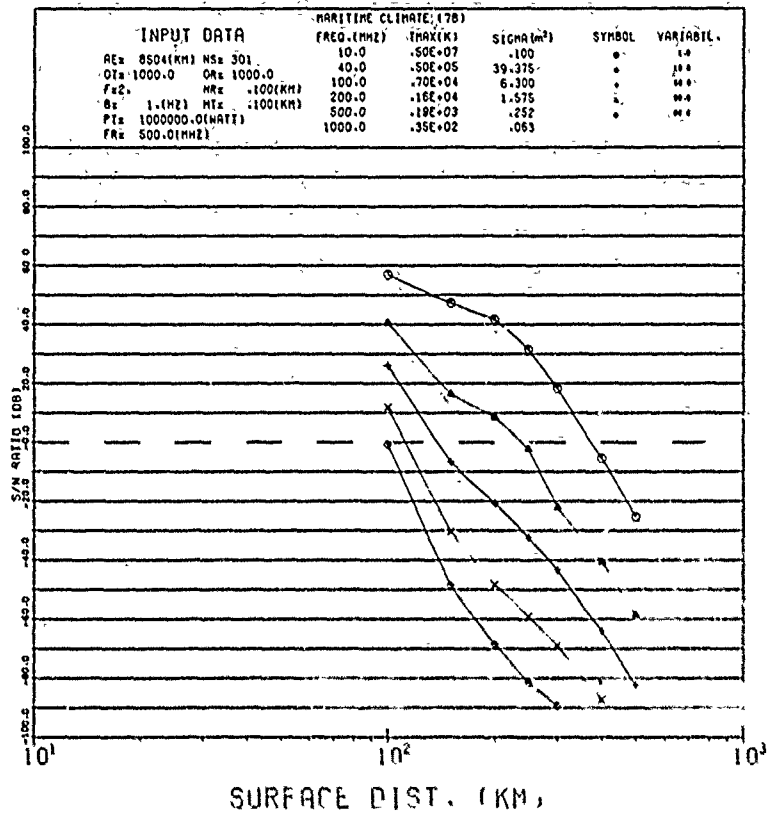


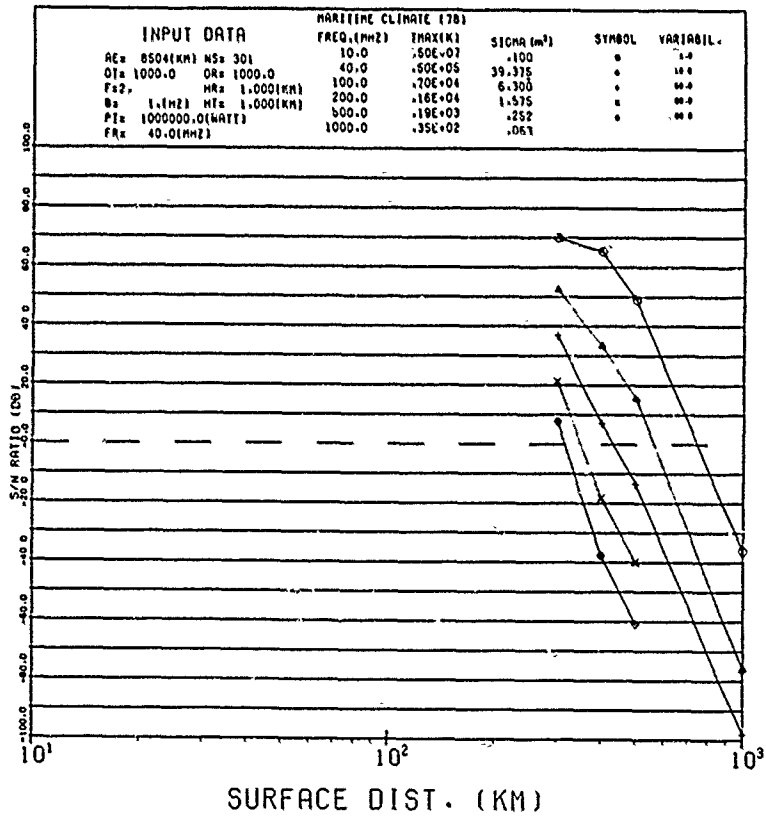
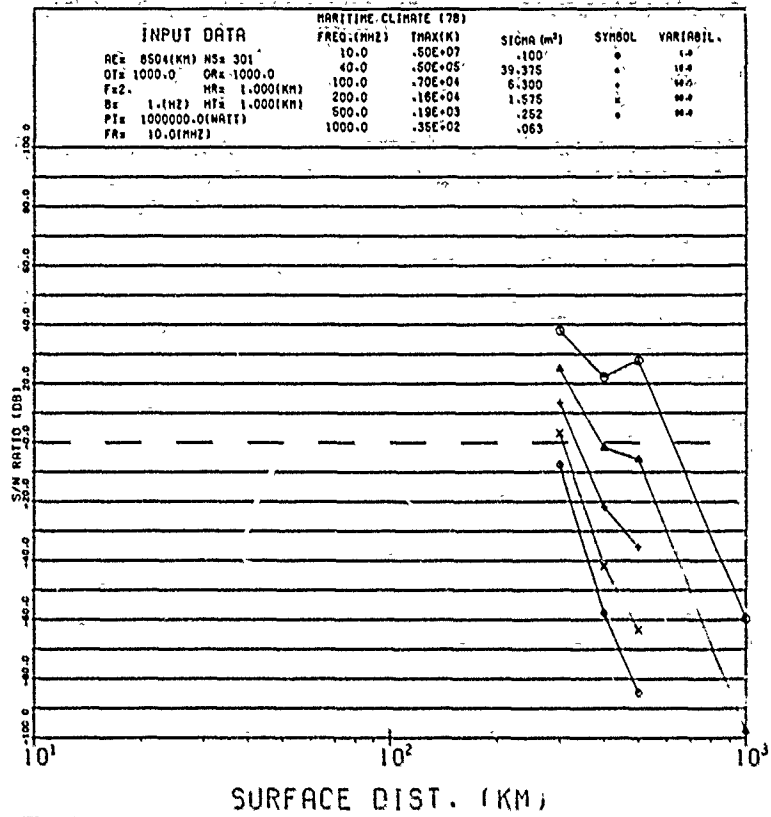


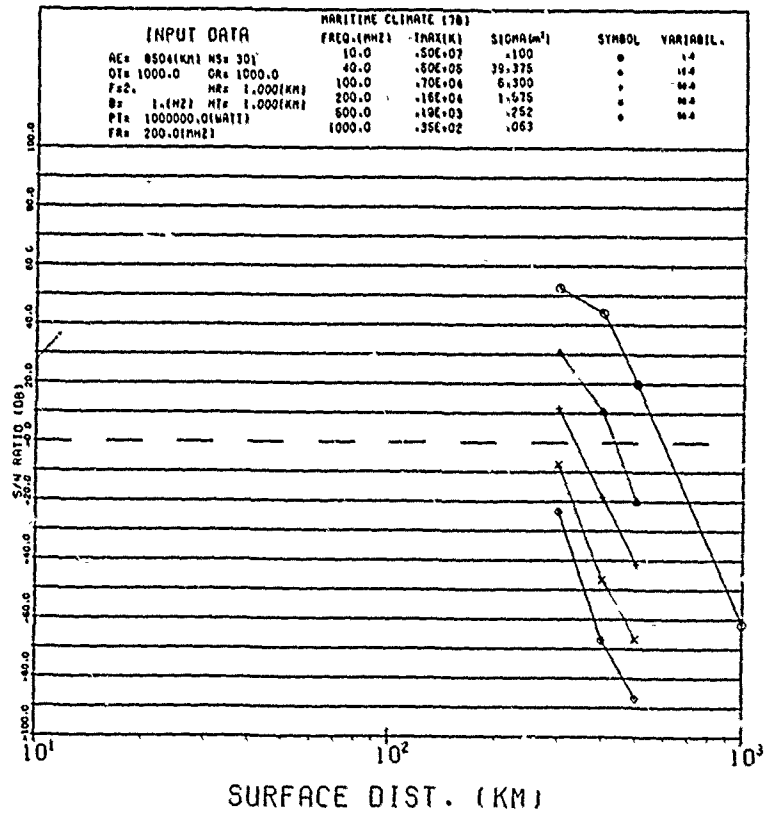
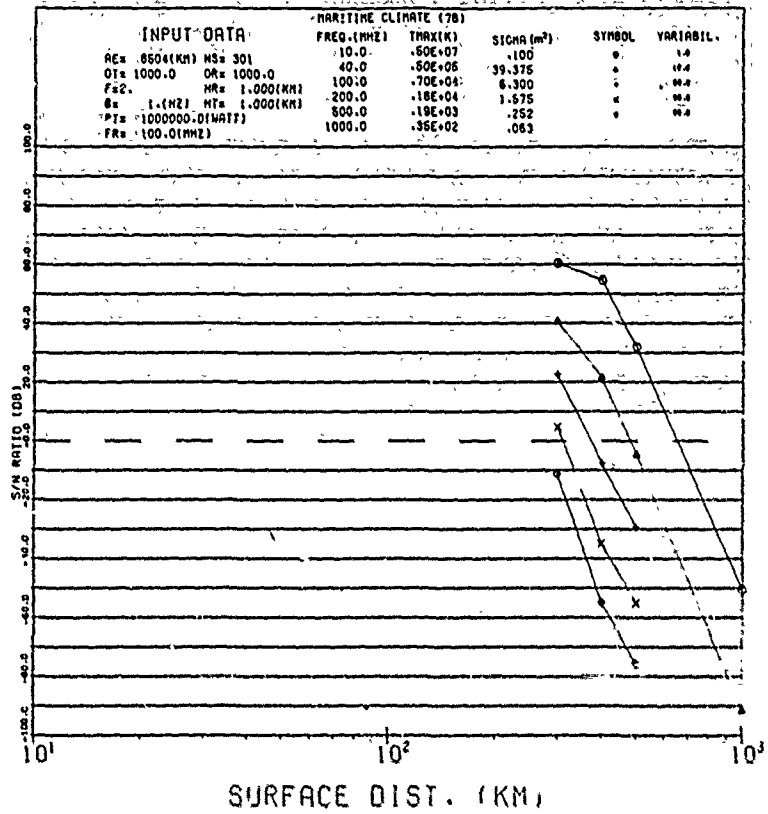


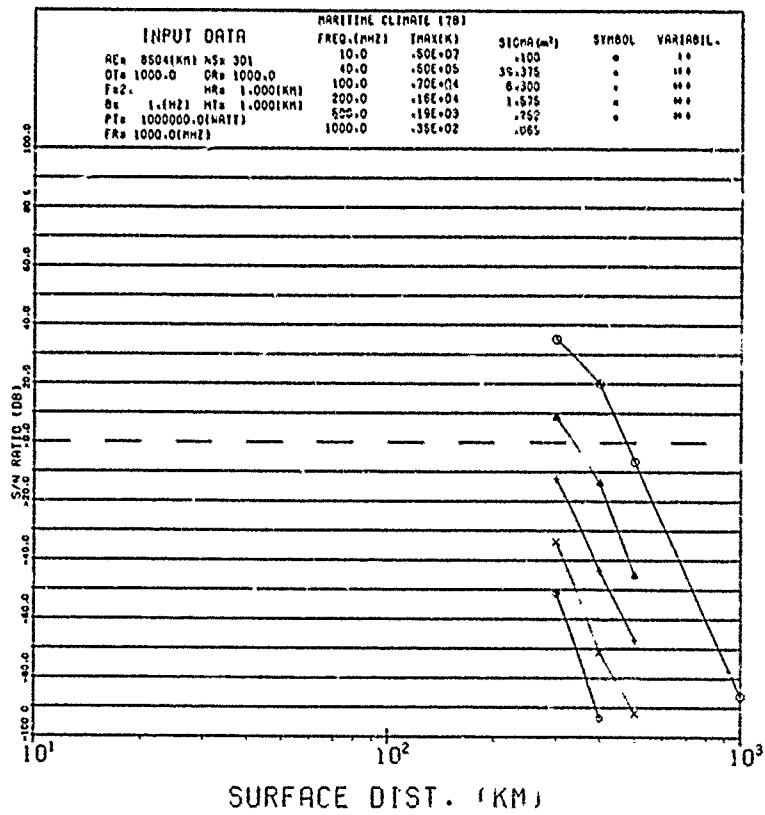
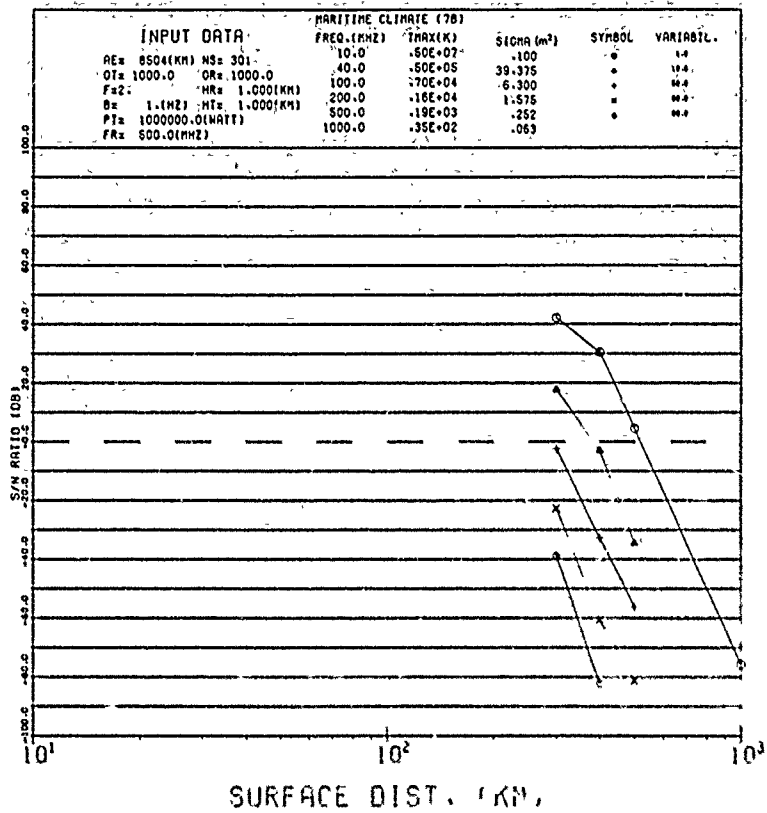


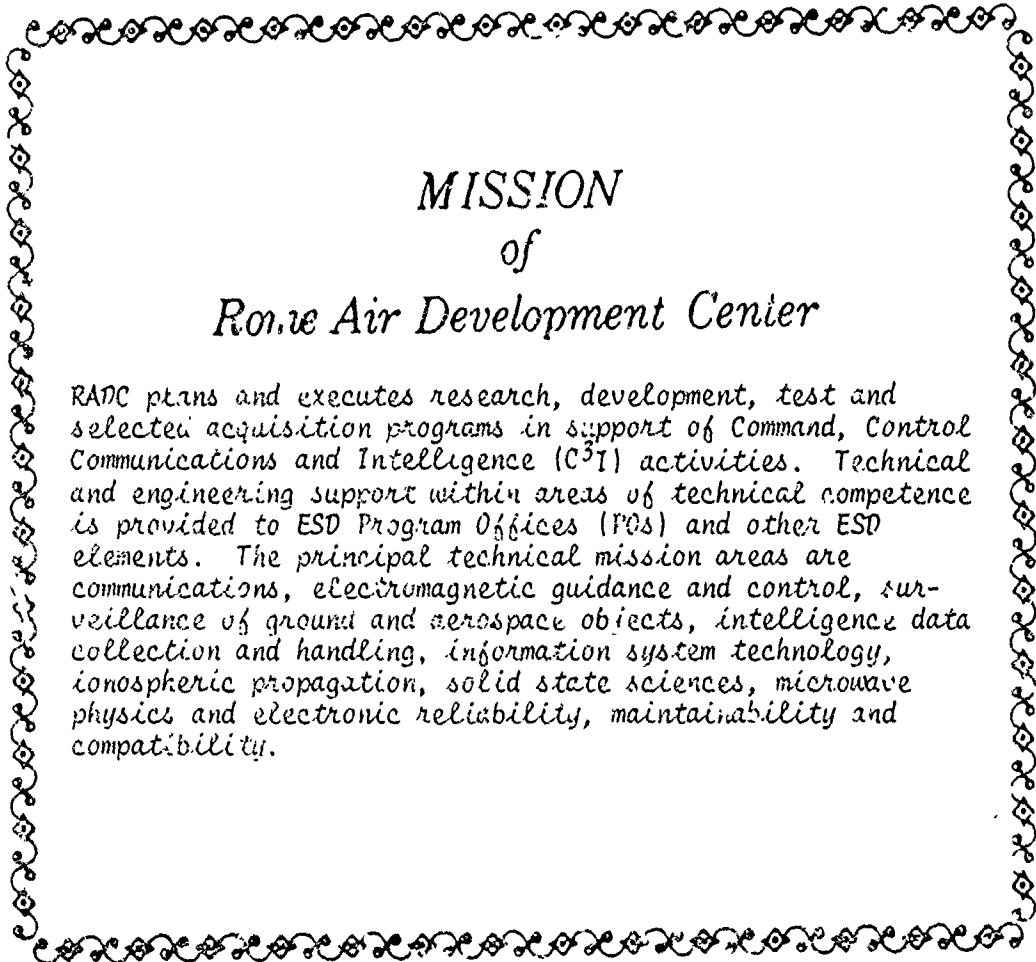












*MISSION*  
*of*  
*Rome Air Development Center*

RADC plans and executes research, development, test and selected acquisition programs in support of Command, Control Communications and Intelligence (C<sup>3</sup>I) activities. Technical and engineering support within areas of technical competence is provided to ESD Program Offices (POs) and other ESD elements. The principal technical mission areas are communications, electromagnetic guidance and control, surveillance of ground and aerospace objects, intelligence data collection and handling, information system technology, ionospheric propagation, solid state sciences, microwave physics and electronic reliability, maintainability and compatibility.